MUTATION IN A LIGHT-REGULATED GLUCAN SYNTHASE-LIKE GENE (*GSL12*) DISPLAYS LIGHT HYPER-RESPONSIVE AND CALLOSE-DEFICIENT PHENOTYPES IN *ARABIDOPSIS*

A Dissertation

by

BO HYUN BYUN

Submitted to the Office of Graduate Studies of
Texas A&M University
in partial fulfillment of the requirements for the degree of

DOCTOR OF PHILOSOPHY

May 2008

Major Subject: Molecular and Environmental Plant Sciences

MUTATION IN A LIGHT-REGULATED GLUCAN SYNTHASE-LIKE GENE (*GSL12*) DISPLAYS LIGHT HYPER-RESPONSIVE AND CALLOSE-DEFICIENT PHENOTYPES IN *ARABIDOPSIS*

A Dissertation

by

BO HYUN BYUN

Submitted to the Office of Graduate Studies of
Texas A&M University
in partial fulfillment of the requirements for the degree of

DOCTOR OF PHILOSOPHY

Approved by:

Chair of Committee,	Alan Pepper
Committee Members,	Clint Magill
	Thomas McKnight
	Arne Lekven
Chair of Interdisciplinary Faculty,	Jean H. Gould

May 2008

Major Subject: Molecular and Environmental Plant Sciences

ABSTRACT

Mutation in a Light-Regulated Glucan Synthase-Like Gene (*GSL12*) Displays Light Hyper-Responsive and Callose-Deficient Phenotypes in *Arabidopsis*. (May 2008)

Bo Hyun Byun, B.S., University of Suwon; M.S., Seoul National University

Chair of Advisory Committee: Dr. Alan Pepper

Light is a very important factor affecting every aspect of plant development. Plant developmental responses to light are sensitive to the direction, intensity, color, and duration of light. Light is perceived by an extensive set of photoreceptors that includes the red/far-red light–absorbing phytochromes and blue/UV-A light–absorbing cryptochromes. The *Arabidopsis* mutant *seedling hyper-responsive to light 6* (*shl*6) has exaggerated developmental responses to available light. In the low light, s*hl*6 seedlings have a phenotype similar to wild-type plants grown in high light, with short hypocotyls, expanded cotyledons, and well-developed first true leaves. In addition, the roots of *shl6* are short and highly branched. The *SHL6* gene was mapped to a position on chromosome 5 between simple sequence length polymorphism (SSLP) markers nga249 and nga151. Two cosmid clones from this interval (introduced by *Agrobacterium*-mediated transformation) complemented the *shl*6 mutant phenotype. One candidate gene identified by complementation is a member of the glycosyltransferase family. The sequence of *shl*6 mutant differs from wild type Columbia allele of this gene (At5g13000) by a single nucleotide substitution in the first exon. This putative *SHL6* gene encodes a member of a glycan synthase-like (GSL12) gene family that includes callose synthase. The β-1,3-D-

glucan callose is found in the cell plate of dividing cells, in pollen mother cell walls, and pollen tubes. Callose synthase and related genes have not been previously implicated in developmental responses to light. We also observed that 90% of Col-0 anthers showed high callose deposition, but *shl6* mutant did not display callose deposition in the anthers. The pollen viability in the *shl6* was lower than Col-0. The epidermal cell elongation in *shl6* hypocotyls was reduced when compared with Col-0. Therefore, we conclude that the mutation in light-regulated *SHL6/GSL12* was involved in the synthesis of callose as well as light signaling.

I dedicate this dissertation to my husband for his love, support and encouragement,

my mother, sisters, and brothers for their love and patience,

and my parents-in-low for their love and encouragement.

ACKNOWLEDGEMENTS

I would sincerely like to thank Dr. Alan Pepper for allowing me to join his lab and guiding me to become a scientist. His constant patience and support have helped me to discover the world of covered plants. I would also like to thank all my committee members (Clint Magill, Arne Leckven, and Thomas McKnight) for their valuable comments, corrections, and encouragement.

I thank Dan Grum for his encouragement and discussions about experiments and for his insightfulness. I would like to thank Robert Corbett for his technical help on making markers and answering my questions with patience. I thank Mi-Seon Sung for introducing me to Dr. Pepper's lab and for her positive mind. I thank Carla Young, Millie Burrell, and her mother for their love and encouragement. I would also like to say thank you to all of the undergraduate student workers for their great efforts to keep our lab in order and for their support.

I thank Dr. Hisashi Koiwa and Dr Chang-ho Kang for helping me to use a UV filter microscope, and Eun-Gyu No for helping me with sequencing candidate genes.

I thank Monique for helping me to teach a Botany 328 lab and for grammar corrections. Finally, I thank my Vision-Mission church friends, including the pastors, for their spiritual support.

.

TABLE OF CONTENTS

CHAPTER Page

LIST OF FIGURES

FIGURE Page

LIST OF TABLES

CHAPTER I

INTRODUCTION

Photomorphogenesis

Being sessile, plants have evolved developmental and physiological responses to various environmental factors including wind, temperature, water and light. Light is a very important factor that affects every aspect of plant development, including seed germination, seedling photomorphogenesis, phototropism, gravitropism, chloroplast movement, shade avoidance, circadian rhythms, and flower induction. Plants modulate their development in response to the direction, intensity, color, and duration of light. After germination, young seedlings have two distinct developments depending on light conditions. In the dark, plants follow skotomorphogenesis (or etiolation), which is characterized by hypocotyl elongation, an apical hook, undeveloped cotyledons and inhibition of chlorophyll and anthocyanin biosynthesis. Once the seedlings are exposed to light, they follow photomorphogenesis or de-etiolation; the hypocotyl stops elongation, shoot apical meristem is activated, chlorophyll and anthocyanin biosynthesis are initiated, and true leaves begin to develop. When plants are exposed to natural light, they receive a broad spectrum of light, ranging from UV to far-red light. Light is perceived by several photoreceptors.

This dissertation follows the style of *Plant Physiology*.

These include the UVA and blue light-absorbing phototropins and cryptochromes, and the phytochromes which mainly absorb red and far-red light (designated PHYA to PHYE in *Arabidopsis*) (Gyula et al., 2003**;** Yamamoto et al., 1998; Quail et al., 1995).

The origin, structure and localization of phytochrome

Phytochrome stands for "plant color" and the name was created to describe the protein pigment that controls photoperiod response and floral induction of certain short-day plants such as cocklebur and soybean (Garner and Allard, 1920). The phytochromes were identified through the observation that the germination of lettuce seeds is induced by red (R) light and repressed by far-red (FR) light (Kendrick and Kronenberg, 1994). Plant phytochromes, which are 240-kDa chromoprotein, have an amino-terminal domain that has four subdomains (P1-P4) and a carboxy-terminal domain that is subdivided into a PAS-related domain (PRD) containing two PAS repeats and a histidine-kinase-related domain (HKRD) (Montgomery and Lagarias, 2002). Phytochromes have two photo-reversible forms. Phytochromes predominately absorb the red and far-red wavelengths. When the inactive Pr form (Pr: red light absorption form) is expose to red light, it is activated by photo-conversion to the biologically active Pfr form (Pfr: far-red absorption form) (Quail, 1997). The activated Pfr form converts back to the Pr form by absorbing far-red light or undergoes dark reversion in the absence of light (Furuya and Song, 1994; Quail, 2002). Phytochromes are of two types based on their stability to light, Type I (photo-labile) and Type II (photo-stable). Type I phytochromes are unstable to light; since they accumulate in the darkness and are degraded rapidly by being exposed to

light, while type II are made in the light (Furuya, 1993). In *Arabidodpsis*, phyA is a type I phytochrome and phyB-E are type II phytochromes (Quail, 1997; Sharrock and Quail, 2002). The photo-conversion of phytochromes induces their translocation from the cytoplasm to the nucleus. For example, phyA is imported into the nucleus in response to continuous far-red light (Nagy and Schafer, 2002). A hypomorphic protein made by the *phyB* fails to translocate into the nucleus (Matsushita et al., 2003). The translocation of phytochromes into the nucleus has an important role in phytochrome signaling (Quail 2002).

Phytochrome signaling

Red light induces the autophosphorylation of oat phyA by attaching to chromophore (Yeh and Lagarias, 1998). phyA can also phosphorylate several proteins including PKS1 (protein kinase substrate 1) (Frankhauser et al., 1999), Aux/IAA (Colon-Carmona et al., 2000), cry1, and cry2 (Ahmad et al., 1998) *in vitro*. Several phytochrome signaling domains have been identified through deletion and site directed mutagenesis studies. For example, the deletion of phyA residue Ser7 in *Arabidopsis* phyA led to hypersensitivity to the far-red light (Casal et al., 2002). The HKRD domain is also an essential signaling region of both phyA and phyB (Krall and Reed, 2000; Fankhauser et al., 1999). PKS1 of a number of phyA intermediates interacts with HKRD and can be phosphorylated by phyA *in vitro* (Fankhauser et al., 1999). PKS1 is an inhibitor of phyB, and is required for phyA-mediated VLFR responses with enhanced cotyledon opening, and inhibition of hypocotyl elongation (Lariguet et al., 2003). An analysis of protein-

protein interactions involved in phytochrome signaling has identified a number of phytochrome-interaction factors (PIFs) including PIF3 and PIF4 (Quail 2002; Kim et al., 2003). PIF3 and PIF 4 are nuclear localized basic helix-loop-helix (bHLH) proteins and are negative regulators of phytochrome signaling (Heim et al., 2003; Toledo-Ortiz et al., 2003). PIF3 binds to a light-responsive G-box cis-element to express skotomorphogenesis genes (Martinez-Garcia et al., 2000). PIF3 acts mainly as a negative regulator of phyB-induced signaling (Kim et al., 2003).

The Pfr form of phytochromes is imported into the nucleus. The Pfr form phosphorylates PIF3 and phosphorylated PIF3 is ubiquitinylated and degraded (Al-Sady et al., 2006; Bauer et al., 2004). PIF4 also binds to the Pfr form of phyB (Huq and Quail, 2002) and is involved in shade-avoidance and red light responses (Huq and Quail, 2002; Salter et al., 2003).

The photomorphogenetic mutants involved in light signaling

Through the use of photomorphogenetic mutants, several genes involved in de-etiolation have been discovered. These mutants have three distinct classes: *cop/det/fus* (constitutive photomorphogenesis/de-etiolated/fusca), long hypocotyl (*hy*), and seedling hyper-responsive to light (*shl*).

In the first class of mutants, dark-grown seedlings have short hypocotyls and phenotypes characteristic of light grown plants (Chory et al., 1989; Wei and Deng, 1996; Osterlund et al., 1999; Holm and Deng, 1999). As negative regulators of photomorphogenesis, *cop/det/fus* (*constitutive photomorphogenesis/de-etiolated/fusca*)

mutant mimic the phenotype of light-grown seedlings, including open, expanded cotyledons, suppression of hypocotyls growth, and anthocyanin accumulation when grown in the dark (Koornneef et al., 1980; Chory, 1992; Ang and Deng, 1994; Wei et al., 1994; Pepper and Chory, 1997). For example, in *det*1 mutants, light-induced genes such as those that encode the ribulose bisphosphate carboxylase small (rbcS) and *large* subunits (rbcL) are expressed in the dark. DET1 is a 62kDa protein located in the nucleus that functions to repress the promoters of light-regulated genes (Pepper et al., 1994). The functional form of DET1 is an approximately 350 kDa protein complex with Damaged DNA Binding Protein 1 (DDB1) (Schroeder et al., 2002). DET1/DBB1 complex has a chromatin-remodeling function and in the dark, DET/DDB1 complex binds to nonacetylated amino-terminal tails of the core histone H2B in the cortex of the nucleosome (Benvenuto et al., 2002; Schroeder et al., 2002). In addition, Schroeder (2002) suggested a model that the DET1/DBB1 complex binding to chromatin may inhibit access of positive regulators involved in photomorphogenesis in the dark and be released by acetylation in the light to stimulate the expression of photoregulated genes, such as *HY5* and *PIP3* (Benvenuto et al., 2002).

As another key negative regulator, COP1 has three motifs: a ring finger zinc-binding motif, a coiled-coil domain, and WD-40 repeats (Deng et al., 1992). The coiled-coil domain of COP1 interacts with the COP1 Interacting Proteins CIP1, CIP4, and CIP7 (Matsui et al., 1995; Torii et al., 1999; Yamamoto et al., 1998; Yamamoto et al., 2001). CIP8 interacts with the ring finger motif of COP1 (Hardtke et al., 2002). COP1 and CIP8 both have ring finger motifs, characteristic of E3 ubiquitin ligases and the interaction of

CIP8 and COP1 participates in proteosome-mediated degradation of two basic domain/leucine zipper (bZIP) transcription factors (HY5 and HYH) (Osterlund et al., 2000; Hardtke et al., 2002; Holm et al., 2002). In addition, COP1 was shown to act with an E3 ubiquitin ligase in the degradation of a number of proteins, including a MYB transcription factor (LAF1), and a basic helix-loop-helix (bHLH) transcription factor (Saijo et al., 2003; Seo et al., 2003; Jang et al., 2005) that are involved in promoting photomorphogenesis (Yang et al., 2005). COP1 subcellular localization depends on light signals. The quantitative abundance of COP1 decreases in the nucleus in a manner dependent on light intensity, whereas in the dark, COP1 is nuclear localized (von Arnim and Deng, 1994; Osterlund and Deng, 1998). COP1 interacting with HY5 acts as a putative E3 ubiquitin ligase and targets the degradation of HY5 via the 26S proteosome pathway in darkness (Osterlund et al., 2000; Schwechheimer and Deng, 2000). In light, COP1 activity is regulated negatively by multiple photoreceptors (Osterlund and Deng, 1998). The direct interaction of cryptochrome with COP1 is involved in the inactivation of COP1 in blue light (Wang et al., 2001; Yang et al., 2001).

The second set of mutants is defective in light perception (Koornneef et al., 1980). These long hypocotyl or *hy* mutants fail to integrate signals from various multiple photoreceptors and have a long hypocotyl phenotype whether they are grown in light or darkness (Koornneef et al., 1980). Most *hy* mutants are defective in photoreceptors or in positive regulators of photomorphogenesis. For example, *hy8*, *hy3*, and *hy4* encode the apoproteins of phytochromeA, phytochromeB, and cryptochrome1, respectively. The *hy*5 gene encodes the basic leucine zipper (bZIP) transcription factor that activates the

transcription of light-induced genes (Ang et al., 1998). Mutation in *Hy5* also cause a defect in light-induced inhibition of hypocotyl elongation in all light conditions, indicating that HY5 acts downstream of phyA, phyB, chrptochromes, and UV-B (Koornneef et al., 1980; Oyama et al., 1997; Ang et al., 1998; Ulm et al., 2004). The *hy5* null mutant also has abnormal root morphology and altered hormone responses (Oyama et al., 1997; Cluis et al., 2004). In addition, HY5 is regulated by COP1 via proteosome-mediated degradation with COP1. Further, HY5 is regulated by UVB Resistance 8 (UVR8). UVR8 is a UVB-specific signaling component that affects the expression of a range of genes essential for UV-B protection (Brown et al., 2005). UVR8 has been shown to associate with chromatin in the *HY5* promoter region by Chromatin immunoprecipitation (ChIP) (Brown et al., 2005).

In a previous study, a new third set of photomorphogenic mutants in genes acting at the interface of light perception and developmental pathways was screened in *Arabidopsis*. Pepper et al. (2001) isolated recessive light-hyperresponsive mutants in eight genetic loci, designated as *seedling hyper-responsive* to *light* (*shl*). Whereas low light grown Col-0 seedlings have elongated hypocotyls and open cotyledons, *shl* seedlings showed a phenotype typical of seedlings grown in high-light, with short hypocotyls, expanded cotyledons, and significant development of first true leaves in low light. *shl* seedlings have an etiolated phenotype like Col-0 seedlings grown in darkness. To eliminate mutants in the *det/cop/fus* class and those with severe pleiotropic developmental defects, mutant seed pools were “counter-screened” in darkness. *SHL* genes act as negative regulators of photomorphogenesis, but they are functionally

distinct from mutants in the *det/cop/fus* class in that they are hyperresponsive to available light, rather than light independent (Chory et al., 1989; Deng et al., 1991; Pepper et al., 2001).

In this study, I identified the gene mutated in one of *shl* mutants, *shl6*, by a map-based cloning approach. We characterized the function of the *SHL*6 gene at the molecular and physiological levels, thus contributing to our understanding the relationship between light signaling and plant development.

CHAPTER II

IDENTIFICATION OF *shl6* MUTANT

Introduction

Being sessile, plants have evolved developmental and physiological responses to various environmental factors such as wind, temperature, water and light. Light is a very important factor that affects every aspect of plant development. Plants modulate their development in response to the direction, intensity, color, and duration of light. After germination, young seedlings have two distinct developments depending on light conditions. In the dark, plants follow skotomorphogenesis (or etiolation), which is characterized by hypocotyl elongation, an apical hook, undeveloped cotyledons and inhibition of chlorophyll and anthocyanin biosynthesis. Once the seedlings are exposed to light, they follow photomorphogenesis or de-etiolation; the hypocotyl stops elongation, shoot apical meristem is activated, chlorophyll and anthocyanin biosynthesis are initiated, and true leaves begin to develop. When plants are exposed to natural light, they receive a broad spectrum of light, ranging from UV to far-red light. Light is perceived by several photoreceptors. These include the UVA and blue light-absorbing phototropins and cryptochromes, and the phytochromes, which mainly absorb red and far-red light (designated PHYA to PHYE in *Arabidopsis*) (Gyula et al., 2003**;** Yamamoto et al., 1998; Quail et al., 1995).

Through the use of photomorphogenetic mutants, several genes involved in de-etiolation have been discovered. These mutants have three distinct classes: *cop/det/fus* (*constitutive photomorphogenesis/de-etiolated/fusca*), *long hypocotyl* (*hy*), and *seedling hyper-responsive* to *light* (*shl*). In the first class of mutants, dark-grown seedlings have short hypocotyls and characteristic phenotypes of light grown plants (Chory et al., 1989; Wei and Deng, 1996; Osterlund et al., 1999; Holm and Deng, 1999). As negative regulators of photomorphogenesis, *cop/det/fus* (*constitutive photomorphogenesis/de-etiolated/fusca*) mutant mimic the phenotype of light-grown seedlings, including open, expanded cotyledons, suppression of hypocotyl growth, and anthocyanin accumulation when grown in the dark (Koornneef et al., 1980; Chory 1992; Ang and Deng, 1994; Wei et al., 1994; Pepper and Chory, 1997). For example, in *det*1 mutants, normally light-induced genes, such as those that encode *ribulose bisphosphate carboxylase small* (*RBCS*) and *large* subunit (*rbcL*) are expressed in the dark. DET1 is located in the nucleus and functions to repress the promoters of the light-regulated genes (Pepper et al., 1994). In the dark, DET1 binds to nonacetylated amino-terminal tails of the core histone H2B in the cortex of the nucleosome (Benvenuto et al., 2002). Thus, DET1 may be released by acetylation in the light to stimulate expression of photoregulated genes, such as HY5 and PIP3.

A second set of mutants is defective in light perception (Koornneef et al., 1980). These *long hypocotyl* or *hy* mutants fail to integrate signals from various multiple photoreceptors and have a long hypocotyl phenotype whether they are grown in light or darkness. Most of *hy* mutants are photoreceptors or positive regulators of

photomorphogenesis mutations. For example, *hy8*, *hy3*, and *hy4* encode the apoproteins of phytochrome A, phytochrome B, and cryptochrome1, respectively. The *hy*5 gene encodes the basic leucine zipper (bZIP) transcription factor that regulates the transcription of light-induced genes (Ang et al., 1998).

Our laboratory has identified a new third set of photomorphogenic mutants in *Arabidopsis* that are hyper-responsive to available light, designated as *seedling hyper-responsive* to *light* (*shl*) (Pepper et. al, 2001). In low light, *shl* seedlings showed a phenotype typical of seedlings grown in high-light, with short hypocotyls, expanded cotyledons, and significant development of first true leaves when grown in low light. One of *shl* mutants, *shl*6 was isolated by screening mutagenized seed lines under a yellow filter, which partially depletes photomorphogenetically active areas of the light spectrum including UV, blue, red and far-red. Unlike other *shl* mutants (Pepper et. al, 2001), *shl6* mutants also have also short, branched roots.

In this chapter, mutant *shl6* was back-crossed with wild type Columbia (Col-0) to analyze the phenotype of F_2 progeny. The light hyper-responsive trait was shown to be determined by a single gene. For map-based cloning of the *shl*6 locus, a mapping population was made from the F_2 of a cross of the *shl6* mutant and the wild type *Landsberg erecta* ecotype (*La-er*). To identify the *SHL6* gene, complementation analysis was employed via *Agrobacterium*-mediated plant transformation.

Results

Isolation of *shl6* mutants

Fifteen independent mutants were isolated from ethyl methane sulfonate (EMS) mutagenized plants (Columbia ecotype) screened under low light using the conditions described by Pepper et al. (2001). When grown under low light, these mutants showed a high light phenotype with short hypocotyl, open cotyledons, and early development of the first true leaves. In the dark, however, they were largely similar to wild type with respect to hypocotyl elongation, folded cotyledons, and inhibition of chlorophyll and anthocyanin biosynthesis. Thus, these mutants were called *seedling hyper-responsive* to *light* (*shl*). s*hl*6, one of these mutants, was crossed with the wild type Columbia ecotype (*Col*-0). In the F_2 generation, short hypocotyls were 14 and long hypocotyls were 47. The observed numbers accepted the principle of segregation (1:3) by a chi-square test (χ^2=16, p<0.5). The result supported the hypothesis that short hypocotyls were caused by a single recessive mutation.

In yellow light (65 μmol m^{-2} s^{-1}), s*hl*6 seedlings have a phenotype similar to wild-type plants grown in high light (110 μmol m^{-2} s^{-1}), with short hypocotyls, expanded cotyledons, and well-developed first true leaves (Figure 2.1A). Unlike several other *shl* mutants, *shl6* had a somewhat shorter hypocotyl in the dark than wild-type (a partially de-etiolated phenotype), and thus did not fit the ideal *shl* phenotypic criteria. However the *shl6* phenotype showed a very strong light dependence (Figure 2.1A and B). In addition, the roots of *shl6* were short and highly branched in all light conditions.

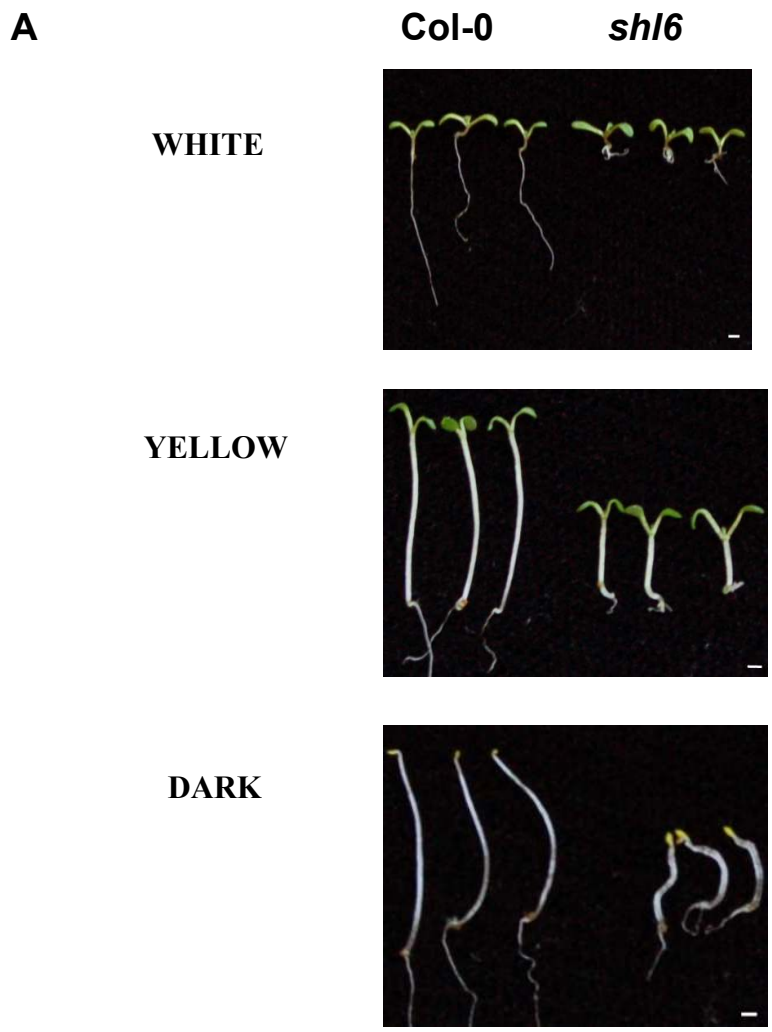

Figure 2.1. Early morphological phenotype of *shl6* mutants

(A) Seven-day-old *shl6* seedlings show differences under high light (110 μmol m^{-2} s^{-1}), yellow (65 μmol m^{-2} s^{-1}), and darkness compared to the wild type (Col-0).
(B) Hypocotyls were measured in high light (110 μmol m^{-2} s^{-1}), yellow (65 μmol m^{-2} s^{-1}), and darkness. Data presented are mean ± SE (n=25).
(C) Root growth responses of Col-0 and *shl6* seedlings to yellow (65 μmol m^{-2} s^{-1}). Data presented are mean ± SE (n=12). Bar means 1mm.

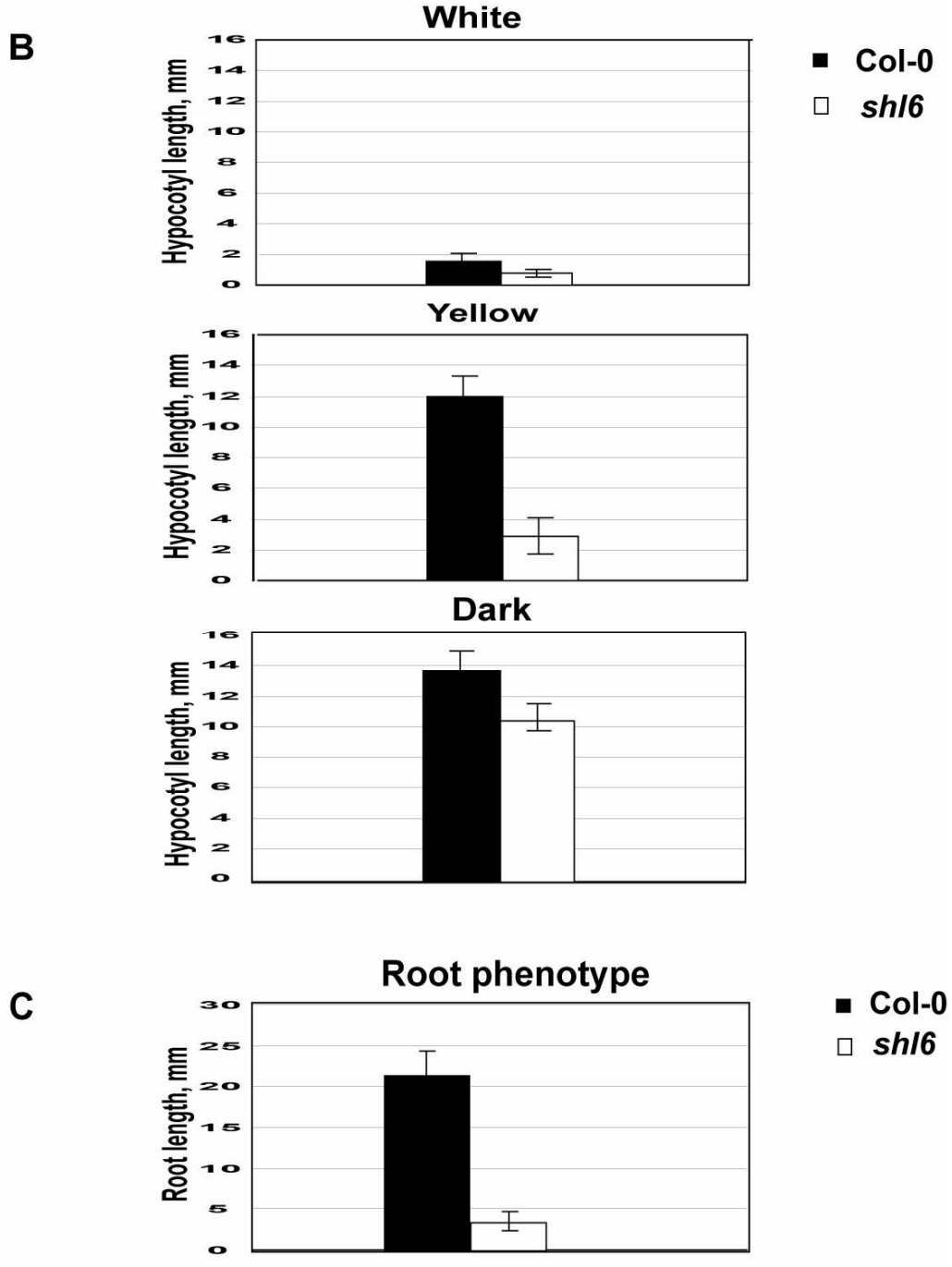

Figure 2.1. Continued.

Identification of the *SHL6* gene

For map-based cloning of the *shl*6 locus, 500 short-hypocotyl plants were selected from the F_2 of a cross between the *shl6* mutant and the wild type *Landsberg erecta* ecotype (*La-er*). To do genetic mapping, twenty four genetic markers (Pepper et al.,2001) were selected to cover the five *Arabidopsis* chromosomes. The *shl6* mutant was linked to simple sequence length polymorphism (SSLP) marker nga225 on chromosome 5. Fine linkage mapping of the 500 mutant F_2 individuals using PCR-based markers localized *shl*6 to the region of chromosome 5 between SSLP markers nga249 and nga151 (Figure 2.2A). Using the genomic sequences released by the international *Arabidopsis* genomic Initiative (Sato et al., 1997, Bevan et al., 1998, and AGI, 2000, Jander et al., 2002) twelve new additional SSLP markers were developed (Table 2.1). The genomic interval containing the *shl*6 locus was narrowed to a 235Kb genomic fragment spanned by bacterial artificial chromosome BAC clones T2L20, T2H18, T19L5, and T31B5 (TAMU BAC library; Cai et al., 1995) (Figure 2.2A).

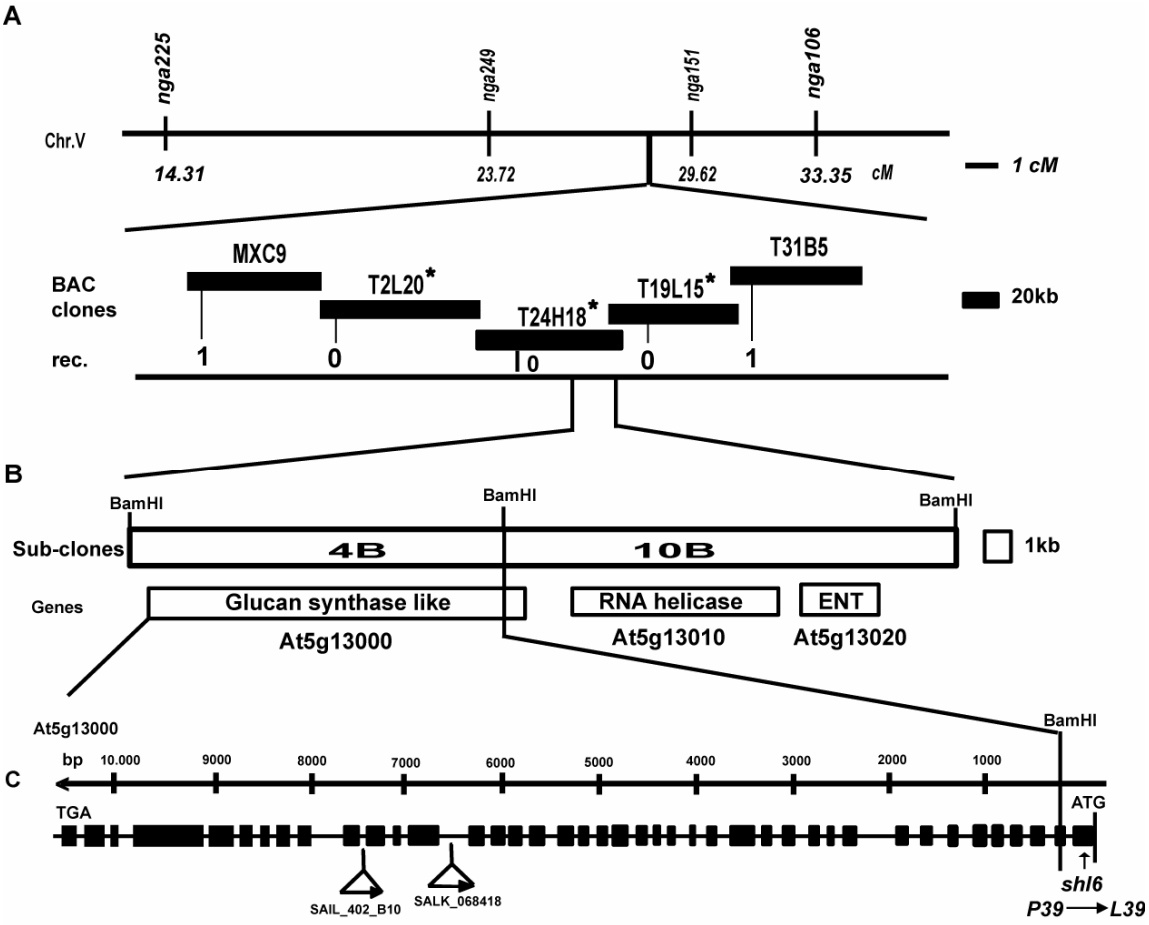

Figure 2.2. Map-based cloning of *SHL6*

(A) *SHL6* was mapped to the BAC clone T24H18 on chromosome 5 by analyzing recombinants produced from crosses. Positions of known SSLP markers used for mapping are indicated. Positions of SSLP markers developed for this work from sequence data are labeled by vertical lines. Asterisks (*) indicate sub-cloned BACs.
(B) Two sub-clones (4B and 10B) complementing *shl6* mutant by *Agrobacterium*-mediated transformation are indicated.
(C) Exon/intron structure of *SHL6*. *SHL6* consists of 42 exons (rectangles) and thick lines are introns. *shl6* caused a Pro-39 to Leu mutation in the first exon of gene At5g13000. Two T-DNA insertion lines (SALK_068418 and SAIL_402_B10) are indicated by open triangles.

Table 2.1. Twelve new SSLP makers on Chromosome 5

Marker Name	PCR primer pair 5´-forward-3´ and 5´-reverse-3´	Map position Physical [a]	
F8F6	F5'-GGTATAATGCGTGTATTCG-3' R5'-CGTGTGGACATCATAAATGCC-3'		F8F6
MJJ3	F5'-GTCCCGTCCAAGGTCATTTA-3' R5'-CTGTTTTCACCGCTAAGTCG-3'		MJJ3
T31P16	F5'-CTTAAGAATTATGGGAACGGAG-3' R5'-GCAGCTAGTGATCGTTAACCCG-3'		T31P16
T5K6	F5'-CTTAATAACCCCTCCTCTCTCG-3' R5'-TGAAGTTGAAGTAGGTGCTC-3'	(10/-10)[b]	T5K6
F2I11C	F5´-CAACGGATGCGATAGATTACCCA-3´ R5´-GCC ATT GAA AAG ACT ATT CCA TTC G-3´		F2I11
T22P22A	F5'-GGAGTTTGCAAACTATTAGACACA-3´ R5'-AGTCATTGTTATGCTACTTGAGG-3'	(-6/6)[b]	T22P22
F14F18	F5'-CAGTTGTTCAGCTACCTATTCAG-3' R5'-TCCATGCTACCCAGAAAAGG-3'	(-8/8)[b]	F14F18
MXC9A	F5´-GCTGATTCAAACCATTCC-3´ R5´-GGTAGGTGTGAACATTTTGG-3´	(-1/1)[b]	MAX9
T2L20	F5´-GCAACCGCCTCTACAATGTC-3´ R5´-GGTAGAGCTCCTGGCAACTTA-3´	(1/-1)[b]	T2L20
T24H18	F5'-AATCGGTCATGGACAAGGGG-3' R5'-CTAACGTTCGGTGGTTGAGTGTC-3'	(8/-8)[b]	T24H18
T19L5A	F5´-CCAAGAATGAGATGAGCTCT-3´ R5´-GTATGATTAGTGCTCGATCCTC-3´	(-4/4)[b]	T19L5
T31B5	F5'-CAGCTCAATTAATCCCAGTAACC-3' R 5'-CGGTCTCGCAGATACTGTG-3'		T31B5

[a] Clone designation [b] Cereon data base: INDEL

To identify *SHL6* gene, four BACs from within this region, T2L20, T2H18, and T19L5, were partially digested with *Hind*III and *Bam*HI, then randomly subcloned into T-DNA transformation vector, pCambia 3300 (Broothaerts et al., 2005), which contains a BASTA-resistance gene (BAR) as a plant selectable gene and a *kanamycin* resistance gene as a bacterial selection marker (Hajdukiewicz et al., 1994). The set of 65 cosmid-containing sub-clones from BACs T2L20, T24H18, and T19L5 was transformed into *Agrobacterium tumefaciens* GV3101 then transformed into homozygous *shl*6 mutant via the floral dip method (Clough and Bent, 1998). After self-fertilization of these primary (T_0) transformants, BASTA-resistant T_1 plants were selected, and screened for T_2 seedlings showing wild-type phenotypes under a yellow filter (e.g. complementation). In two independent transformations, two adjacent but non-overlapping cosmid clones, designated 4B and 10B, from BAC T24H18, complemented the *shl*6 mutant phenotype (Figure 2.3). 4B contains two hypothetical genes, At5g12990 encoding *CLV3/ESR* 40 (*CLE40*) and At5g13000 encoding glucan synthase. However, At5g13000 gene did not have a promoter or start codon within the 4B clone. Interestingly, only three of seven 4B transformants (43%) complemented homozygous *shl6* mutants (Figure 2.3A).

10B had two complete putative genes, At5g13010 encoding RNA helicase and At5g13020 encoding *EMSY N-terminal (ENT) domain*. The 10B clone also contained nucleotides from the promoter region to the second exon of At5g13000. Unlike 4B transformants, 100% of 10B transformants complemented *shl6* mutants. However, 10B transformants only showed a partial complementation phenotype: hypocotyl length of 10B transformants fell between wild-type (Col-0) and *shl6* mutants (Figure 2.3B).

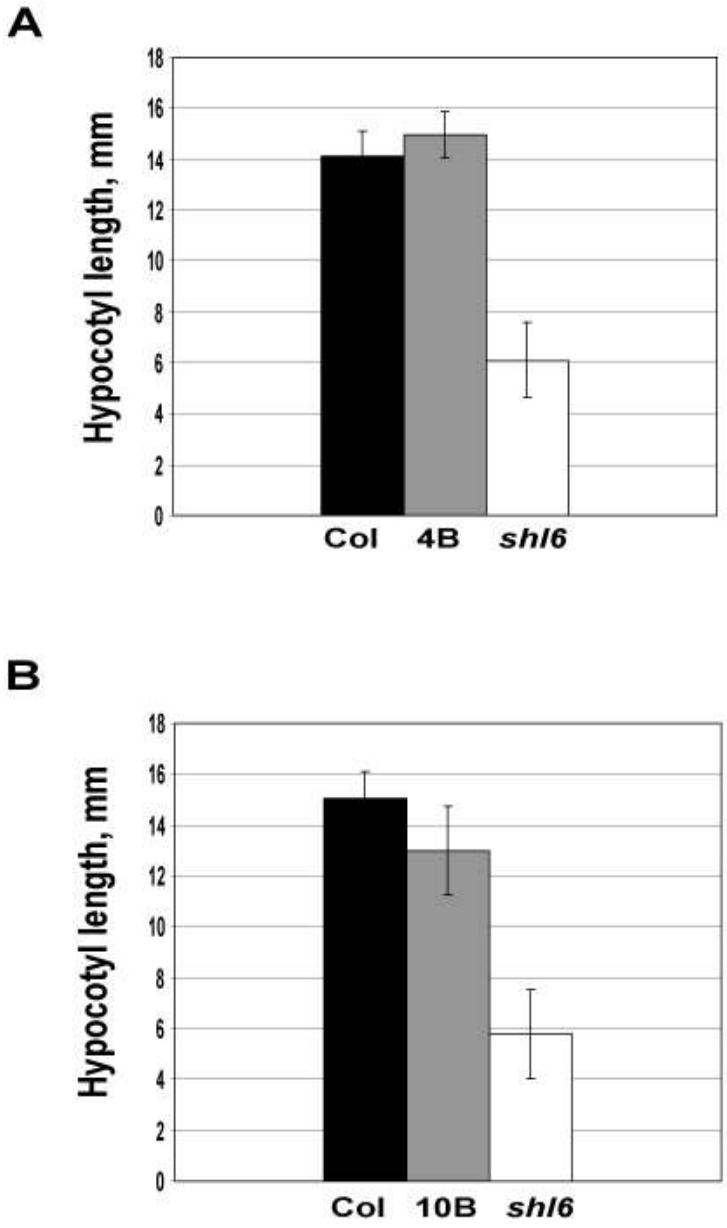

Figure 2.3. Complementation analysis of 4B and 10B cosmid clones

(A) Three of seven (43%) 4B transformants complemented homozygous *shl6* mutants. **(B)** Hypocotyl length of 10B transformants fell between Col-0 and *shl6* mutants. 10B transformants partially complemented shl6 mutants. Data presented are mean ± SE.

To determine whether the *shl6* mutant contained a point mutation in four candidate genes for two cosmid clones (4B and 10B), each 4kb of this whole genomic region (approximately 24kb) from both the *shl6* mutant and Col-0 was amplified by PCR and sequenced via primer walking (Table 2.2). Whereas single strand sequencing of three candidate genes, At5g12990, At5g13010, and At5g13020 yielded no difference between the mutant and Col-0, the only sequencing of Atg13000 revealed that the sequence of *shl6* mutant within this genomic region only differed from Col-0 allele by a single base-pair change (C to T), which caused a predicted proline to leucine amino acid substitution mutation in the first exon of gene At5g13000. The point mutation region of SHL6 protein is highly conserved among 12 homologous genes (GSL1-12) in *Arabidopasis*. The At5g13000 gene is discussed in detail at the end of this chapter.

The verification of 4B and 10B transformant lines

In the previous data, sequencing showed that the missense mutation was only in the At5g13000 gene. Whereas the point mutation was in the portion of the gene contained in the 10B clone, most of the gene is 4B clone. The 10B and 4B clones are not overlapping. To verify that the gene structure of transformed lines 4B and 10B confirm that no Col-0 pollen contamination had covered, we performed PCR with primer sets consisting of one primer from border sequences (LB or RB) of T-DNA vector (pCambia 3300) and the other from genomic sequences using genomic DNA from both 4B and 10B transformants as a template (Figure 2.4A).

Table 2.2. Primers used for sequencing *GSL12*

Primer	Sequence (5´→3´)	Annealing temperature (° C)*	Position[a]
GS-PF	GATTCAGTATGTGCGTGGGATT	64	-1214
GS-1F	CTTTGCGTACTTAGCAGCTAAGTAGC	64	-225
GS-PR	ACAGTGACGAACAGAGATGCAAC	65	-123
GS1-1	GGTTCTGCTTTCTCCCTTAGGTC	64	262
GS1-2	GCTGACAAAGGCATACCAAACTG	66	750
GS1-3	GGCTTCAAGAAATGTTTGGATTTC	65	1197
GS1-4	GATGATCAAGCATTGACAGAAGTG	64	1683
GS1-5	GCTAAGGAGCTATAACTTGCACGC	65	2166
GS-2F	ATTCACAGGAGGCTCAAAGAAGC	66	2653
GS-1R	GACCTTTACGACTGTGTGAAAGC	63	2757
GS2-1	TCGATCGAATGTGGAGCTTCTA	65	3169
GS2-2	GAGTTGGTTTGGGAGTGCTAT	61	3667
GS2-3	GAAGAGTAAGATTCGTGATGAGAC	59	4199
GS2-4	GCCTTGGAGAGGTATGCATTTT	65	4687
GS2-5	GCATTTGGACTATTCATAGGGA	61	5198
GS-3F	AGCCTCTATGATCACTTTGTCAAG	62	5756
GS-2R	ACGAAGATATTGGACCAATTGACA	65	5853
GS3-1	GAACCAGTAACAGAAGCTTGGAA	63	6176
GS3-2	GTTTTCGTTACTTAACTGGTGGGG	65	6704
GS3-3	ACTATCGAAAAGCCTTGGAGC	63	7166
GS3-4	GCCTAAGTCAACTGATCATTCTAC	59	7685
GS3-5	CGTGGAGAAGGTTTACAGACAA	62	8170
GS-4F	CATAGACTCTAACTGATGTCCTCGC	63	8840
GS-3R	CTCAATACAAAACATTGGCAATCC	64	8869
GS4-1	CTCGAACAAGGTTTAAGTACGCA	64	9270
GS4-2	CTATGTGGTTCATGGTCGGGA	66	9706
GS4-3	TCTCAGACTGTTTCGGTTGGAA	65	10219
GS4-4	CGAGATAGTAATGGGACTGTT	63	10583
GS-4R	GAAAGCTTTGTTGTCGCTGTATC	63	11003

[a] Measured in bp from 5'end of primer to the start of predicted experimental transcription
* Calculated by nearest neighbor salt-agusted

The 4B-specific primer pair from 4B clone was used to do PCR with both 4B transformants and 10B transformants. Likewise, the 10B-specific primer set was also used to do PCR with both 4B and 10B transformants. In the 4B transformants, 4B-specific primer pair via PCR amplified an expected 1.4 kb DNA fragment. Artifactual products were amplified in wild-type Col-0 and the same size DNA fragment was also amplified in 10B transformants. 4BR and M13F primers amplified an expected 0.8 kb DNA fragment. In addition, 10BF and M13R primer pair also amplified an expected 1.3 kb DNA fragment and 10BR and M13F primers also amplified an expected 0.7 kb PCR products in 10B transformants. 4B and 10B primer pairs did not amplify their DNA fragments in 10B and 4B transformants, respectively. Therefore, the 4B and 10B clones are adjacent but they are not overlapping. In addition, 4B transformants have only the 4B clone and 10B transformants also contains only the 10B clone (Figure 2.4B).

The previous data revealed the gene spans two clones (4B and 10B), but they are not overlapping. To reject another possibility that *shl6* complementation by 4B and 10B clones may be caused by wild-type Col-0 pollen contamination, we verified that 4B or 10B transformants are in a homozygous *shl6* genotype background. PCR based genotyping was performed. Fortunately, the sequences of *GSL12* provide an important clue to detect homozygous *shl6*. The genomic sequences, ccatC site that is a mutated region in *shl6*, in Col-0 created a *BccI* restrict enzyme site, but ccatC to ccatT change in *shl6* prevented the *BccI* restriction enzyme reaction (Figure 2.5A).

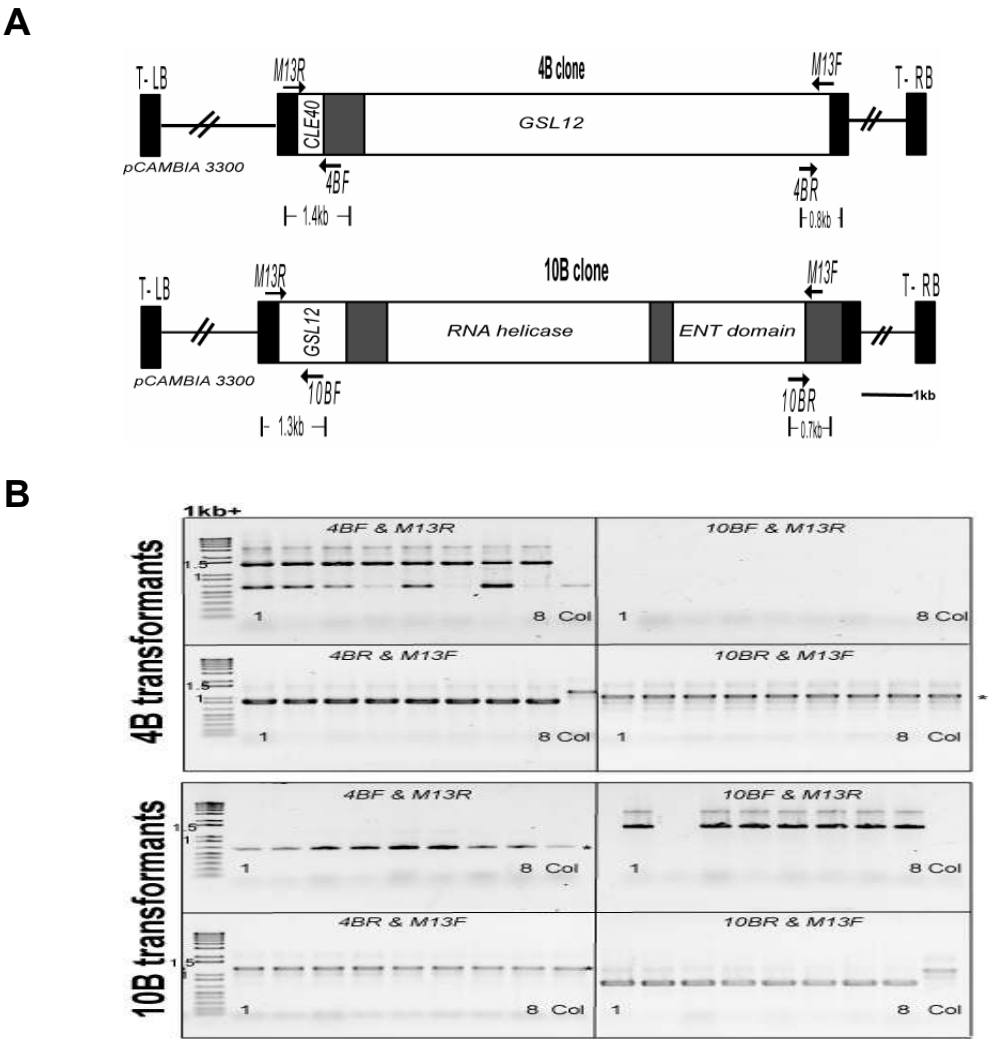

Figure 2.4. Verification of T-DNA insertion of 4B and 10B cosmid clones

(A) Primer sets were designated in 4B and 10B clones. M13F, M13R are from border sequences (LB or RB) of T-DNA vector (pCambia 3300) and 4BF/4BR, and 10BF/10BR are from T-DNA inserted genomic sequences. Bar indicates 1kb.
(B) Each primer set was used for PCR and 1kb^{+}DNA ladder (Invitrogen, USA) was used. In independent eight 4B transformants, 4BF primer pair via PCR amplified 1.4kb DNA fragment. 4BR and M13F primers amplified 0.8 kb PCR products. 10BF and M13R primer pair also amplified 1.3 kb DNA fragment and 10BR and M13F primers also amplified 0.7 kb PCR products in eight independent 10B transformants. Asterisks (*) indicate artificial DNA products. Col-0 and *shl6* were used as controls in the right lanes of a 2% agarose gel.

As a consequence, Col-0 and the *shl6* mutant can be distinguished by *BccI* restriction fragment analysis. BccI-R and BccI-F primers amplified 541bp DNA in Col-0 and 4B transformants containing the polymorphic *BccI* recognition site (Figure 2.5A). After treatment of *BccI* restriction enzyme, Col-0 had 141bp, 204bp and 196bp fragments, and 4B transformants had 141bp and 400bp DNA fragments (Figure 2.5B). 10B transformants were also verified by PCR-based genotyping. After amplifying PCR products with BccI-R-1 and BccI-F, the PCR products were cut by *BccI* restriction enzyme. Col-0 had 5 different DNA fragments including 136bp, 204bp, 406bp, 358bp and 230bp. 10B transformants had 136bp, 610bp, 358bp and 230bp DNA fragments (Figure 2.5B). PCR based genotyping comparisons to Columbia showed both 4B and 10B transformants have homozygous *shl6* backgrounds.

Complementation of the *shl6* mutant with a full length At5g13000 clone

The 4B clone had most of the *GSL12* gene except for the promoter region to the second exon region. The only 10B clone contained the region that is mutated in the first exon of the *GSL12*. Thus, the previous results raise two important questions: (1) how did a small DNA fragment in 10B clone complement *shl6* mutant, and (2) could full-length *GSL12* gene complement *shl6* mutant.

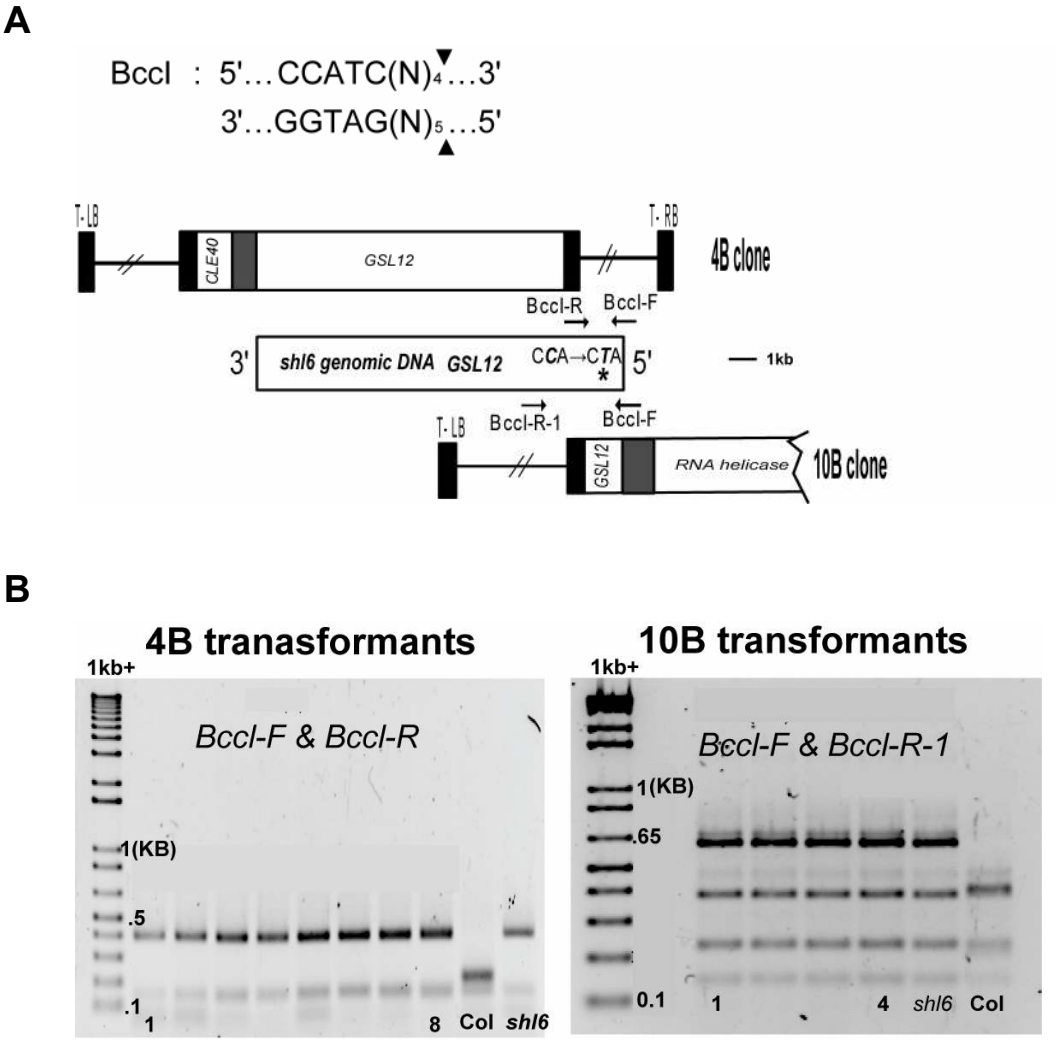

Figure 2.5. Verification of homozygous *shl6* mutant

(A) The genomic sequences, ccatC site that is a mutated region in *shl6*, in Col-0 created a *BccI* restrict enzyme site. BccI-R and BccI-F primers were used for PCR in 4B transformants and Col-0. PCR in 10B transformants and Col-0 was performed by BccI-R-1 and Bcc-F primers. Asterisks (*) indicated a point mutation in *shl6*.
(B) Amplified PCR products in Col-0 and independent eight 4B transformants were treated by *BccI* restriction enzyme. Col-0 had 141bp, 204bp and 196bp, and 4B transformants had 141bp and 400bp DNA fragments. PCR products amplified by BccI-R-1 and BccI-F in Col-0 and independent four 10B transformants were treated by *BccI* restriction enzyme. Col-0 had 5 different DNA fragments including 136bp, 204bp, 406bp, 358bp and 230bp. 10B transformants had 136bp, 610bp, 358bp and 230bp DNA fragments. 204bp and 196 bp DNA fragments were overlapped and they were shown to one band. Col-0 and *shl6* were used as controls in the right of 2% agarose gel.

Eventually, the identification of *SHL6* was confirmed by the complementation analysis of the full-length *GSL12* gene via *Agrobacterium*-mediated plant transformation (Clough and Bent, 1998). To make a full-length GSL12 clone was difficult. Because the length of *GSL12* is approximately 13kb including promoter, we failed to amplify full-length *GSL12* by PCR. Thus, full-length *GSL12* clone was constructed from segment of 4B clone and modified 10B clone. The 10B clone was reconstructed first by partial digestion with *SalI* restriction enzyme, yielding the segment from the promoter to the 2nd exon (1.8kb) of *GSL12* gene (Figure 2.6). This clone was called a re-constructed clone (ReC1). The ReC1 clone was also used to confirm that the small DNA fragment included complemented *shl6* mutant. As a negative control, only vector was transferred into *shl6* plants. The hypocotyls of *shl6*, EV (only vector), ReC1 transgenic, and Col-0 plants were measured under white (110 μmol m^{-2} s^{-1}), yellow (65 μmol m^{-2} s^{-1}), and darkness (Figure 2.7A and B). As a result, interestingly, transformation with the ReC1 clone partially complemented *shl6* in a manner matching the 10B transformants (Figure 2.7C).

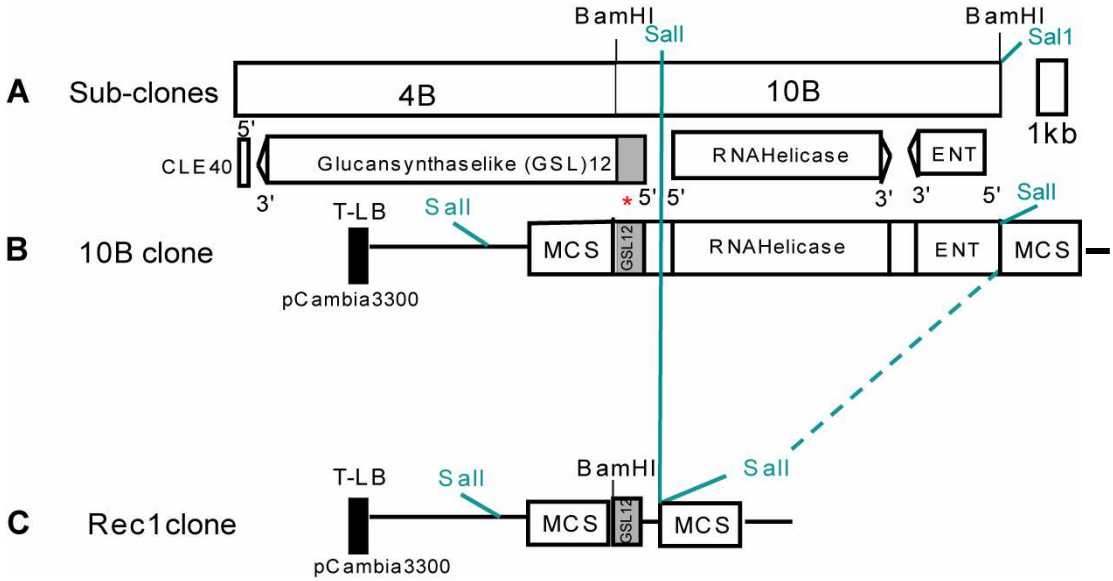

Figure 2.6. ReC1 clone construction

(A) 4B and 10B *BamHI* fragments were sub-cloned in pCambia 3300. Partial *CLE 40* (~0.2 kb) and *GSL12* (~10 kb) were in 4B clone and 10B contained partial *GSl12* fragment (~1.8 kb), full-length *RNA helicase*, and *ENT domain* genes. An asterisk (*) indicates a mis-sense mutation in *shl6*.
(B) The 10B clone was partially digested by *SalI*. RNA helicase and ENT domain were deleted from 10B clone and *GSL12* small fragment (~1.8 kb) was re-ligated. MCS means multiple cloning sites. T-LB (T-DNA left border), and T-RB (T-DNA right border)
(C) Re-constructed clone (ReC) 1 was in pCambia 3300, and transferred into *shl6* mutant plants. T-RB was not shown.

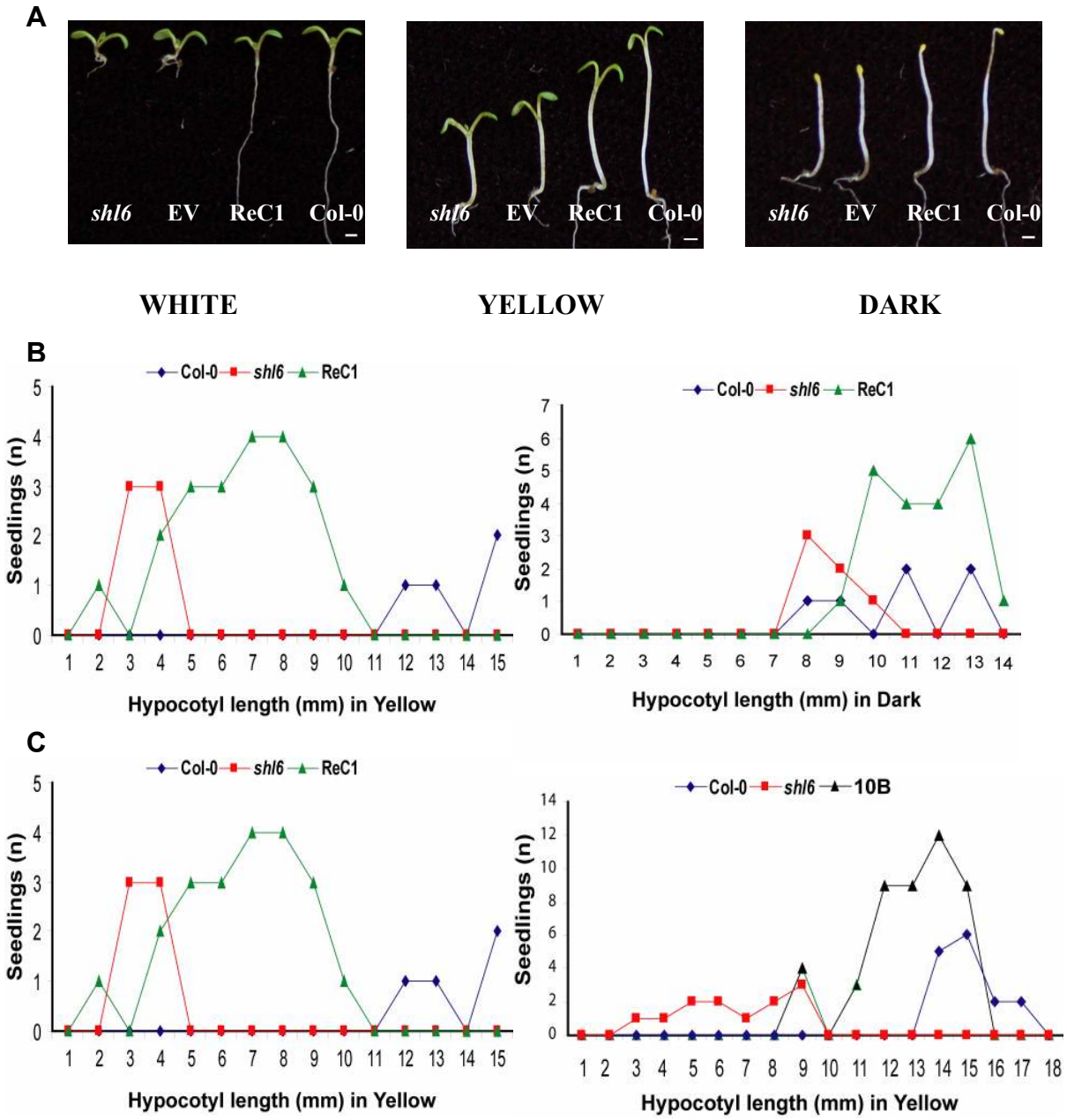

Figure 2.7 Complementation analysis of ReC1 clone

(A) and **(B)** 7-d old *shl6*, EV (no insert: only vector)), ReC1 transgenic and Col-0 seedlings were analyzed under high light (110 μmol m^{-2} s^{-1}), yellow (65 μmol m^{-2} s^{-1}), and darkness.
(C) Hypocotyls of *shl6* seedlings grown under yellow were compared with those of 10B transgenic seedlings. Bars mean 1mm.

Finally, to construct a full-length *GSL12* clone in pCAMBIA 3300, partial *GSL12* fragment from 4B clone was digested by *BamHI*, and then the digested partial *GSL12* fragment was inserted adjacent to the 2nd exon of the *GSL12* gene *BamHI* fragment in the ReC1 clone (Figure 2.8). The orientation of partial *GSL12* fragment was confirmed by *EcoRI* restriction enzyme digestion (Data not shown). Eight independent lines transformed by the GSL12 clone completely complemented *shl6* in low light (Figure 2.9). Therefore, we concluded that this *GSL12* (At5g13000) gene is the *SHL6* gene through the transformation analysis of small DNA fragment and full-length *GSL12*.

SHL6 encodes *Glucan Synthase Like* (*GSL12*) gene

The putative *SHL*6 gene encodes *glucan synthase-like* or *callose synthase-like* (*GSL12*) gene. Through sequence similarity, twelve putative *glucan synthase like* (*GSL1-12*) sequences were revealed over the five chromosomes of *Arabidopsis* (Hong et al, 2001a); the 12 *GSL* genes for these proteins were also annotated independently by a group in Stanford (http://cellwall.stanford.edu/gsl/index.shtml).

GSL1-12 genes have homology with yeast *FK506 hypersensitivity (FKS)* genes, a well characterized β-1,3-glucan synthase (Douglas et al., 1994; Cabib et al., 2001; Dijkgraaf et al., 2002).

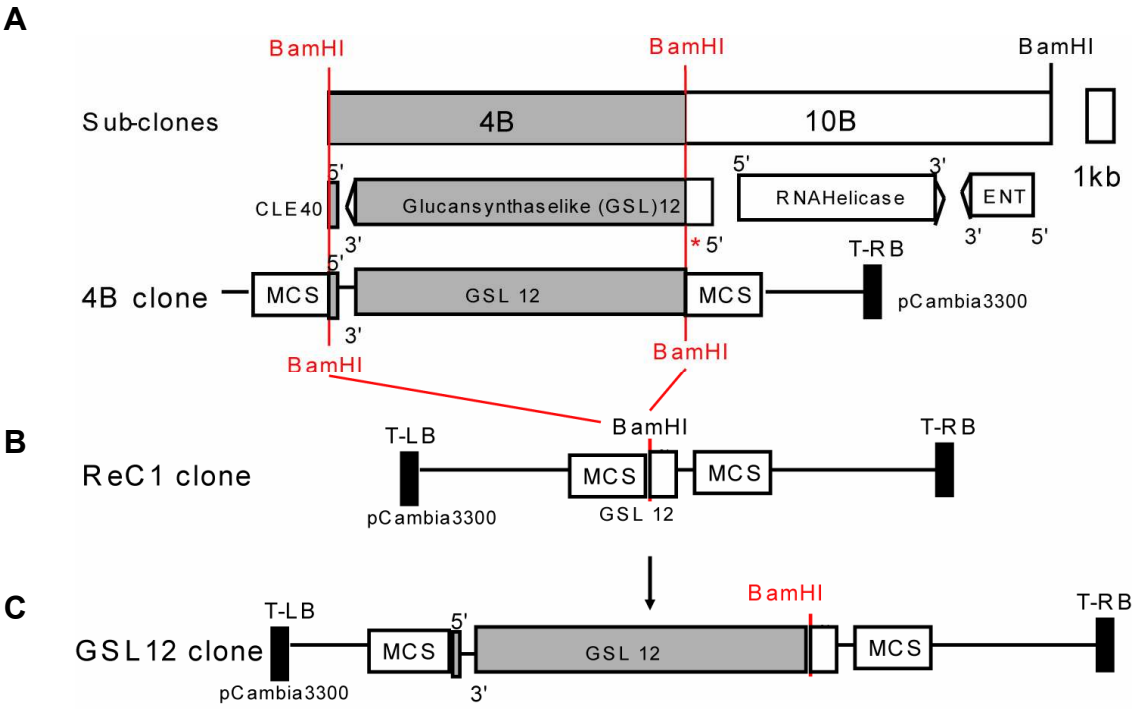

Figure 2.8. Construction of full-length *GSL12* clone

(A) 4B sub-cloned by *BamHI* was digested again by *BamHI* to get partial *GSL12* fragment (~10 kb). An asterisk (*) indicated a point mutation in *shl6*.
(B) ReC1 clone was digested by *BamHI* and then the digested partial *GSL12* fragment was inserted into the region by *BamHI* in the pReC1 clone.
(C) Full-length *GSL12* clone was transferred to *shl6* plants via *Agrobacterium*-mediated transformation. MCS means multiple cloning sites. T-LB and RB mean T-DNA left and right borders.

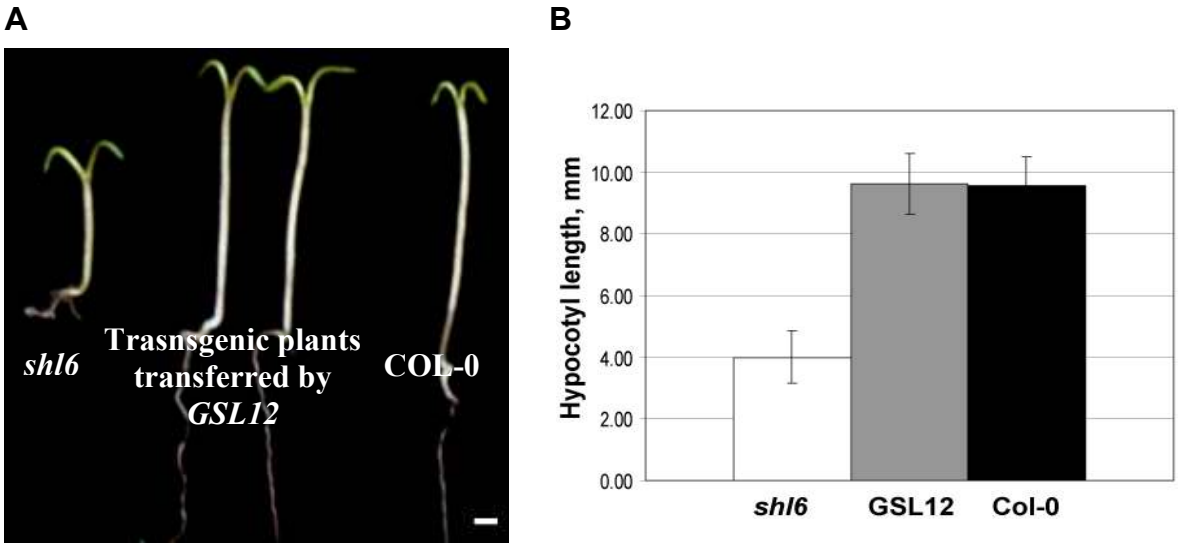

Figure 2.9. Complementation analysis of *GSL12*

(A) 7-d old *shl6*, GSL12 transgenic and Col-0 seedlings were analyzed under yellow (65 μmol m^{-2} s^{-1}). A bar = 1mm.
(B) Hypocotyls of *shl6* seedlings grown under yellow filter were compared with those of Col-0 seedlings. Data presented are mean ± SE.

Partial alignment of the predicted amino acid sequences of the 12 members performed by ClustalW 1.83 suggested that the *shl6* missense mutation alters a highly conserved motif, a proline-rich domain (PRD) (Prosite file, PS50099) (Figure 2.10A). *GSL* genes in *Arabidopsis* are separated into two groups, one made of genes containing 2-3 exons (*GSL1*and *GSL5*) and the other up to 50 exons (*GSL 2,3,4,6,7,8,9,* and *10*). Phylogenetic comparisons suggest that GSL12 is more closely related to GSL6, 3 and 9 (http://cellwall.genomics.purdue.edu) (Figure 2.10B).

The predicted protein structure for SHL6 is shown in Figure 2.11. *GSL12* is approximately 11.3kb in length, has 42 exons based on AGI gene models, and encodes an 1889-amino acid protein with a predicted molecular mass of approximately 217 kD. Hydropathy analysis of GSL12 using the Kyte-Doolittle method indicated that it is an integral membrane protein with 11 transmembrane helices (http://workbench.sdsc.edu) (Figure 2.11A). The N terminus (501 amino acids) is hydrophilic and lacks an apparent cleavable signal sequence. The predicted protein domain analysis (http://www.ebi.ac.uk and http://pfam.sanger.ac.uk) indicates that the N- terminus (91-189 amino acids) includes a *histidine-containing phosphotransfer* (HPT) domain, and the C-terminus (1076-1876 amino acids) has a *glucan_synthase* domain (Figure 2.11B).

A

```
GSL6_          ----------MAQRREPD----PPPPQRRILRTQ-------------TVGSLGEAMLDSE 33
GSL3_          ----------MAQRKGPD----PPPPQRRILRTQ-------------TAGNLGEAMLDSE 33
GSL9_          ----------MNQ----------PNRGQILQTV-------------FSHFFPVASPDSE 26
GSL12_         ----------MSATRGGPDQGPSQPQQRRIIRTQ-------------TAGNLGES-FDSE 36
GSL2_          ----------MAQSSTSHD--SGPQGLMRRPSRS-------------AATTVSIEVFDHE 35
GSL7_          ----------MASTSSGGRGEDGRPPQMQPVRSMSRKMT-RAGTMMIEHPNEDERPIDSE 49
GSL11_         ----------MEASSSG---------TAELPRSLSRRAPSRATTMMIDRPNEDASAMDSE 41
GSL4_          MSHEIVPVDPIDVPSTSYSRPILGPREDSPERATEFTRS------LTFREHVSSEPFDSE 54
GSL1_          ------------------------------------------------------------
GSL5_          ------------------------------------------------------------
GSL8_          ------------------------------------------------------------
GSL10_         ----------MSRAESSWERLVNAALRRDRTGGV-------------AGGNQSSIVGYV 36

                         *
GSL6_          VVPSSLVE-IAPILRVANEVEASNPRVA--YLCRF----------------YAFEKAHRL 74
GSL3_          VVPSSLVE-IAPILRVANEVEASNPRVA--YLCRF----------------YAFEKAHRL 74
GSL9_          LVPSSLHEDITPILRVAKDVEDTNPRSL--FLQDLDIKSVDDSINILSGHSHALDKANEL 84
GSL12_         VVPSSLVE-IAPILRVANEVESSNPRVA--YLCRF----------------YAFEKAHRL 77
GSL2_          VVPASLGT-IAPILRVAAEIEHERPRVA--YLCRF----------------YAFEKAHRL 76
GSL7_          LVPSSLAS-IAPILRVANDIDQDNARVA--YLCRF----------------HAFEKAHRM 90
GSL11_         LVPSSLAS-IAPILRVANEIEKDNPRVA--YLCRF----------------HAFEKAHRM 82
GSL4_          RLPATLASEIQRFLRIANLVESEEPRIA--YLCRF----------------HAFEIAHHM 96
GSL1_          ------------------------------------------------------------
GSL5_          ------------------------------------------------------------
GSL8_          ----------------------------------------------------MAQNL 5
GSL10_         PSSLSNNRDIDAILRAADEIQDEDPNIARILCE------------------HGYSLAQNL 78
```

B

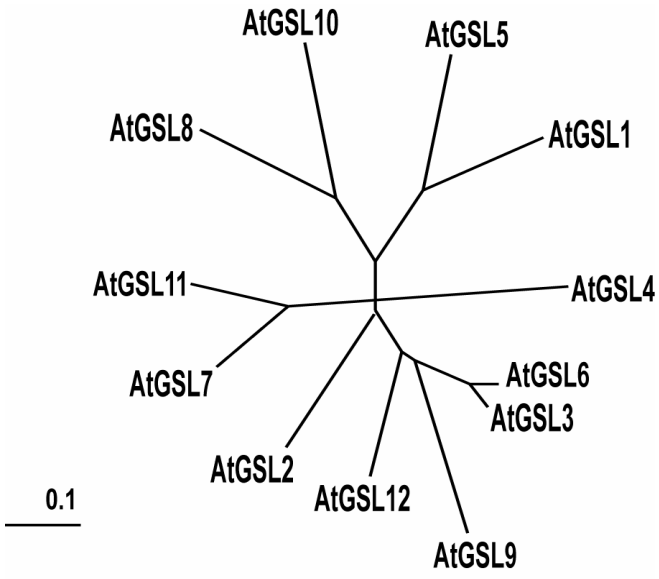

Figure 2.10. Structure of the SHL6 protein

(A) Partial alignment of the predicted amino acid sequences of the 12 members of the *Arabidopsis* GSL family. Asterisk (*) indicates position of the *shl6/gsl12* mutation. Multiple alignment of GSL amino acid sequences were done by ClustalW 1.83.
(B) Phylogenetic tree of putative GSL proteins from *Arabidopsis*. Bar indicated 0.1 substitutions per site.

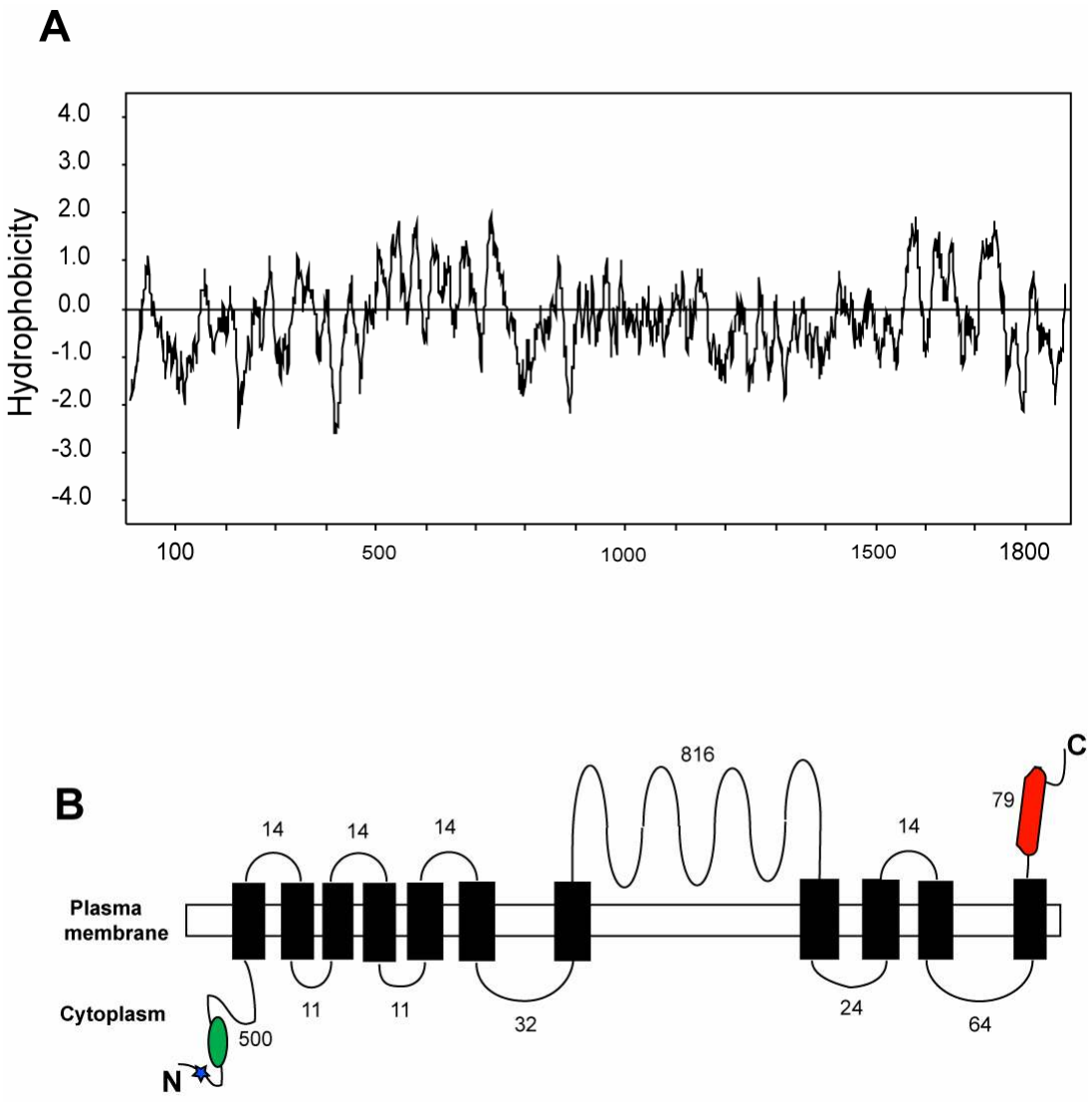

Figure 2.11. Predicted transmembrane topology model of AtGSL12 protein in a plasma membrane

(A) Hydropathy analysis of GSL12 indicated that it is an integral membrane protein with 11 transmembrane helices by using Kyte-doolittle method.
(B) The predicted protein domain analysis displayed that solid black rectangles indicated predicted transmembrane domains. A green circle indicates a histidine-containing phosphotransfer, HPT, domain (91-189 amino acids) in the N- terminus, and red rectangle indicates a glucan_synthase domain (1076-1876 amino acids) in the C-terminus. A blue star indicates the mutated position in *shl6.*

Discussion

In this study we describe the isolation and characterization of the *Arabidopsis shl6* mutant hyper-responsive to light. We used a map-based cloning to locate the *SHL6* gene and identified that complementation places *SHL6* in the glucan synthase family.

Identification of *SHL6*

To identify photomorphogenetic mutants that are hyper-responsive to available light, fifteen mutants were isolated from ethyl methane sulfonate (EMS) mutagenized plants (Columbia ecotype) screened under low light (Pepper et. al, 2001). Using a map-based cloning strategy, we have shown that *shl6* is a single recessive mutation, causing a high-light growth phenotype: short hypocotyl, open cotyledons, and early development of the first true leaves in plants grown under low light (Figure 2.1). Homozygous *shl*6 plants also showed short, highly branched roots (Figure 2.1C). The genomic interval containing the *shl*6 locus was narrowed to a 235Kb genomic fragment spanned by bacterial artificial chromosome BAC clones T2L20, T2H18, T19L5, and T31B5 through fine linkage mapping (Figure 2.2A). Surprisingly, independent transformations with two different cosmid clones designated 4B and 10B from BAC T24H18 that include adjacent but non-overlapping sequences, complemented the *shl*6 mutant phenotypes (Figure 2.2B).

Sequence analysis of this genomic region for the two cosmid clones via primer walking showed that the sequence of *shl6* mutant within this genomic region only differed from wild type Columbia allele by a single nucleotide substitution, which

caused a proline to leucine amino acid substitution mutation in the first exon of gene At5g13000 that encodes a *glucan synthase-like (GSL) 12* gene. GSL12 is a putative callose synthase and unknown protein. Interestingly, the 4B cosmid contains a 5' truncated region of *GSL12* gene, deleted from the promoter to the second exon. 10B cosmid has the promoter region through the second exon of *GSL12*. Three of seven (43%) 4B transformants occasionally complemented homozygous *shl6* mutants. While the 10B fragment usually complemented, the hypocotyl phenotype of 10B transformants was intermediate between wild-type (Col-0) and *shl6* mutants. The 10B transformants partially complemented *shl6* mutants (Figure 2.3). We suggest that the complementation with this 4B clone is induced by the endogenous promoter of some gene close to 4B fragment. The reason is that less than 50% of 4B transformants have BASTA-resistance, but they were not complemented to wild type phenotype. In contrast, all 10B transformants containing BASTA-resistance partially complemented *shl6* mutants.

Therefore, we concluded that two independent, not overlapping cosmid clones (4B and 10B) complemented *shl6* mutant (Figure 2.4-5). *shl6* mutant complemented by a small DNA fragment of ReC clone (Figure 2.7) may be explained by *α-complentation*. The *E. coli* enzyme β-galactosidase is a homo-tetramer of the protein product of the *lacZ* gene. Certain mutations in the 5' region of *lacZ* prevent subunit association. This enzyme is *non-functional* (it will not hydrolyze lactose or other -galactosides). In this type of mutants, subunit assembly (and enzyme activity) is restored by the presence of a small (26 amino acids) amino-terminal fragment of the *lacZ* product (Yanisch-Perron et al., 1985). However, it is still unknown how the small DNA fragment can function.

Finally, full-length *GSL12* gene complemented *shl6* mutant. The P39L amino acid change inhibited hypocotyl and root elongation in *shl6* mutant under yellow. The point mutation region may be a significant motif to regulate hypocotyl and root elongation.

SHL6/GSL12 protein is a putative transmembrane protein

SHL6 encoding *GSL12* lacks an apparent cleavable signal sequence and hydrophilic in N terminus (501 amino acids) (http://workbench.sdsc.edu). The predicted protein domain analysis (http://www.ebi.ac.uk and http://pfam.sanger.ac.uk) displayed that the N- terminus (91-189 amino acids) includes a histidine-containing phosphotransfer (HPT) domain and the C-terminus (1076-1876 amino acids) has a glucan_synthase domain. *GSL* genes have similar homology with yeast *FK506 hypersensitivity (FKS)* genes, a well characterized β-1,3-glucan synthase family (Douglas et al., 1994; Cabib et al., 2001; Dijkgraaf et al., 2002). Multiple alignment of the predicted amino acid sequences of the 12 members performed by ClustalW 1.83 suggested the position of the *shl6* mutation was within a highly conserved motif, proline-rich domain (PRD) (Prosite file, PS50099) (Figure 2.10A). It is also suggested based on the *shl6* phenotype that the mutation in the conserved PRD may be involved in hypocotyl and root development.

A phylogenetic tree of twelve putative GSL proteins suggested that GSL12 is more closely related to GSL6, 3 and 9 (http://cellwall.genomics.perdue.edu) (Figure 2.10B). Callose synthase and related genes have not been previously implicated in

developmental responses to light. How *GSL12* is involved in light signaling is addressed in the next chapter.

Materials and methods

Plant materials and growth conditions

Arabidopsis ecotype Col-0 seeds were obtained from the laboratory stocks of Joanne Chory. *shl6* mutant was isolated from ethyl methane sulfonate (EMS) mutagenized plants (Col-*gl*) screened under low light (Pepper et al., 2001). *shl6* was back-crossed twice to wild-type Col-0 and homozygous *shl6* mutant was isolated by their short hypocotyls in yellow light (65 μmol m^{-2} s^{-1}). Seeds were surface-sterilized (Chory et al, 1989), resuspended in sterile 0.1% (w/v) phytagar, and then stored overnight at 4 °C. Seeds were then plated on Murashige-Skoog plates (1x Murashige-Skooge salts, 0.8% phytagar, 1XGamborg's B5 vitamin mixture, 2% (w/v) sucrose). Seeds were placed at 25 °C for at least 4h in white light (100 μ $molm^{-2}s^{-1}$) and then grown in continuous yellow light (65 μmol m^{-2} s^{-1}) for 7 days.

Hypocotyl measurements

For hypocotyl length measurements, seeds were dispersed onto Murashige and Skoog plates containing 2% (w/v) sucrose in a 7 mm grid pattern to ensure even spacing. Seeds were placed at 25 °C for at least 4h in white light (100 μ $molm^{-2}s^{-1}$) prior to placement in continuous white light (100 μ $molm^{-2}s^{-1}$), low light (30μ$molm^{-2}s^{-1}$) and the dark for 9 days. Hypocotyl length is determined as the distance between the top of the

collet root hairs, to the 'V' made by the cotyledon shoulder (Scheres et al., 1994). Hypocotyls were straightened using forceps if necessary, and then were measured by using a 0.5mm scale ruler, and the mean ± SE calculated for each data set. Hypocotyls of seedlings that were growing appressed to the agar media, as well as those with obvious developmental abnormalities, were not measured.

Light source

White light was supplied by an equal mixture of cool-white (CW) and Grow-lux wide-spectrum fluorescent bulbs (Sylvania, Danvers, MA). A 2472 yellow-green acrylic filter (Polycast Technology, Stamford, CT) with a transmission maximum of ±550 produced light that was partially depleted in the photomorphogenetically active UV, B, R, and FR regions of the spectrum. Dark experiments were performed in a passively ventilated dark box. Red light was supplied by CW fluorescence bulbs filtered through a Kopp 2-73 red glass filter (Kopp Glass, Pittsburgh, PA, USA). Blue light was supplied by CW fluorescent bulbs filtered through a Kopp 5-57 blue filter. Far-red enriched light was provided by a 60W incandescent bulb filtered through a Kopp 2-64 glass filter (R/FR ratio of ± 0.32). Fluence rates of white, R, and B light were measured with a quantum photometer (model LI-189, LI-COR, Lincoln, NE). Fluence rates of FR light were measured using a radiometer (model IL1400, International Light, Newburyport, MA) with FR probe (model SEL033, International Light).

Mapping

Homozygous *shl6* plants in Col-0 background were crossed as females to wild-type Ler-er. F_1 progeny were scored and several F_1 plants exhibiting long hypocotyl plants under low light were self-pollinated to obtain a F_2 progeny. Genomic DNA was isolated from F_2 progeny exhibiting short hypocotyl plants using the micropreparation method described by Pepper and Chory (1997). Initial mapping of *shl6* mutant was performed using simple sequence length polymorphic (SSLP) markers from The *Arabidopsis* Information Resource (http://www.arabidopsis.org; Bell and Ecker, 1994; Lukowitz et al., 2000) and the PCR-based Cleaved Amplified Polymorphic Sequence (CAPS) (Konieczny and Ausubel, 1993) markers. Additional markers for fine mapping were generated based on the information made available by CEREON (Jander et al., 2002). Publicly available *Arabidopsis* sequence and *Arabidopsis* BAC fingerprint database were used to tile the *shl6* interval with BACs and develop additional PCR-based markers (http://www.tigr.org/tdb/at/at.html, and http://www.arabidopsis.org). DNA was amplified in 20-μL reactions as described by Bell and Ecker (1994).

Analysis of SSLP amplification products was performed using 2% standard agarose plus 2% Metaphor® agarose (Cambrex, North Brunswick, NJ, USA) gels. Samples were electrophoresed at 5.3 V cm^{-1} in 0.5× TBE buffer (45 mM Tris-Borate, 1 mM EDTA, pH 8), with buffer-chilling to 4 °C. When high resolution was required, we employed a vertical acrylamide gel electrophoresis system in which samples were electrophoresed at 12 V cm^{-1} in a 10 cm high × 33 cm wide × 1 mm thick vertical gel rig (CBS Scientific, Del Mar, CA, USA) containing 7% polyacrylamide with 10% v/v

Spreadex NAB polymer® (Elchrom Scientific, Cham, Switzerland) in 1× TAE buffer (45 mM Tris-Acetate, 1 mM EDTA, pH 8).

Sequence analysis

To sequence the *shl6* mutant allele, PCR fragments (approximately 3kb) were amplified from genomic DNA of the *shl6* mutant and Col-0 to be used as templates for direct sequencing. The PCR reaction was used along with *TaKaRa LA Taq*™ polymerase (TaKaRA) that has a superior proofreading function due to a robust 3´-> 5´exonuclease activity. Purified PCR products (Qiagen PCR purification kit) were used for sequencing reactions using the BigDye™ (Applied Biosystems) protocol. Primers (Table 2.2) were designed to produce overlapping sequencing products (approximately 500bp) at ~3kb intervals. Sequencing reactions were purified by Sepadex G-50 spin columns and the purified sequencing reactions were analyzed by using an Applied Biosystems 3100 capillary DNA sequencer. The single base difference between SHL6 and *shl6* was confirmed by re-sequencing from the Col-0 and *shl6* templates.

Complementation analysis

To test complementation, the first clone (pRC) was re-constructed by *SalI* digestion yielding from the promoter to the 2nd exon (1.8kb) of *GSL12* gene that the 10B contains. Thus, the pRC clone was constructed by deletion the rest of the fragment except for the promoter region and the second exon region of the *GSL12* from inserted genomic sequences of the 10B clone. The second clone (pGSL12) has the full-length of

the *GSL12* genomic sequence (13kb) of Columbia. To make pGSL12 clone into pCAMBIA 3300, partial *GSL12* fragment in 4B clone was digested by *BamHI*, and then the digested partial *GSL12* fragment was inserted into the next to the 2nd exon of the *GSL12* gene digested by *BamHI* in the pReC1 clone (Figure 2.6). Two reconstructed clones (pRC and pGSL12) were moved into *Agrobacterium tumefaciens* GV3101 (Koncz et al., 1983) by electroporation, and were used to transform *Arabidopsis shl6/shl6* mutants via the floral dip method (Clough and Bent, 1998). Primary seeds from transformed plants were planted to soil and were selected by BASTA after 8weeks. For hypocotyl analysis, T_2 seeds harvested from selected BASTA-resistant *shl6* plants were dispersed onto MS plates containing 2% (w/v) sucrose. T_2 seeds were placed at 25 °C for at least 4h in white light (100 μ $molm^{-2}s^{-1}$) prior to placement in low light (30μ$molm^{-2}s^{-1}$) for 9 days.

CHAPTER III

MOLECULAR CHARACTERIZATION OF *SHL6*

Introduction

Our laboratory has identified a new third set of photomorphogenic mutants in *Arabidopsis* that are hyper-responsive to available light, designated as *seedling hyper-responsive* to *light* (*shl*) (Pepper et. al, 2001). In low light, *shl* seedlings showed a phenotype typical of seedlings grown in high-light, with short hypocotyls, expanded cotyledons, and significant development of first true leaves when grown in low light. One of *shl* mutants, *shl*6 was isolated by screening mutagenized seed lines under a yellow filter.

In the previous chapter, we mentioned that *shl6* was caused by a single recessive mutation. In yellow light (65 μmol m^{-2} s^{-1}), s*hl*6 seedlings have short hypocotyls, expanded cotyledons, and well-developed first true leaves. In addition, the roots of *shl6* were short and highly branched in all light conditions. *shl6* mutant was mapped to the region of chromosome 5 between SSLP markers *nga249* and *nga151*. Further, the sequence of *shl6* mutant revealed that a single base-pair was different from Col-0 allele, which caused a predicted proline to leucine amino acid substitution mutation in the first exon of a glucan *synthase-like 12* (*GSL12*) gene (At5g13000). Finally, *SHL6* was identified by the complementation analysis of the full-length *GSL12* via *Agrobacterium*-

mediated plant transformation (Clough and Bent, 1998). We concluded that *SHL6* encodes *GSL12* (At5g13000) gene.

In this chapter, we showed that *SHL6* is regulated by light via several approaches. Light is also an important factor for transition from vegetative to reproductive growth, called flowering time because the timing of flowering is strictly modulated by the direction, intensity, color, and duration of light (Simpson and Dean, 2002). *Arabidopsis* is a facultative long-day plant because flower initiation is accelerated under long-day photoperiod but delayed under short-day photoperiod (Searle and Coupland, 2004).

The molecular mechanism of flowering regulation by light has been well described in *Arabidopsis*. The flowering time is partially regulated by the CONSTANTS (CO; a zinc finger transcriptor factor) protein that plays a critical role in the photoperiodic flowering pathway. The abundance of *CO* mRNA was reduced in *phyA* and *cry2* mutants but was increased in *phyB* mutant (Cerdan and Chory, 2003). It has been recently suggested that CO protein is subject to posttranscriptial regulation by light signals, and different photoreceptors act in modulating of CO activity (Valverde et al., 2004). In this model, CRY2 and PHYA stabilize the CO protein under blue and far-red light, but PHYB destabilizes CO protein under red light to generate the shade avoidance response. The stabilized CO induces the expression of another flowering regulator, FLOWERING LOCUS T (FT; a small protein with similarity to RAF-kinase inhibitor), which is the proximal inducer of flowering (Kardailsky et al., 1999; Kobayashi et al., 1999).

Furthermore, we also examined responses induced by red, far-red, and blue light in wild type (Col-0) and *shl6* mutant seedlings to determine whether the *shl6* mutants have

altered hypocotyl morphology in a particular wavelength of light. To examine whether transcript levels of *SHL6* are regulated in Col-0 and *shl6* seedlings grown under dark, yellow, red, and high light, the mRNA levels of *SHL6* was examined by quantitative RT-PCR, using gene-specific primers. Flowering time as a developmental process involved by light was observed in *shl6* compared with Col-0 plants. Finally, we determined whether transcript levels of *SHL6* are regulated by organ specificity in seedlings by using quantitative RT-PCR.

Results

shl6 mutant exhibits hyper-responsiveness to multiple wavelength conditions in seedling development

In the previous experiments, the hypocotyl length of 7-d-old *shl6* mutant and wild type (Col-0) seedlings grown under dark, white (110 μmol m^{-2} s^{-1}), and yellow (65 μmol m^{-2} s^{-1}) were measured (Figure 2.1). The hypocotyl elongation of *shl6* mutants was significantly inhibited and the first true leaf of *shl6* developed earlier than Col-0 under yellow light. s*hl6* had an etiolated phenotype, but with only partially inhibited hypocotyl elongation under dark conditions.

To determine whether the *shl6* mutants have altered morphology in response to a particular wave length among blue, red, and far-red light that could be related to CRY and PHY, we examined the growth of 5-d-old seedlings under multiple wave lengths such as red, far-red, and blue light. As a result, the red, far-red, and blue light conditions induced a reduction in the hypocotyl elongation of the *shl6* mutant compared with Col-0 and the *shl6* mutant seedlings also showed shorter hypocotyls compared with Col-0 seedlings over the ranges of red, far-red, and blue fluence rates (Figure 3.1A).

To determine which light wavelengths more significantly affect the hypocotyl elongation of the *shl6* mutant, the hypocotyl length of *shl6* and Col-0 in red, far-red and blue light conditions was normalized to the hypocotyl length of *shl6* and Col-0, respectively in the dark. Differences of the normalized *shl6* hypocotyls from normalized Col-0 hypocotyls showed an average of 27.5 % reduction in red, 20 % reduction in far-red, and 17.5 % reduction in blue light (Figure 3.1B). Thus, this normalization data suggested *shl6* seedlings exhibited most hyper-responsiveness to red light.

Figure 3.1. *shl6* hyper-responsive hypocotyl growth in red, far-red, and blue light

(A) Hypocotyl growth response of 5-d-old Col-0 and *shl6* mutants under various fluence rates of constant red, far-red, and blue light. Data are presented as mean±SE (n=28).
(B) Hypocotyl lengths were normalized to hypocotyl length in the dark under various flucence rates of constant red, far-red, and blue light. Each point represents the normalized mean ± SE of the seedlings grown for 5 d. Red, blue, and far-red light fluences are measured in μmol m^{-2} s^{-1} unit. Error bars represent the SE after each *shl6* and Col-0 seedling was normalized to the average hypocotyls length of *shl6* and Col-0 seedlings, respectively grown in the dark.

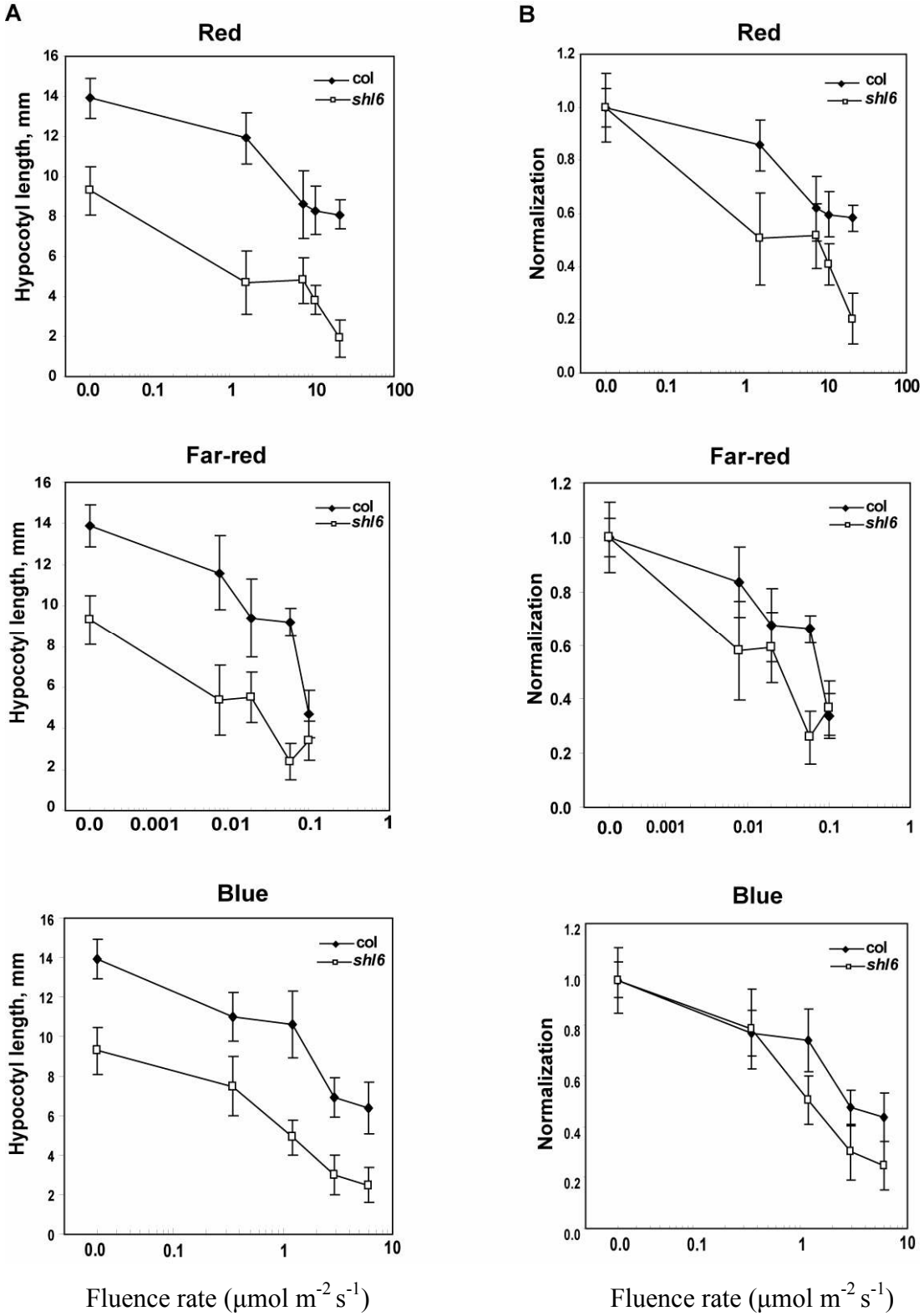
A
Red
Hypocotyl length, mm
col
shl6
0.0
0.1
1
10
100
Far-red
0.001
0.01
Blue
Fluence rate (µmol m-2 s-1)
B
Red
Normalization
Far-red
Blue
Fluence rate (µmol m-2 s-1)

SHL6 transcript accumulation is light-regulated

In the dark, Col-0 seedlings follow etiolation, which is characterized by hypocotyl elongation, an apical hook, undeveloped cotyledons and inhibition of chlorophyll and anthocyanin biosynthesis. Once the seedlings are exposed to light, they follow photomorphogenesis; the hypocotyl stops elongation, and true leaves begin to develop. When plants are exposed to natural light, light is perceived by several photoreceptors including the UVA and blue light-absorbing phototropins and cryptochromes, and the phytochromes which mainly absorb red and far-red (Gyula et al., 2003**;** Yamamoto et al., 1998; Quail et al., 1995). Thus, we examined whether transcript levels of *SHL6* are regulated during etiolation and photomorphogenesis in 5-d-old Col-0 seedlings grown under dark, white (110 μmol m^{-2} s^{-1}), yellow (65μmol m^{-2} s^{-1}), and red (22μmol m^{-2} s^{-1}) light by quantitative real time reverse transcriptase (RT)-PCR, using a gene-specific primer pair. The *SHL6* transcript levels were found to be induced two-fold in Col-0 seedlings grown in the dark compared to light-grown seedlings grown in different light conditions such as white, yellow, and red light (Figure 3.2A).

In the previous experiments, we examined the hypocotyl growth responses of Col-0 and *shl6* to red, far-red, and blue light at a relatively broad range of light intensities and showed that *shl6* seedlings were hyper-responsive to red, far-red, and blue light conditions (Figure 3.2A). However, red light had a greater effect on *shl6* hypocotyl growth after normalization (Figure 3.1B). Therefore, we next determined whether *SHL6* expression was altered in 5-d-old *shl6* seedlings. qRT-PCR analysis showed that the transcript level of *SHL6* in the *shl6* mutant was reduced more in dark

and red than in Col-0, but *SHL6* mRNA expression levels in *shl6* seedlings grown in white, and yellow light were similar to those in the Col-0 seedlings, even hypocotyl elongation of the *shl6* mutant was more reduced than that of Col-0. To confirm that the expression of *SHL6* mRNA is responsible for transgenic GSL12 complemented by a full-length *SHL6*, qRT-PCR was performed in the same light conditions (Figure 3.2B). The reduction in transcript accumulation in *shl6* mutants was eliminated by GSL12 transgenic seedlings and the expression of mRNA in transgenic GSL12 seedlings was higher than that in Col-0 because transgenic GSL12 plants contain both the endogenous genomic *GSL12* gene and exogenous *GSL12* DNA fragment from T-DNA insertion (Figure 3.2B). The expression levels (ΔCt) of the *SHL6* transcript were calculated by subtracting the C_t for *EF1a* primer from each C_t for tissue samples (Table 3.1). Higher -Δ C_t values for *SHL6* in dark, white, yellow, and red light indicated higher expression of *SHL6* because the *SHL6* transcript was more highly expressed than control *EF1a* gene.

Table 3.1. C_t values for genes analyzed using RT-PCR

		Col-0		*shl6*		GSL12	
Gene	Treatment [a]	Average C_t [b]	StDv[c]	Average C_t	StDv	Average C_t	StDv
SHL6/GSL12	Dark	27.65	0.11	26.69	0.15	26.47	0.44
	Yellow	26.25	0.18	26.11	0.06	25.60	0.20
	Red	26.25	0.05	25.65	0.09	25.68	0.20
	White	26.76	0.10	26.16	0.04	25.01	0.09
EF1a	Dark	29.76	0.23	28.13	0.30	29.69	0.48
	Yellow	27.09	0.11	27.05	0.05	27.69	0.09
	Red	27.20	0.11	26.02	0.05	28.61	0.27
	White	27.73	0.14	27.26	0.14	27.22	0.11

[a] Dark (0µmol m^{-2} s^{-1}), Yellow (65µmol m^{-2} s^{-1}), Red (22µmol m^{-2} s^{-1}), and White (110µmol m^{-2} s^{-1})

[b] Average Ct Values for 3 replicates

[c] Standard Deviation for 3 replicates

A

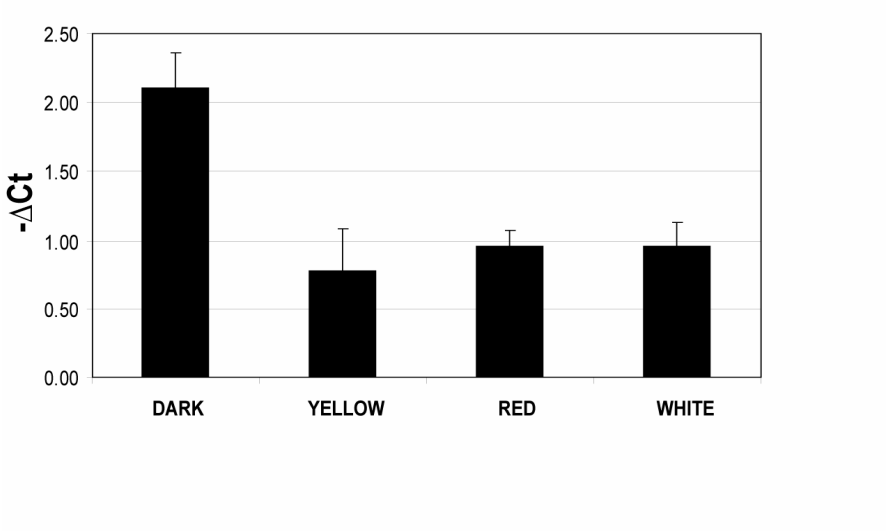

B

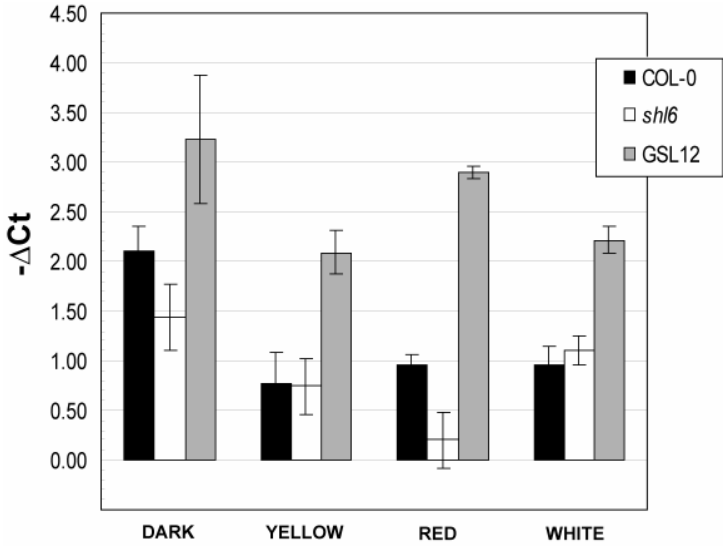

Figure 3.2. Expression levels of *SHL6*

(A) and **(B)** mRNA expression levels of *SHL6* in 5-d-old Col-0, *shl6*, and transgenic GSL12 seedlings under different light conditions including yellow (65μmol m^{-2} s^{-1}) red (22μmol m^{-2} s^{-1}), and white (110μmol m^{-2} s^{-1}). Expression of genes was analyzed by qRT-PCR reactions. Higher a -Δ C_t value for *SHL6* mRNA indicated higher an expression level because the *SHL6* transcript was more highly expressed than control *EF1a* gene. Error bars indicate standard deviation of Δ C_t values calculated by $(\sigma^2_{\text{gene}} + \sigma^2_{\text{control}})^{1/2}$.

The *shl6* plants flower early in both long and short days

Flowering time is strictly modulated by the direction, intensity, color, and duration of light (Simpson and Dean, 2002). *Arabidopsis* is a facultative long day plant that flowers earlier in long day (16-h light/8-h dark) than in short days (8-h light/16-h dark). To determine whether *SHL6* is involved in the regulation of flowering time, the *shl6* mutant plants were compared to Col-0 during growth under both long-days and short-days, respectively. We found that *shl6* plants flowered earlier than Col-0 plants in both long and short days (Figure 3.3). Whereas wild type plants started flowering after the formation of 15±1.1 leaves, the *shl6* mutants flower after producing 9.6±1.1 leaves in long-days. The *shl6* mutant plants started flowering after 30±2.6 leaves and Col-0 plants flower after producing 37± 4.8 leaves in short days. The data of *shl6* in short-days showed significantly earlier flowering compared with Col-0 (t-test, $p<0.01$).

A

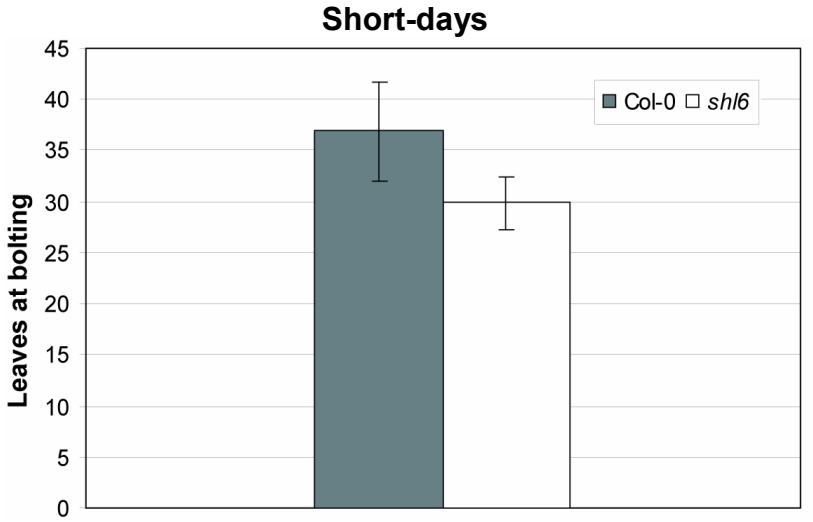

B

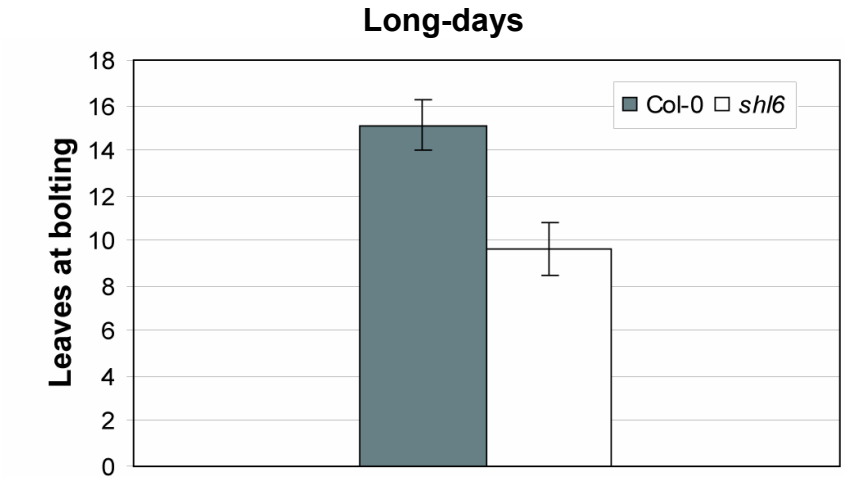

Figure 3.3. The *shl6* plants flower early relative to Col-0 in both long and short days

(A) and **(B)** Graphs represent mean (±SD) number of rosette and cauline leaves at bolting for Col-0, and *shl6* plants grown under short day conditions (8-h light/16-h dark) and long day conditions (16-h light/8-h dark). Error bars indicate SD (standard deviation) (n=10).

Organ-specific gene expression

In low light, Col-0 seedlings elongated hypocotyls and opened cotyledons (Pepper et al., 2001). To determine whether transcript levels of *SHL6* are regulated in an organ specific manner in seedlings, SHL6 mRNA levels were examined by quantitative RT-PCR, using a gene-specific primer pair. An *EF1a* primer pair was used as the constitutively expressed internal control.

Total RNA was extracted from the cotyledons, hypocotyls, and roots of 5-d-old Col-0 seedlings grown in low light ($22\mu mol^{-2}sec^{-1}$), and then cDNAs were made by reverse transcription and used as templates for qRT-PCR with a gene-specific primer pair for *SHL6*. The *SHL6* transcript was more highly expressed than the control *EF1a* gene, and ubiquitously, to a detectable level, in cotyledons, hypocotyls, and roots. However, it was relatively more abundant in the cotyledon (2-fold induction) (Figure 3.4). The expression levels (ΔC_t) of the *SHL6* transcript were calculated by subtracting the C_t for *EF1a* primer from each C_t for tissue samples. Higher $-\Delta C_t$ value for *SHL6* in cotyledons, hypocoyls, and roots indicated a higher expression level because the *SHL6* transcript was more highly expressed than the control *EF1a* gene.

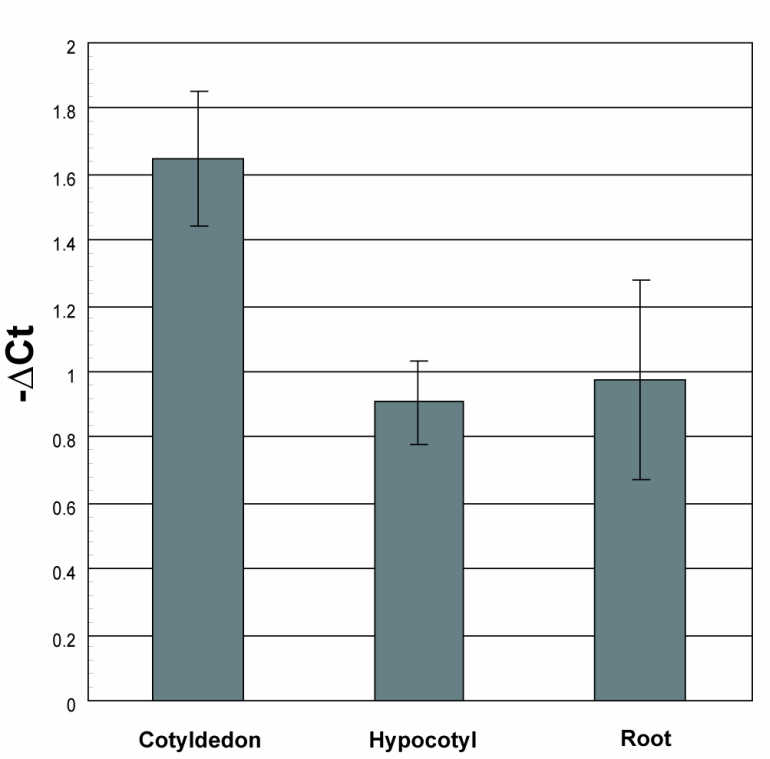

Figure 3.4. *SHL6* mRNA expression levels in organs of Col-0 seedlings

RNA was extracted from each tissue: cotyledons, hypocotyls, and roots of 5-d-old seedlings. Expression of genes was analyzed in quantitative RT-PCR reactions. Higher a -ΔCt value for *SHL6* mRNA indicated higher an expression level because the *SHL6* transcript was more highly expressed than control *EF1a* gene. Error bars indicate standard deviation of ΔCt value calculated by $(\sigma^2_{\text{gene}} + \sigma^2_{\text{control}})^{1/2}$.

Discussion

In this study we provided molecular genetic evidence for that *SHL6,* a gene encodes a glucan synthase-like 12 (*GSL12*) that has a role in regulation of light signaling.

SHL6/GSL12 is regulated to multiple wave lengths of light

The *shl6* seedlings also showed shorter hypocotyls compared with Col-0 seedlings over the ranges of the red, far-red, blue fluence rates used (Figure 3.1A). However, normalization data account for relative hypocotyl elongation showed *shl6* seedlings are most hyper-responsive to red light (Figure 3.1B). Since plants homozygous for *shl6* exhibited hyper-responsiveness to multiple wave lengths of light, these results suggest that the normal allele of *SHL6* acts as a negative regulator of photomormogentic growth.

Furthermore, the mRNA levels of *SHL6* examined by quantitative RT-PCR showed two-fold induction in Col-0 seedlings grown in dark in comparison to white, yellow, and red light (Figure 3.2A). It is suggested that *SHL6/GSL12* may be involved in hypocotyl elongation in the dark by transferring cell wall components including glucose to synthesize callose. *AtGSL6 (CALS1)* closely related to *SHL6* sequences is involved in cell plate formation (Hong et al., 2001b). To build the cell plate at cytokinesis, amount callose needs to be deposited with in a few minutes after the tubulovescular network (Samuels et al., 1995; Verma, 2001). Hong and his colleagues (2001) suggested a model that UDP-glucose transferase (UGT1) acts in transferring UDP-glucose from sucrose

synthase (SuSy) to the glucose (callose) synthase complex for rapid synthesis of callose. Therefore, light- regulated hypocotyl elongation by *SHL6* may be related to callose involved in cell plate formation.

qRT-PCR analysis showed that the transcript level of *SHL6* in the *shl6* mutant was reduced in dark and red grown *shl6* seedlings in comparison to wild-type. However, interestingly, *SHL6* mRNA levels in *shl6* seedlings grown in white and also in yellow light were similar to those in the Col-0 seedlings although hypocotyl elongation of *shl6* mutant was reduced more than in Col-0 plants. The reduction in transcript accumulation in *shl6* mutants was eliminated by GSL12 transgenic seedlings. Expression of mRNA in *GSL12* seedlings was higher than that in Col-0 because GSL12 plants contain both an endogenous genomic *GSL12* gene and an exogenous *GSL12* DNA fragment from T-DNA insertion (Figure 3.2B). These results showed that the transcript levels were affected by post-transcriptional regulation although *shl6* was a point mutation. One possibility is that the reduction in transcript accumulation in *shl6* mutants is caused by an nonsense or missense-mediated RNA decay system (Nyström-Lahti et al., 1999; Pertea et al., 2007) and missense-mediated RNA decay might be regulated by light. Exonic splicing enhancers (ESEs) are discrete sequences within exons that promote both constitutive and regulated splicing (Blencowe, 2000). ESEs can be disrupted by single nonsense, missense, and translationally silent point mutation (Liu et al., 2001). Coding-region single nucleotide polymorphisms (cSNPs) within an ESE may affect the patterns or efficiency of mRNA splicing (Liu et al., 2001; Cargill et al., 1999). It is possible that the point-mutated region in *SHL6* may contain ESE domains.

shl6 mutant flowers early in both short-day and long-day periods

Arabidopsis is a facultative long day plant that flowers earlier in long day (16-h light/8-h dark) than in short days (8-h light/16-h dark). We found that the *shl6* plants flowered earlier than Col-0 plants in both long and short days (Figure 3.4). PHYA and CRY2 promoted flowering in both long-day and short-day photoperiods (Guo et al., 1998; Mockler et al., 2003), whereas *phyB* seedlings have an elongated, early flowering phenotype characteristic of the shade-avoidance of wild-type seedlings grown under a low R/FR light (Smith and Whitelam, 1997). CO and FT proteins modulated by photoreceptors (PHYA and CRY2) promote flowering (Kardailsky et al., 1999; Kobayashi et al., 1999). Therefore, *SHL6* may act as a negative regulator in photomorphogenesis to suppress down-stream genes (CO and FT) of photoreceptors.

In addition, CO and FT proteins are expressed specifically in vascular bundles of leaves (Takada and Goto, 2003). Furthermore, the CO and FT protein acts in vascular bundles to induce photoperiodic flowering (An et al., 2004). PHYB and CRY2 photoreceptors are expressed in vascular bundles, epidermal, and mesophyll in cotyledons, unlike CO and FT (Somers and Quail, 1995; Goosey et al., 1997; Toth et al., 2001).

The examination of the functional site of *PHYB* for the regulation of flowering has demonstrated that PHYB-GFP expressed in mesophyll cells regulates flowering, but PHYB-GFP expressed in vascular bundles does not (Endo et al., 2005). In addition, *FT* expression in vascular bundles was suppressed by PHYB-GFP expressed in mesophyll cells (Endo et al., 2005). CRY2-GFP fusion protein with tissue-specific promoters was

analyzed by the regulation of flowering. CRY2-GFP expression in vascular bundles advanced flowering by promoting the expression of *FT* (Endo et al., 2007). Hence, Endo et al. (2007) suggested that CRY2 and PHYB function in different tissues within the leaf, but coordinately regulate flowering in response to light signaling.

The expression of one member of *GSL* family genes in *Arabidopsis*, (*AtGSL2:GUS)* was also detected in the vascular tissues of cotyledons, hypocortyls, and roots of transgenic plants (Dong et al., 2005). The *SHL6* transcript was more highly expressed than the control *EF1a* gene, in all tissues tested, including cotyledon, hypocotyl, and root: however, it was more relatively abundant in the cotyledon (Figure 3.4).

Therefore, *SHL6* transcrtipts may be expressed in vascular tissues of cotyledon, hypocotyl, and root. It is suggested that *SHL6* transcripts were highly expressed in cotyledons because vascular tissues are more abundant in cotyledons than in hypocotyls and roots. Another reason is that light is perceived by leaves (Knott, 1934; Endo, 2007), so light-regulated *SHL6* mRNA could be expressed in cotyledons higher than in roots and hypocotyls.

Materials and methods

Plant materials and growth conditions

Arabidopsis ecotype Col-0 seeds were obtained from the laboratory stocks of Joanne Chory. The *shl6* mutant was back-crossed twice to wild-type Col-0 and homozygous shl6 mutant was isolated by their short hypocotyls in low light (24µmolm^{-2}s^{-1}). Seeds were surface sterilized (Chory et al, 1989), resuspended in sterile 0.1% (w/v) phytagar, and then stored overnight at 4 °C. Seeds were then plated on Murashige-Skoog plates (1x Murashige-Skooge salts, 0.8% phytagar, 1XGamborg's B5 vitamin mixture, 2% (w/v) sucrose). Seeds were placed at 25 °C for at least 4h in white light (100 µ molm^{-2}s^{-1}) and then grown in continuous low light (30µmolm^{-2}s^{-1}) for 9 days.

Hypocotyl measurements

For hypocotyl length measurements, seeds were dispersed onto Murashige and Skoog plates containing 2% (w/v) sucrose in a 7 mm grid pattern to ensure even spacing. Seeds were placed at 25 °C for at least 4h in white light (100 µ molm^{-2}s^{-1}) prior to placement in continuous white light (100 µ molm^{-2}s^{-1}), low light (30µmolm^{-2}s^{-1}) and the dark for 9 days. Hypocotyl length is determined as the distance between the top of the collet root hairs, to the 'V' made by the cotyledon shoulder (Scheres et al., 1994). Hypocotyls were straightened using forceps if necessary, and then were measured by using 0.5mm scale ruler, and the mean ± SE calculated for each data set. Hypocotyls of seedlings that were growing appressed to the agar media, as well as those with obvious developmental abnormalities, were not measured.

Light source

White light was supplied by an equal mixture of cool-white (CW) and Grow-lux wide-spectrum fluorescent bulbs (Sylvania, Danvers, MA). A 2472 yellow-green acrylic filter (Polycast Technology, Stamford, CT) with a transmission maximum of ±550 produced light that was partially depleted in the photomorphogenetically active UV, B, R, and FR regions of the spectrum. Dark experiments were performed in a passively ventilated dark box. Red light was supplied by CW fluorescence bulbs filter through a Kopp 2-73 red glass filter (Kopp Glass, Pittsburgh, PA, USA). Blue light was supplied by CW fluorescent bulbs filtered through a Kopp 5-57 blue filter. Far-red enriched light was provided by a 60W incandescent bulb filtered through a Kopp 2-64 glass filter (R/FR ratio of ± 0.32). Fluence rates of white, R, and B light were measured with a quantum photometer (model LI-189, LI-COR, Lincoln, NE). Fluence rates of FR light were measured using a radiometer (model IL1400, International Light, Newburyport, MA) with FR probe (model SEL033, International Light).

Expression analysis by quantitative RT-PCR

To study the expression of *SHL6* gene in *Arabidopsis*, RNA was isolated with the Qiagen Plant RNeasy RNA extraction kit. RNA samples were isolated from Col-0, shl6 mutant, and transformant GSL12. Seedlings where grown as previously described under continuous white light (110 $\mu molm^{-2}s^{-1}$), yellow light (70 $\mu molm^{-2}s^{-1}$), red light (22 $\mu molm^{-2}s^{-1}$), and in the dark. As an additional experiment, RNA samples were collected from flower bud, mature flower, silique, leaf, stem, and root tissues. Amount of RNA

was measured by using Beckman DU60 Spectrophotometer and quality of the RNA was tested by agarose gel electrophoresis. To remove genomic DNA, DNAseI treatment (DNA *free*™ kit, Ambion, Austin, TX) was used. 400 ng of RNA was reverse transcribed by using SuperScript™ III First-Strand Synthesis SuperMix (Invitrogen, USA). The resulting single stranded cDNA was thereafter used as template in quantitative real-time PCR (qRT-PCR) reactions. qRT-PCR was performed with *POWER* SYBR® Green PCR master mix (Applied Biosystem, USA) with an ABI 7900HT real-time (RT) PCR machine. The cDNA was normalized relative to the level of constitutively expressed (elongation factor a1) *EF1a* gene (EF930-F, 5'-TCGAATCCTCAAAACTCTATCCGCA-3'; EF930-R, 5'-GGAGAAGAAACGAAGCTATAACACG-3') as a control. qRT-PCR reactions were carried out with a gene specific primer for *SHL6* (CS-F, 5'-TATCCTTGCCTTTATGCCCACAGGTT-3'; CS-R,5'-TGATCCCCAGAATCCTGCTCTATGA-3') in a volume of 10 µl. The PCR program was as follows: incubation for 2 min at 50 °C, then 2 min at 95 °C, and 60°C for 1 minute. To verify the amplification of single PCR products, it was followed by 40 cycles of denaturation at 94 °C for 15 s, annealing at 60 °C for 15 s and a 2% ramping to 95°C. All measurements were repeated twice. To check non-specific amplification products, amplified fragments were analyzed by 2% agarose gel electrophoresis and then digested by a unique restriction enzyme (*HinfI*) site in the CS primers.

Flowering time experiments

Flowering time was analyzed in both short-day and long-day conditions. Seeds were soak in 0.1% phytoagar solution, cold-treated for 3d at 4°C, and transplanted with even spacing into pots containing the same compost sand mixture. The pots were moved to a growth room maintained at 22°C for measuring flowering time. Seeds were grown under a 16-h light/ 8-h dark photoperiod for long days and an 8-h light/16-h dark photoperiod for short days. Flowering time was determined by counting the total of number of rosette and cauline leaves at bolting.

CHAPTER IV

PHENOTYPICAL CHARACTERIZATION OF *SHL6*

Introduction

Arabidopsis plants homozygous for the mutation *shl6* are hyper-responsive to available light. It is one of a number of mutants designated as *seedling hyper-responsive* to *light* (*shl*) (Pepper et. al, 2001). In low light, *shl6* seedlings have a phenotype typical of seedlings grown in high-light. That is they have short hypocotyls, expanded cotyledons, and significant development of the first true leaves even when grown in low light. *SHL6* was mapped to the region of chromosome 5 between SSLP markers nga249 and nga151. Further, the DNA sequence of the *shl6* mutation revealed that a single base-pair difference from the wild-type Col-0 allele causes a predicted proline to leucine amino acid substitution mutation in the first exon of a glucan *synthase like gene 12* (*GSL12*) (At5g13000). *SHL6* was identified by complementation using the full-length *GSL12* via *Agrobacterium*-mediated plant transformation (Clough and Bent, 1998).

In the previous chapter, in order to further our understanding of the role of *SHL6* encoding *GSL12* in photomorphogenesis, we characterized *SHL6* molecular functions. The *shl6* mutant seedlings showed hyper-responsiveness to red, far-red, and blue light. The transcript level of *SHL6* was regulated in Col-0 and *shl6* seedlings grown under dark, yellow, red, and white light. The *shl6* plants flowered early in the both short-days and long-days. *SHL6* expression was highly induced in the cotyledons.

In this chapter, as the first approach, we used SALK and SAIL lines (Alonso et al., 2003) containing T-DNA inserts in the candidate genes in order to investigate the loss of function mutant of *SHL6*.

In addition, we have used several approaches to further our understanding of the physiological role of *SHL6* as an enzyme involved in callose synthesis.

Callose, a β-1,3-glucan, is widely distributed in higher plants and carries out several important functions during normal plant growth and development (Aspinall and Kessler, 1957). Callose is readily detected in tissue sections, including sieve plates of phloem elements, pollen mother cells, pollen grain, and pollen tubes through UV-light induced florescence after dying with aniline blue (Stone and Clarke, 1992). Callose is also localized at the cell plate, and in plasmodesmata, root hairs, cotton seed hairs, and spiral thickenings in tracheids (Stone and Clarke, 1992). In addition, the deposition of callose is induced by wounding, pathogen infection, and physiological stress (Jacobs et al., 2003; Kauss, 1996; Stone and Clarke, 1992).

Callose is synthesized by callose synthases encoded by a family of glucan synthase-like genes (*GSL*) (Cui et al., 2001; Doblin et al., 2001; Hong et al., 2001a; Østergaard et al., 2002). *GSL* genes have homology with yeast *K506 hypersensitivity (FKS)* genes that encode the catalytic subunit of β-1,3-glucan synthase (Douglas et al., 1994; Cabib et al., 2001; Dijkgraaf et al., 2002). Through sequence similarity, twelve *GSL (AtGSL1-12)* genes have been identified in *Arabidopsis* (Richmond and Somerville, 2000; Hong et al, 2001); the genes for these proteins were also annotated independently by a group in Stanford (http://cellwall.stanford.edu/gsl/index.shtml). CSL1 (GSL6) and

CSL12 (GSL5) have been localized at the site of cell plate formation and to the site of pathogen infection, respectively (Hong et al., 2001a; Jacobs et al., 2003; Nishimura et al., 2003).

Recently, mutation analysis of callose synthase genes in *Arabidopsis* indicated the function of callose at the molecular level. *cals5(gsl2)* mutants exhibited male sterility and lacked the normal callose wall affecting the exine pattern of the microspores. It was suggested that *CalS5 (AtGSL2)* is responsible for the synthesis of callose in the temporary callose wall of the microspores and is essential for exine formation during microsporogenesis (Dong et al., 2005). Two closely related and linked genes, *GSL1* and *GSL5* play a redundant but essential role in both sporophyte and pollen development and their protein are localized in pollen mother cell walls and pollen tubes (Enns et al., 2005 and Dong et al, 2005). However, Nishikawa and colleagues (2005) published that three additional *cals5* alleles have shown altered exine patterns, but the mutants produce fertile pollen. In addition, one of these alleles *(cals5-3)* led to successful fertilization in self-pollinated plants, although the mutant also lacked detectable callose in its pollen tubes. The results suggested that callose is essential for pollen wall patterning, but not required for pollen tube function (Nishikawa et al., 2005).

Here, we also attempted to determine whether *SHL6* is involved in callose synthesis by observing callose deposition and pollen viability because pollen grains temporally make callose cell wall. Finally, we examined call wall elongation in seedlings to prove whether *SHL6* is an enzyme of the callose synthesis complex that is involved in cell division. Finally, we determined whether the transcriptional level of

SHL6 is regulated in these tissues because abnormal morphologies are observed in flowers, siliques, roots, leaves, and stems.

Results

The phenotypical characterization of SALK and SAIL knock-out insertion in At5g13000

In a separate effort to determine effects of the loss of function of *SHL6*, nine mutant lines with T-DNA insertions in candidate genes At5g13000, At5g13010, and At5g13020 were obtained from sequenced-indexed mutant collections, designated SALK (Salk Institute Genomic Analysis Laboratory; http://signal.salk.edu/cgi-bin/tdnaexpress) and SAIL (Syngenta Arabidopsis Insertion Library; http://www.tmri.org/en/partnership/sail_collection.aspx.) (Table 4.1) (Alonso et al., 2003). The SALK and SAIL T-DNA seed collections were generated from T-DNA insertion mutagenesis of *Arabidopsis* Col-0. To verify homozygous T-DNA lines from the pool of seeds, two primer pairs were designed. One primer pair was gene-specific primers (GSP-F and GSP-R) and the other primer pair was a T-DNA left border primer (LBaI) paired with GSP-F or GSP-R (Figure 4.1A). The homozygous SALK and SAIL mutant hypocotyls were also measured in low light to find the light hyper-responsive phenotype similar to *shl6*.

PCR with the two primer pairs using target DNA from SALK_019541 and SALK_062354 lines that have T-DNA insertions in an exon or intron in the At5g13010 (RNA helicase) did not reveal any homozygous lines. No homozygous progeny were detected among F_2 progeny of confirmed heterozygous parents. The implication is

homozygosity for T-DNA insertion in At5g13010 created a lethal phenotype. Although a homozygous T-DNA insertion in the exon of the At5g13020 (ENT domain) was found, the homozygous mutants did not have the *shl6* mutant phenotypes in low light. However a SALK_068418 line inserted in an intron in At5g13000 (*glucan synthase-like*) showed a hypocotyl length phenotype intermediate between Columbia and the *shl6* in low light. Crosses between verified homozygous SALK_068418 and the homozygous *shl*6 produced F_1 progeny with an incomplete or partial complementation phenotype: the hypocotyls of F_1 progeny complemented *shl6*, but the root phenotype of F_1 progeny did not complement *shl6* in low light and had short roots (Figure 4.1B; Table 4.1).

Table 4.1. Tested SALK and SAIL T-DNA lines

Gene name	SALK and SAIL T-DNA	Position	Description
Glucan synthase (At5g13000)	SALK_068418	INTRON	All homozygous lines, but only F_1 (*shl6*xSALK_068418) progeny showed short roots.
	SAIL_402_B10	INTRON	
	SAIL_650_A08	5´UTR	
RNA helicase (At5g13010)	SALK_019541	EXON	No homozygous lines No *shl6* phenotype
	SALK_062354	INTRON	
	SALK_030464	3´UTR	
ENT domain (At5g 13020)	SALK_023962	EXON	Homozygous lines, but no *shl6* phenotype
	SALK_023966	EXON	
	SALK_106147	EXON	

Figure 4.1. Verification of SALK T-DNA insertion and crosses to *shl6*

(A) To confirm the presence of the expected T-DNA insertion, PCR was used. *LBa1* and *LBb1* were used for border primers of T-DNA. *GSP-R* and *GSP-F* are gene specific primers. If a SALK has a wild type genotype, product is amplified only by *GSP* primers. A heterozygous genotype (*HZ*) has two PCR products, one from wild type and the other from homozygous genotype (*HM*). A homozygous genotype is only amplified by *LBa1* or *LBb1* and *GSP-F* primers.
(B) In crosses between verified homozygous SALK_068418 and homozygous *shl*6, the hypocotyl length of F_1 progeny was same as that of Col-0, but the root phenotype of F_1 progeny was shorter than that of Col-0. Data represent mean ±SE (n=11).

A

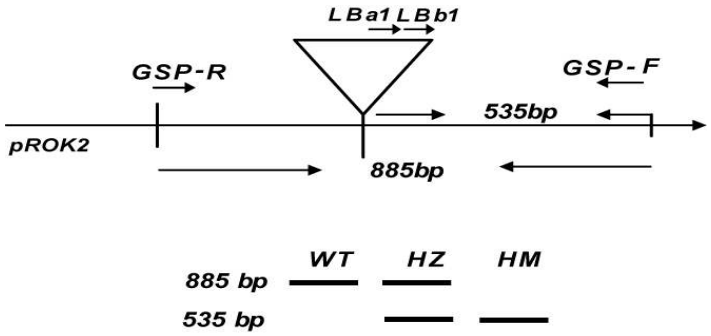

B

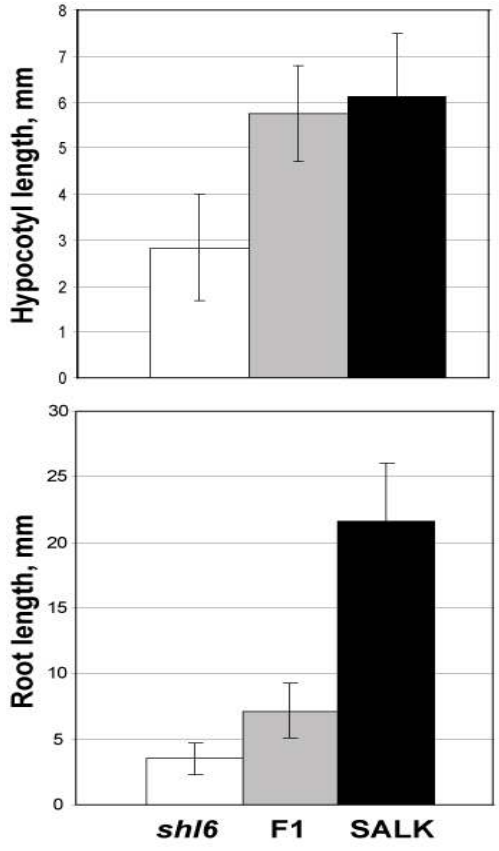

The *shl6/gsl12* mutant displays multiple developmental phenotypes in *Arabidopsis*

In the previous data, germinating *shl6* plants displayed a phenotype in high light (110 μmol m^{-2} s^{-1}), yellow (65 μmol m^{-2} s^{-1}), and darkness that were visible on petri dishes in 7-d-old seedlings (Figure 2.1). Compared to Col-0, *shl6* seedlings showed a reduction in hypocotyl and root growth in the yellow light.

The Col-0 petal and silique lengths were used to determine relative differences displayed by the *shl6* mutant plants. Once plants were transferred to soil, the observable differences between wild-type (Col-0) and *shl6* mutant phenotype were maintained. The mean petal length in ten-week-old Col-0 plants was 3.3 ±0.25 mm and that of *shl6* mutant plants was 2.25±0.26 mm (Figure 4.2A). The silique length of *shl6* mutant plants was variable (Figure 4.2B). Twenty siliques of Col-0 and *shl6* plants were collected and measured. The silique length (7.65±1.57 mm) of *shl6* was less than that of Col-0 (12.8±1.2 mm). Most of the siliques in *shl6* mutant plants contained no or only few seeds (data not shown). Corrected probability ($p<0.005$) values indicate statistical significance of the differences in mean petal and silique lengths between Col-0 and *shl6*, as determined by *t*-test analysis. Values below $p=0.05$ were considered as being statistically significant for differences in petal and silique lengths between Col-0 and *shl6* mutant plants.

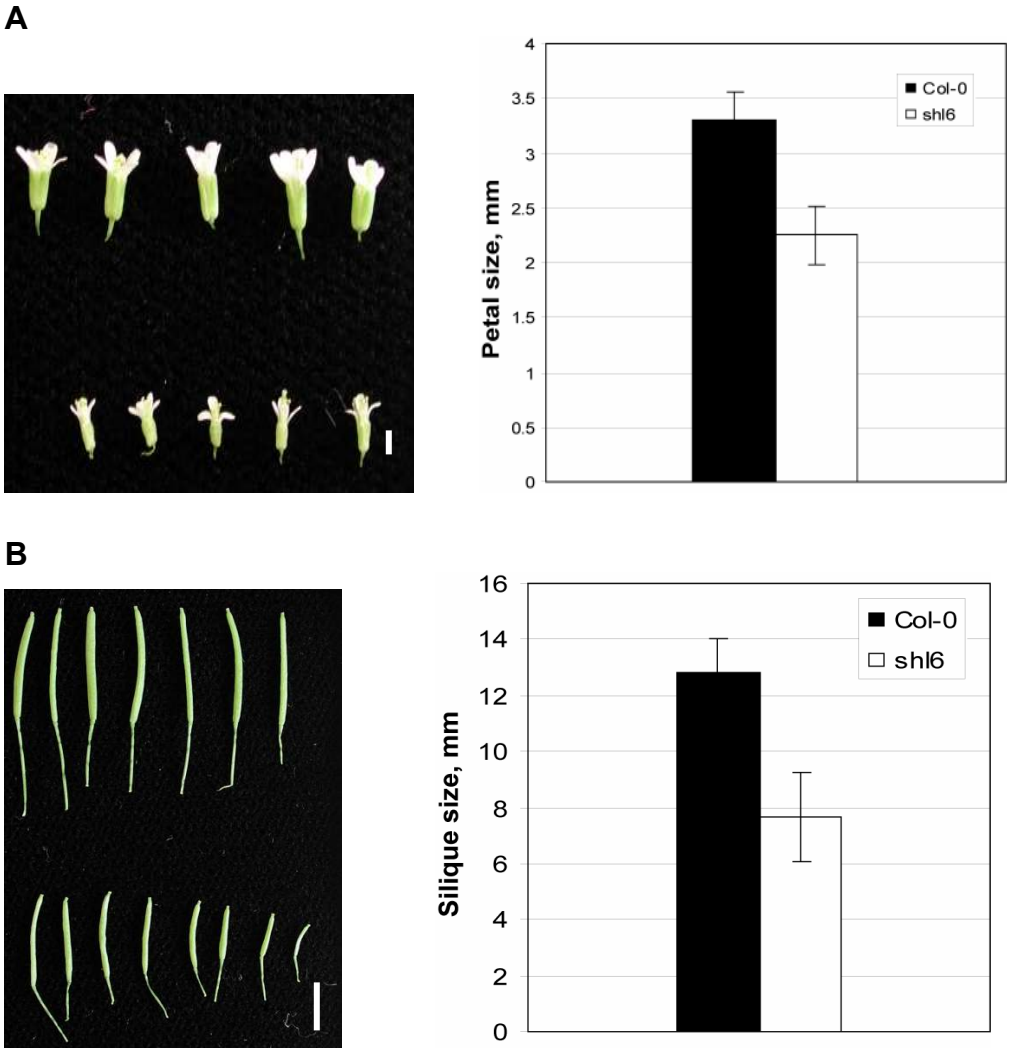

Figure 4.2. Flower and silique morphology of *SHL6*

Mature flowers and siliques from Col-0 and *shl6* mutant plants were compared.
(A) The mean petal length of *shl6* (2.25±0.26 mm) was highly reduced when compared to Col-0 (3.3 ±0.25 mm) (t-test, $p<0.005$) (n=10). Bar=1 mm
(B) The mean siliquelength of *shl6* (7.65±1.57 mm) were smaller than Col-0 (12.8±1.2 mm) (t-test, $p<0.005$). Error bars indicate SD (standard deviation) (n=20). Bar=5mm

Effects of *shl6* mutant on anther morphology and callose deposition

The mutation in *SHL6* also causes a dramatic reduction in fertility. Reciprocal crosses between *shl6* and wild-type plants (Col-0) were usually successful when *shl6* plants were pollinated, but failed when *shl6* was used as the pollen donor, indicating reduced male fertility. The *shl6* mutant plants developed abnormal flowers with abnormal heart-shaped anthers (Figure 4.3A) and were partially or completely sterile.

To determine whether these abnormal anthers were caused by defective callose, 0.01% aniline blue was used to stain callose (Worrall et al., 1992). Stained callose was observed under a microscope (Olympus, BX51) with fluorescence and UV (a standard U-mnu2) filters. Whereas 90% of anthers of wild type plants showed high callose deposition, callose was not observed in anthers of *shl6* mutant plants (Figure 4.3B). The callose deposition region contained vascular bundle and connective tissue (Goldberg et al., 1993). To examine callose deposition in pollen tube, self-pollinated pistils were stained by 0.01% aniline blue. The callose plug appeared in the pollen tube of both Col-0 and *shl6* mutant, but the size of callose plug of *shl6* was smaller than Col-0 (Figure 4.3C, D). Although pollen tubes from self-pollinated pistils were observed, most of callose plugs of *shl6* were smaller than those of Col-0 (Data not shown).

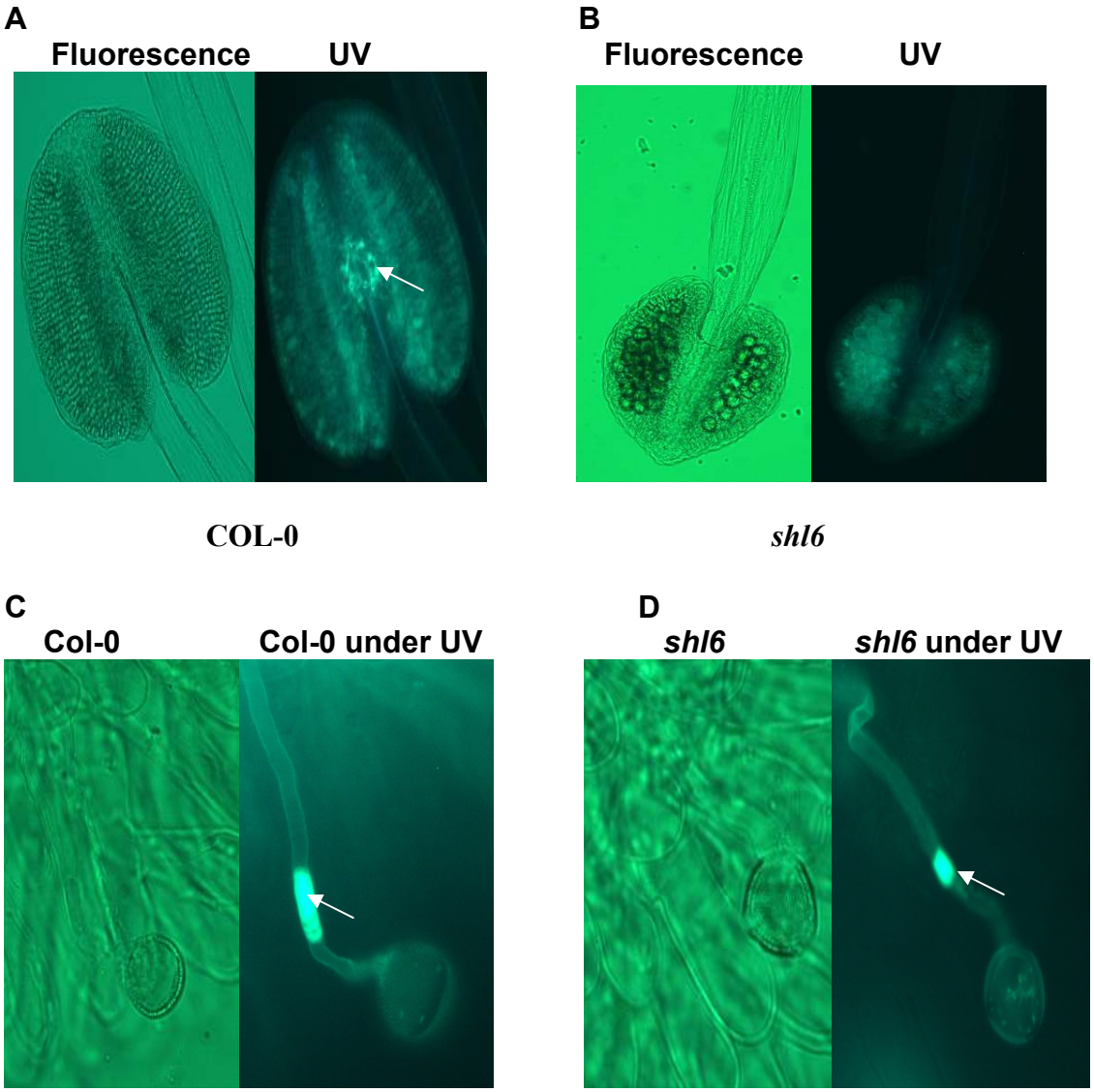

Figure 4.3. Determination of callose deposition in anthers and pollen tubes

(A) Most anthers of Col-0 flowers showed high callose deposition in the middle of anthers stained with 0.01% aniline blue.
(B) Abnormal anthers in *shl6* flowers were associated with the diminished callose. Self-pollinated pistils in Col-0 and *shl6* were stained using 0.01% aniline blue.
(C) and **(D)** The callose plug appeared in the pollen tube of both Col-0 and *shl6*.
Stained callose (arrow) was observed under a microscope with fluorescence and UV filters. (A) and (B) were observed under 10X Objective and (C) and (D) under 40X objective.

Pollen viability in the *shl6* mutant plants

The partial male sterility seen at pollination may be caused by the abnormal anther structure and differences in callose deposition in anthers of Col-0 and *shl6* mutant plants (Figure 4.3). To determine how many pollen grains in the malformed anthers were viable, fluorescein diacetate (FDA) (Heslop-Harrison, J. and Heslop-Harrison, Y., 1970; Regan and Moffatt, 1990) was used to measure pollen viability. Viable grains in both Col-0 and *shl6* glowed yellow from the inside illuminating sperm and vegetative nuclei when view under a microscope (Olympus, BX51) with fluorescence and UV (a standard U-mnu2) filters (Figure 4.4A, B). Many pollen grains in *shl6* mutant were small and collapsed. Unlike normal pollen grains, collapsed pollens did not glow yellow when observed under a UV filter microscope (Figure 4.4B). To measure pollen viability, the fraction of pollen grains stained by FDA was scored. At least 100 pollen grains were counted in each of four replicates. The survival ratios gained from the four replicates were averaged. In this experiments, the pollen viability in *shl6* was (48%) lower than that in Col-0 (87%) (Figure 4.4C).

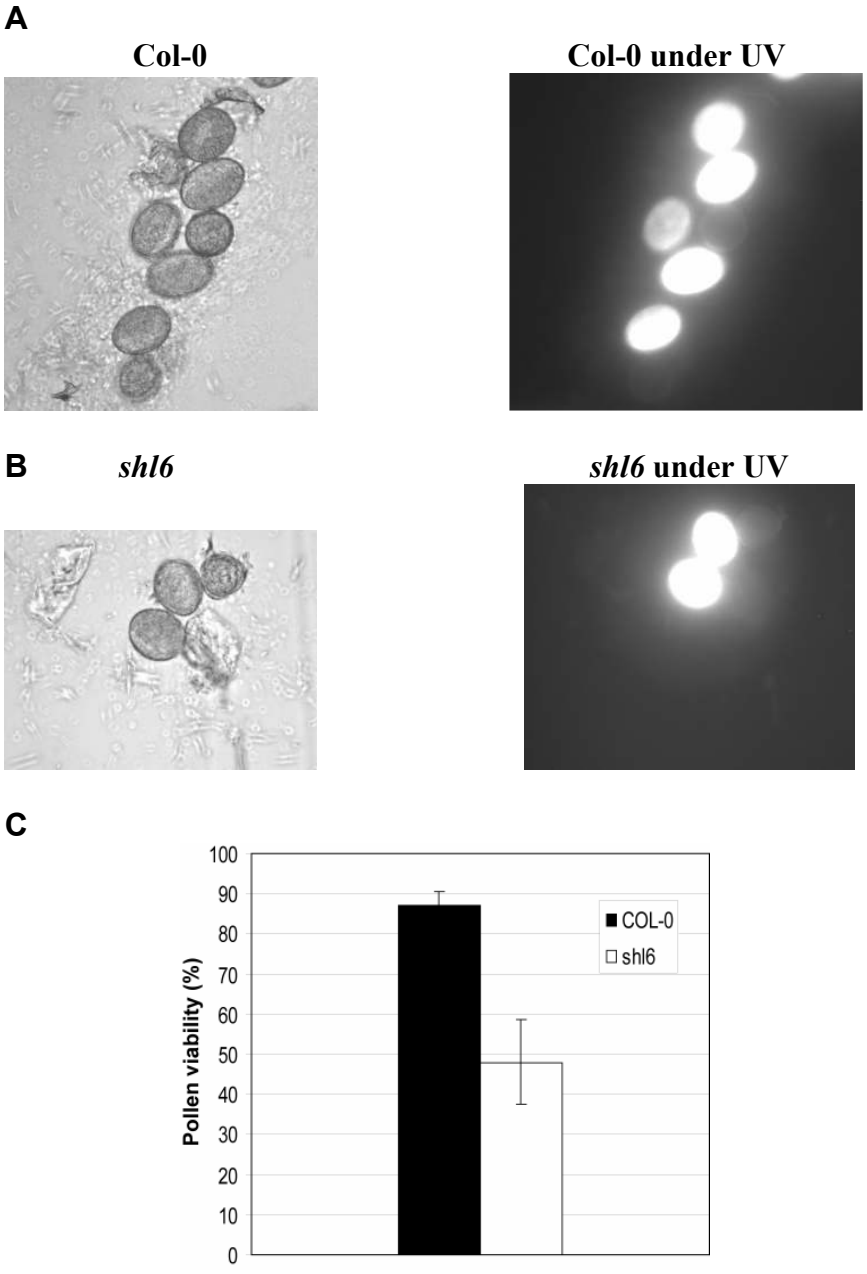

Figure 4.4. Pollen viability in the *shl6* mutant

(A) and **(B)** Viable pollen grains in Col-0 and *shl6* anthers glowed under a UV filter microscope filter.
(C) Average pollen viability of pollen grains was examined. Pollen viability in Col-0 was 87±3.6% and *shl6* was 48±10.7%. Error bars indicate SD (standard deviation). The pollen grains were observed under 40X objective.

The short-hypocotyl phenotype in *shl6* mutant is caused by a reduction in cell size

In the previous experiments, we observed that 7-d-old *shl6* seedlings had shorter hypocotyls than wild type under low light (24 μmol m^{-2} s^{-1}) (Figure 2.1). To investigate the cellular basis of the short-hypocotyls in low light-grown *shl6* seedlings, both the *shl6* and Col-0 hypocotyls were used for agarose imprints to evaluate epidermal cell morphology (Mathur and Koncz, 1997). The average epidermal cell length in hypocotyls of 5-d-old seedlings was shown in Figure 4.5. The length of the epidermal cells by agarose impression revealed that the *shl6* cell length (0.28±0.06 mm) were reduced in their longitudinal length compared with Col-0 (0.44±0.18 mm) (Figure 4.5). In the graph, corrected probability ($p<0.005$) values indicated the statistical significance of the differences in mean hypocotyl cell length between Col-0 and *shl6*, as determined by *t*-test analysis. Values below $p=0.05$ were considered as being statistically significant for differences in hypocotyl length between Col-0 and *shl6* mutant seedlings.

A

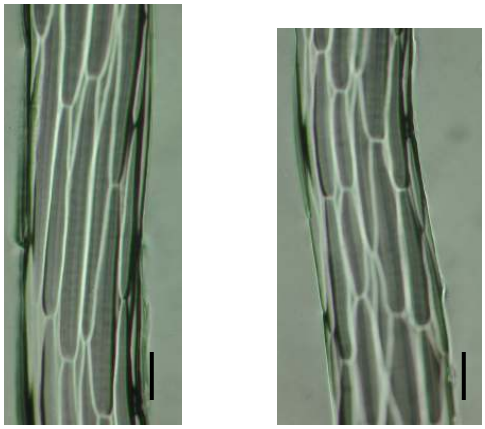

Col-0 ***shl6***

B

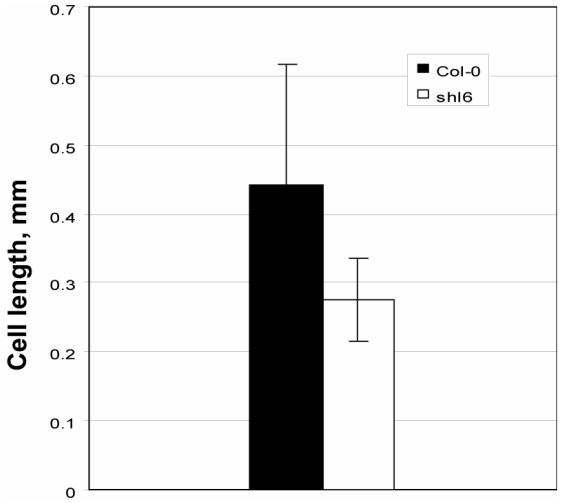

Figure 4.5. Measurement of hypocotyl cell length

(A) Col-0 and *shl6* seedlings were grown under low light (24 μmol m^{-2} s^{-1}) for 5 days. Epidermal cells of hypocotyls were examined by agarose impression. Images of agarose impression from seedlings grown under low light were displayed at actual size for measurment**.**
(B) Average cell length was measured in the agarose imprints. The mean hypocotyl cell length in Col-0 was 0.44±0.18 mm and *shl6* was 0.28±0.06 mm (t-test, $p<0.005$). Error bars represent SD (standard deviation) (n=10) Bars=0.1mm.

Transcript analysis of *SHL6* in various organs

One of the 12 putative callose synthase family genes, *GSL5,*was abundantly expressed in flowers (Østergaard et al., 2002). *GSL1,* which is closely linked to *GSL5* and *GSL5* also were subsequently found to be expressed in all tissues including roots, leaves, siliques, stems, and flowers (Enns et al., 2005). Therefore, it was of interest to determine whether transcript levels of *SHL6* are also regulated by organ specificity. Expression was examined by quantitative RT-PCR, using a gene-specific primer for *SHL6*. Total RNA was extracted from the flower buds, mature flowers, siliques, stems, leaves, and roots of 90-d Col-0 and *shl6* plants grown in long days (16-h light/ 8-h dark), and then cDNA was made by reverse transcription and used as templates for qRT-PCR. A specific primer for the constitutively expressed gene *EF1a* was used as internal control.

The *SHL6/GSL12* transcript in flower buds, mature flowers, siliques, stems, leaves, and roots tissues was more highly expressed than the control *EF1a* gene. However, the *SHL6/GSL12* transcript level in roots was 4-fold higher than flower buds, mature flowers, stems, or leaves (Figure 4.6A, Table 4.2). In addition, 90-d old *shl6* mutant plants showed pleiotropic phenotypes different from Col-0 plants. The *shl6* plants displayed abnormal development in flowers, siliques, and stems as seen in figures 4.1 and 4.5, as well as in leaves and roots (data not shown). The *shl6* stems were bent and weak (Figure 4.7A). The mean stem length of *shl6* mutant plants (21.8±3.5 cm) was shorter than that of Col-0 (28.3±3.4 cm) (Figure 4.7B). To determine whether *SHL6*

expression is altered in the *shl6* mutant tissues including flower buds, mature flowers, siliques, stems, leaves, and roots, qRT-PCR analysis was applied.

The transcript level of *SHL6/GSL12* in the *shl6* mutant was reduced in those tissues compared to Col-0. However, the *SHL6* mRNA in the *shl6* plants in root and stem was reduced to a much greater extent than in mature flower, silique, and leaf tissues (Figure 4.6B). The expression levels (ΔC_t) of the *SHL6* transcript were calculated by subtracting the C_t for *EF1a* primer from each C_t for tissue samples. The higher $-\Delta C_t$ values for *SHL6* in those tissues indicates higher expressions of *SHL6* because the *SHL6* transcript was more highly expressed than control *EF1a* gene.

Table 4.2. C_t values for genes analyzed using RT-PCR

		Col-0		*shl6*	
Gene	Tissue [a]	Average C_t [b]	StDv[c]	Average C_t	StDv
SHL6/GSL12	FB	23.94	0.06	24.35	0.24
	MF	25.23	0.06	24.77	0.12
	Siliq	26.96	0.14	28.50	0.26
	Stem	25.88	0.10	29.21	0.70
	Leaf	27.01	0.11	27.81	0.22
	Root	25.19	0.35	0.19	0.14
EF1a	FB	25.35	0.14	25.50	0.04
	MF	26.47	0.08	25.44	0.07
	Siliq	29.00	0.49	29.71	0.12
	Stem	27.42	0.04	29.99	0.34
	Leaf	29.64	1.07	29.04	0.42
	Root	28.65	0.05	27.49	0.25

[a] FB (Flower Buds), MF (Mature Flowers), Siliq. (Siliques), Stem (Stems), Leaf (Leaves), Root (Roots)

[b] Average Ct Values for 3-4 replicates

[c] Standard Deviation for 3-4 replicates

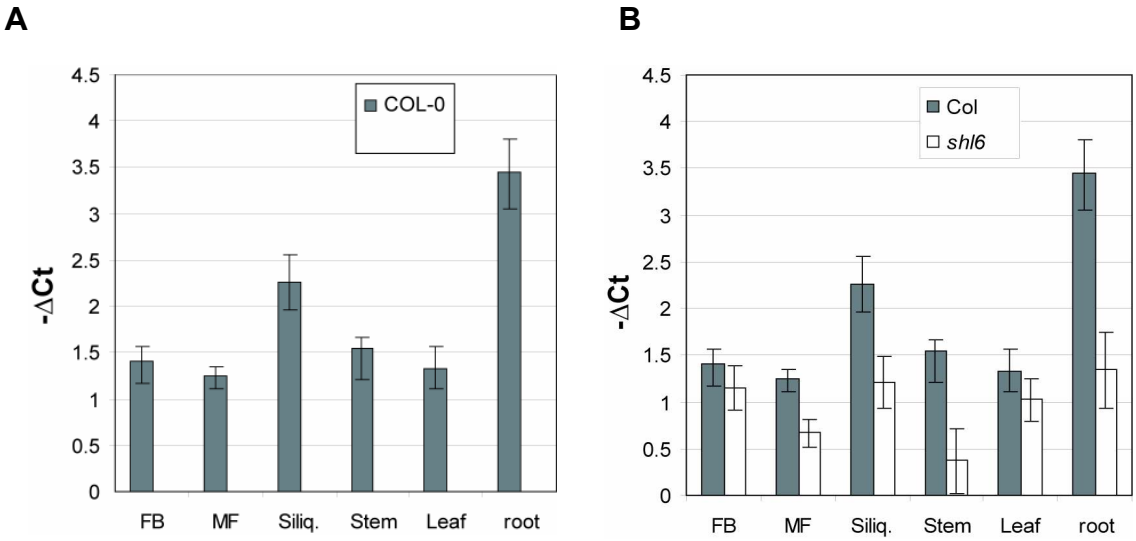

Figure 4.6. Transcription levels of *SHL6* in various *Arabidopsis* organs

(A) RNAs were extracted from various tissues including flower buds (FB), mature flowers (MF), siliques (Siliq), stems, leaves, and roots of Col-0 plants grown 90-d in the long-days.
(B) The *SHL6* transcript expression in Col-0 plants was compared to those in *shl6* mutant plants. Expression of genes was analyzed by quantitative RT-PCR reactions.
The higher -ΔCt value for SHL6 in all tissues indicates a higher expression level because the *SHL6* transcript was more highly expressed than the control *EF1a* gene. Error bars indicate standard deviation of ΔCt value calculated by $(\sigma^2_{gene}+\sigma^2_{control})^{1/2}$.

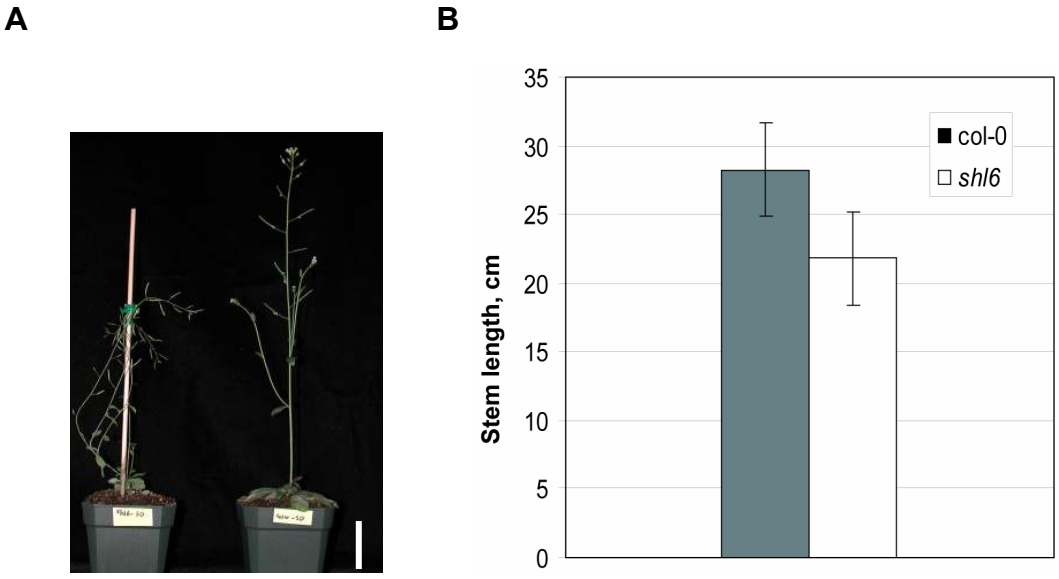

Figure 4.7. Measurement of stem length

(A) Col-0 and *shl6* plants were grown under low light (24 μmol m^{-2} s^{-1}) for 90 days. Images of *Arabidopsis* plants grown in a long day chamber are displayed**.**
(B) Stem lengths were measured from rosette leaves to the top. The mean stem length was measured using a ruler**.** Error bars represent SD (standard deviation) (n=15). Bar=5cm.

Discussion

In this study, we provided phenotypical characterization for the normal role of *SHL6* which encodes a glucan synthase-like (*GSL12*) gene involved in callose synthesis. Mutants lacking normal *SHL6* expression led to partial male sterility, altered levels of expression and altered morphology.

The role of *SHL6* in root development

GSL1 and *GSL5* as *GSL* family genes in *Arabidopsis* are linked, within 8cM of each other. Enns and his colleagues (2005) recently reported that *GSL5* gene was necessary for normal development. The *gsl1-1/gsl1-1 gsl5*/+ mutant lines appeared normal; however, the plants from the *gsl1-1*/+*gsl5/gsl5* mutant lines had extremely small rosette leaves, shorter primary roots, flowers and siliques.

We used a loss of function mutant, a SALK_068418 T-DNA insertion line in an intron in the *SHL6* to characterize the *shl6* mutation. Plants homozygous for this T-DNA-*gsl12* allele showed intermediate hypocotyl phenotype between Col-0 and *shl6* which can be explained by diminished expression due to the insertion occurring in an intron. However, crosses between homozygous SALK_068418 plants and homozygous *shl*6 mutants produce F_1 progeny that showed that short hypocotyl was complemented, but root phenotype was not complemented in low light (Figure 4.1B). Although the complemented hypocotyl phenotype was expected due to the T-DNA being inserted in an intron, the failed complementation in root of F_1 progeny suggests that that the *shl6/gsl12* is indeed an allele of *SHL6*/*GSL12* gene which includes a T-DNA insertion in

SALK_068418 plants, and implicates this gene in normal root development. Interestingly, *shl6/gsl12* seedlings showed different hypocotyl elongation depending on light intensity, but had light-independent short roots.

The role of *SHL6* in anther development

In flowering plants, the anthers contain highly specialized reproductive and somatic cells that are required for male fertility. In flowering plants, male meiosis and male gametophyte development occur in the anther (Goldberg et al., 1993; Ma, 2005; McCormick, 1993). In developing anthers of angiosperm, microsporocytes produce a temporal cell wall of callose between the primary cell wall and the plasma membrane (Currier and Webster, 1964). It is believed that the callose wall is formed temporarily to prevent cell cohesion and fusion. At the end of meiosis, the callose cell wall is degraded by β-1,3-glucanase (callase) and microspores are released in the locular space (Steiglitz, 1977; Steiglitz and Stern, 1973).

We described here that homozygous *shl6* plants had smaller flowers, and siliques. The mutation also caused a dramatic reduction in male fertility. This was supported by a previous report concerning *GSL2 (CalS5)*, one of 12 *GSL* genes in *Arabidopsis* (Dong et al., 2005). Knockout mutations of the *GSL2 (CalS5)* gene by T-DNA insertion also had short siliques and flowers. The homozygous *gsl2 (cals5)* mutant plants resulted in a severe reduction in male fertility (Dong et al., 2005). Consistent with their function, the *shl6* mutant plants developed abnormal flowers with heart-shaped anthers (Figure 4.3A) and were partially or completely sterile. Whereas 90% of anthers of Col-0 plants showed

high callose deposition, callose was not observed in anthers of the *shl6* mutant plants (Figure 4.3B). The callose deposition region contained vascular bundle and connective tissues (Goldberg et al., 1993). Therefore, we measured pollen viability in both Col-0 and the *shl6* mutant for the next step.

The role of *SHL6* in pollen development

The timing of callose wall formation and degradation is pivotal for normal pollen development as shown by the effects of several mutants that alter the callose cell wall of Petunia (Izhar and Frankel, 1971; Warmke and Overman, 1972). Dong et al., 2005 described that callose synthesized by GSL2 (CalS5) is essential for the development of pollen walls required for fertile pollen in *Arabidopsis*.

The collapsed, unviable pollen grains in both Col-0 and *shl6* were distinguished from viable grains that glowed yellow under a microscope (Olympus, BX51) with fluorescence and UV (a standard U-mnu2) filters (Figure 4.4A, and B). Whereas 52% of the pollen grains in the *shl6/gsl12* mutant were small and collapsed, 87% of the pollen grains in Col-0 were viable (Figure 4.4C). It is suggested that low pollen viability in *shl6* may be caused by a deficiency in SHL6. However, it remains unproven that low viability is directly related to decreased callose cell wall formation during pollen development or frequent formation of abnormal heart-shaped anthers lacking callose deposition (Figure 4.3).

The role of *SHL6* for cell elongation

Yeast *K506 hypersensitivity (FKS)* genes homologous with *GSLs* in *Arabidopsis* encode the catalytic subunit of β-1,3-glucan synthase (Douglas et al., 1994; Cabib et al., 2001; Dijkgraaf et al., 2002). *FKS1* expression is cell cycle regulated and more abundant during vegetative growth. In *Arabidopsis*, CalS1(AtGSL6) interacts with two cell plate-associated proteins, phragmoplastin and a UDP-glucose transferase and was found in the cell plate of dividing cells by localization of the GFP-tagged CalS1 protein (Verma and Hong, 2001; Hong et al., 2001a, 2001b). It is possible that CalS1 forms a complex at the cell plate (Hong et al., 2001a).

The cells in *shl6* hypocotyls were reduced in their longitudinal length compared with Col-0 hypocotyls (Figure 4.5). These results show that the differences in hypocotyl length reflect differences in both cell length and cell elongation. The hypocotyl and cell measurements suggested that the *SHL6* gene directly effects hypocotyl cell elongation. In the future, the SHL6 subcellular localization detected via GFP-tagged SHL6 protein may prove whether SHL6 is another cell plate-specific callose synthase involved in callose deposition at the forming cell plate. This would suggest that reduced epidermal cell length in *shl6* mutant hypocotyls is caused by abnormal cell division involved in cell plate formation.

Transcriptional regulation of *SHL6* in the various organs of the Col-0 and the *shl6* mutant plants

The transcript levels of *GSL1* and *GSL5* have been characterized previously by RT-PCR (Enns et al., 2005). The two genes were expressed in all organs including root, young rosette, rosette, cauline leaf, stem, bud cluster, and silique (Enns et al., 2005). However, when the transcript level of *SHL6* in Col-0 plants was compared by quantitative RT-PCR, the *SHL6* transcripts were differently regulated. In roots, the *SHL6* expression was 4-fold higher than in flower buds, mature flowers, stems, and leaves (Figure 4.6A).

The *SHL6* expression level was also altered in the *shl6* mutant. The transcript level of *SHL6* in the *shl6* mutant was decreased in flower buds, mature flowers, stems, leaves, and roots compared to Col-0. Furthermore, the transcript levels of *SHL6* in the *shl6* roots and stems were more highly reduced than those in Col-0 (Figure 4.6B). In the previous data, the loss-of function mutant in *SHL6* showed abnormal development in flowers, siliques, stems, roots, and leaves (Figure 4.2). The results suggest that reduced *SHL6* transcripts may be involved in abnormal phenotypes in multiple stages of development.

Materials and methods

Plant materials and growth conditions

Arabidopsis ecotype Col-*gl1* seed were obtained from Lehle Seeds (Round Rock, TX). The mutant Col-*gl1* line *shl6* was previously mutagenized by ethyl methane sulfonate (EMS) and screened under low light (Pepper et al., 2001). *Arabidopsis* ecotype Col-0 seeds were obtained from the laboratory stocks of Joanne Chory. *shl6* mutant was back-crossed twice to WT Col-0 and homozygous shl6 mutant was isolated by their short hypocotyls in low light (24$\mu molm^{-2}s^{-1}$).

Seeds were surface sterilized (Chory et al, 1989), resuspended in sterile 0.1% (w/v) phytagar, and then chilled for overnight at 4 °C. Seedlings were germinated at 23°C ±0.5°C under 8-h light/16-h dark photoperiod for 10d. Uniformly sized seedlings were moved to a 16-h light/8-h dark growth room and then grown with even spacing into pots containing the same compost/ sand mixture for phenotype analysis.

Expression analysis by quantitative RT-PCR

To study the expression of *SHL6* gene in *Arabidopsis*, RNA was isolated with the Qiagen Plant RNeasy RNA extraction kit. RNA samples were isolated from Col-0, shl6 mutant, and transformant GSL12. Seedlings were grown as previously described under continuous white light (110 $\mu molm^{-2}s^{-1}$), yellow light (70 $\mu molm^{-2}s^{-1}$), red (22 $\mu molm^{-2}s^{-1}$), and in the dark (Figure 4.2). As an additional experiment, RNA samples were collected from flower bud, mature flower, silique, leaf, stem, and root (Figure 4.6). Amount of RNA was measured by using Beckman DU60 Spectrophotometer and quality

of the RNA was tested by agarose gel electrophoresis. To remove genomic DNA, DNAseI treatment (DNA free™ kit, Ambion, Austin, TX) was used. 400 ng of RNA was reverse transcribed by using SuperScript™ III First-Strand Synthesis SuperMix (Invitrogen, USA). The resulting single stranded cDNA was thereafter used as template in quantitative real-time PCR (qRT-PCR) reactions. qRT-PCR was performed with *POWER* SYBR® Green PCR master mix (Applied Biosystem, USA) with an ABI 7900HT real-time (RT) PCR machine. The cDNA was normalized in dependence of the level of constitutively expressed (elongation factor a1) *EF1a* gene (EF930-F, 5'-TCGAATCCTCAAAACTCTATCCGCA-3'; EF930-R, 5'-GGAGAAGAAACGAAGCTATAACACG-3') as a control. qRT-PCR reactions were carried out with a gene specific primer for *SHL6* (CS-F, 5'-TATCCTTGCCTTTATGCCCACAGGTT-3'; CS-R,5'-TGATCCCCAGAATCCTGCTCTATGA-3') in a volume of 10 µl. The PCR program was as follows: incubation for 2 min at 50 °C, then 2 min at 95 °C, and 60°C for 1 minute. To verify the amplification of single PCR products, it was followed by 40 cycles of denaturation at 94 °C for 15 s, annealing at 60 °C for 15 s and a 2% ramping to 95°C. All measurements were repeated twice. To check non-specific amplification products, amplified fragments were analyzed by 2% agarose gel electrophoresis and then digested by a unique restrict enzyme (*HinfI*) in the CS primers.

Callose staining in pollen tube and anthers

For staining callose in pollen tubes, pistils and anthers were submerged in about 250µl acetic acid fixed for 1.5 hours. Tissue was left in fixative overnight. Tissue was softened by submerging into 1 M NaOH solution overnight. Softened tissue was gently washed 3 times with 50 mM KPO_4 buffer. The tissue was stained with 200µl of 0.01% aniline blue for 5-10 minutes (Worrall, et al., 1992). The stained tissue was transferred to a slide, mounting media added, and observed under a microscope (Olympus, BX51) with fluorescence and UV (a standard U-mnu2: excitation filter= 360-420nm;emission= 420nm) filters. Images were applied by a Magnafire Application Software 2.0 (Karl Storz Imaging).

Pollen viability assay

Anthers were stained in fluorescein diacetate (FDA) solution and observed by a fluorescent microscope using a UV filter (Heslop-Harrison, J. and Heslop-Harrison, Y., 1970). Stock solution of FDA in acetate was poured into 10ml of 10% sucrose solution drop-by-drop until the color turned grayish or milky. Pollen was placed on a hemacytometer slide by rubbing, tipping, or scratching grains out of anthers. One to two drops of the 10% sucrose and FDA solution was added and left for three minutes. The grains were covered by a coverslip and observed under a fluorescent microscope using a UV filter. Viable grains glowed a bright yellow from the inside illuminating sperm and vegetative nuclei. At least 100 pollen grains were counted in each of four replicates. Data was indicated by mean ±SD (standard deviation).

Analysis of hypocotyl cell growth

To observe the epidermal cell size and shape of 5-d-old *shl6* and Col-0 seedling grown under low light condition (24μmol$m^{-2}s^{-1}$), the method of epidermal imprints using agarose was used (Mathur and Koncz, 1997). Hypocotyls were dissected from seedlings and quickly laid out on the 3% low melting point agarose on a glass surface. It was placed at 4°C for five minutes in refrigerator to solidify the agarose. The hypocotyls were peeled away from the agarose and images of the impression were photographed using a ZeissM^2BIO fluorescence combination zoom stereo/compound microscope equipped with a Zeiss AxioCam color digital camera. Pictures of the hypocotyls impression were taken using the Zeiss Axio Vision software version 3.0.6. A hemacytometer was used to convert pixels to actual μm. Adobe Photoshop 7.0 was used to analyzed the images of hypocotyl cells.

CHAPTER V

CONCLUSIONS

Plant development is influenced by various environmental conditions. One of the most important factors is light quantity, quality, and duration. Plants have evolved several different photoreceptors for light perception and use light as the energy source for their growth. Plants implement developmental program depending on light, a process called "photomorphogenesis". Dr. Pepper and his colleagues (2001) have identified mutations in genes acting at the interface of light perception and developmental pathway-"downstream" from the photoreceptors and photoreceptor-specific signaling elements. They isolated recessive light-hyper-responsive mutants in eight genetic loci, designated as *seedling hyper-responsive* to *light* (*shl*).

In this study, the primary goal was to identify a gene related to *shl6*, one of the *shl* mutants by using map-based cloning and to characterize the role of the gene to further our understanding of photomorphogenesis.

The *Arabidopsis* mutant *shl*6 has developmental responses that are exaggerated on exposure to available light. In the low light, s*hl*6 seedlings have short hypocotyls, expanded cotyledons, and well-developed first true leaves. In addition, the roots of *shl6* are short and highly branched. The *SHL6* gene was mapped to a position on chromosome 5 between single sequence length polymorphism (SSLP) markers *nga*249 and *nga*151 via map-based cloning. We showed that *SHL6* gene encodes a glucan synthase like *(GSL12)*. In addition, the role of *SHL6* in light signaling was elucidated. The

transcriptional level of *SHL6* was regulated in Col-0 and the *shl6* seedlings grown under dark, yellow, red, and white light. The timing of flowering is under strict control of the light environment (Simpson and Dean, 2002). Mutant *shl6* plants flowered early in the both short-days and long-days. *SHL6* expression was highly induced in the cotyledons.

Another purpose of this research was to investigate the function of *SHL6*, a gene that encodes a callose synthase like *(GSL12)* and its role in the synthesis of callose. Positive evidence included observations showing: 1) Callose was highly deposited in the vascular bundle and connective tissues of Col-0 anthers, but not in the same tissues of *shl6* anthers. 2) Pollen grains temporally make callose as part of cell wall during microsporogenesis (Dong et al., 2005). The pollen viability is low in *shl6* when compared to Col-0. 3) Callose is also localized at the cell plate (Hong et al., 2001a). The reduced epidermal cell length in *shl6* hypocotyls may be caused by abnormal cell division involved in cell plate formation. Therefore, light regulated *SHL6* is also involved in callose synthesis.

Here, a model of the role of *SHL6* coupling light signaling and the synthesis of callose is proposed. Time of flowering is a good example to understand light signaling. The *shl6* mutant plants flower early when grown under both long days and short days. The *SHL6* may be a negative regulator of key flowering regulators, *FLOWERING LOCUS T (FT)* and *CONSTANS (CO)*. FT, CO, and PHYTOCHROME AND FLOWERING TIME (PFT1) are flowering regulators that act downstream of PHYB (Cerdan and Chory, 2003; Holliday et al., 2003; Valverde et al., 2004). Expression of *FT* in the vascular bundles was suppressed by *PHYB-GFP* expressed in the mesophyll and

increased by *CRY2-GFP* expressed vascular bundles (Endo et al., 2005 and 2007). These results revealed that a novel mechanism of inter-tissue signaling from mesophyll to vascular bundles is a critical step for the regulation of flowering by PHYB. However, it is unknown how a protein in a cell is regulated by an exogenous signal. SHL6, as an intermediate signal molecule may be working between PHYB and FT proteins (Figure 5.1).

Three reasons to support this hypothesis are suggested. The first is that *SHL6* mRNA expression in *shl6* mutant seedlings was substantially reduced in red light (Figure 3.2). It implicates that *SHL6* may be regulated by *PHYB*. The second reason is that *SHL6* is highly expressed in cotyledons (Figure 3.4). Although we do not have proof that *SHL6* is expressed in vascular bundles, the expression of one member of the *GSL* gene family in *Arabidopsis*, (*AtGSL2:GUS)* was detected in the vascular tissues of cotyledons, hypocortyls, and roots of transgenic plants (Dong et al., 2005).

Future studies

How is *SHL6* gene regulated in the light signaling pathway?

The first future study is to determine that *SHL6* is directly or indirectly regulated in the light signal pathway. *HY5* acts as one of downstream genes of *PHYA, PHYB*, cryptochromes (*CRY1 and CRY2*), and *UV-B* (Ang and Deng, 1994). *HY5* encoding a constitutively nuclear bZIP transcription factor is a positive regulator in photomorphogenesis (Hardtke and Deng, 2000).

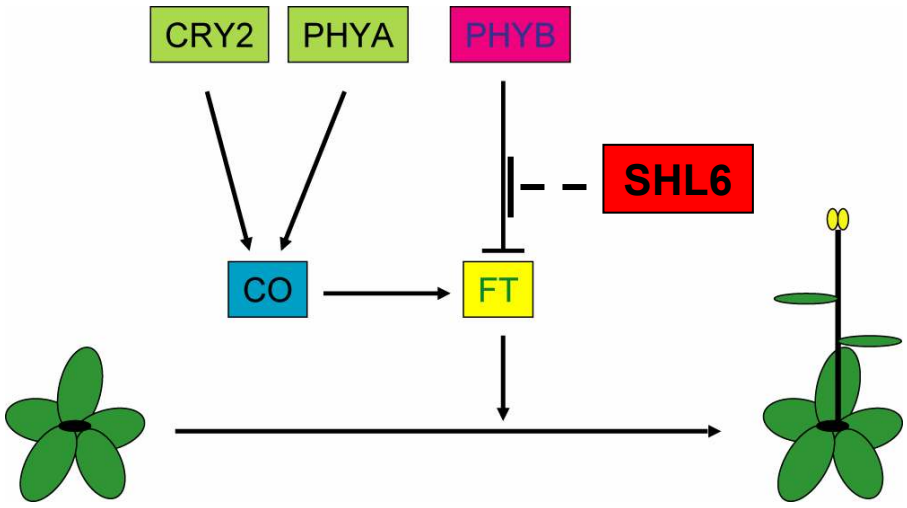

Figure 5.1. A model of the role of *SHL6* involved in flowering time.

PHYA and *CRY2* seem to induce *CO* activity. CO protein directly activates FT expression to promote flowering. *FT* mRNA expression is also repressed by *PHYB*. The placement of *SHL6* is deduced from the work presented here. *PHYB*-regulated *SHL6* may suppress flowering.

Whereas *hy5* hypocotyls elongated in all light conditions (Oyama et al., 1997; Cluis et al., 2004), *shl6* hypocotyls were inhibited under low light. Therefore, to see whether *SHL6* and *HY5* interacted in vivo, we will generate double mutants (*shl6/shl6 hy5/hy5*) through crossing *shl6* and *hy5*. The *shl6/hy5* hypocotyls measured under low light will elucidate *SHL6* acts as a downstream or upstream gene of *HY5*.

How is *SHL6* gene involved in the flowering pathway?

We demonstrated that *SHL6* is involved in photoperiodic flowering, one of plant responses affected by the light signaling pathway because the *shl6* plants flowered early in both long-days and short-days. To identify how *SHL6* as a negative regulator suppresses flowering, an alternative strategie will be performed.

To determine whether the *SHL6* expression affects *CO* and *FT* transcripts promoting flowering, the abundance of *CO* and *FT* mRNA will be calculated in wild type Col-0 and *shl6* plants via qRT-PCR. The abundance of *CO* mRNA was reduced in *phyA* and *cry2* mutants, but was increased in *phyB* mutant (Cerdan and Chory, 2003). Thus, *SHL6* hyper-responsive to red light will show that *SHL6*, one of downstream genes of *PHYB* directly inhibits the *CO* and *FT* mRNA expression in *shl6* plants.

LITERATURE CITED

Ahmad M, Jarillo JA, Smirnova O, Cashmore AR (1998). The CRY1 blue light photoreceptor of *Arabidopsis* interacts with phytochrome A *in vitro*. Mol Cell **1**, 939–948

Alonso JM, Stepanova AN, Leisse TJ, Kim CJ, Chen H, Shinn P, Stevenson DK, Zimmerman J, Barajas P, Cheuk R, Gadrinab C, Heller C, Jeske A, Koesema E, Meyers CC, Parker H, Prednis L, Ansari Y, Choy N, Deen H, Geralt M, Hazari N, Hom E, Karnes M, Mulholland C, Ndubaku R, Schmidt I, Guzman P, Aguilar-Henonin L, Schmid M, Weigel D, Carter DE, Marchand T, Risseeuw E, Brogden D, Zeko A, Crosby WL, Berry CC, Ecker JR (2003). Genome-wide insertional mutagenesis of *Arabidopsis thaliana*. Science **310**, 653-657

Al-Sady B, Ni W, Kircher S, Schäfer E and Quail PH (2006). Photoactivated phytochrome induces rapid PIF3 phosphorylation prior to proteasome-mediated degradation. Mol Cell **23**, 439–446

An H, Roussot C, Suarez-Lopez P, Corbesier L, Vincent C, Pineiro M, Hepworth S, Mouradov A, Justin S, Turnbull C, Coupland G (2004). CONSTANS acts in the phloem to regulate a systemic signal that induces photoperiodic flowering of *Arabidopsis*. Development **131**, 3615–3626

Ang LH, Deng XW (1994). Regulatory hierarchy of photomorphogenic loci: Allele-specific and light-dependent interaction between the *HY5* and *COP1* loci. Plant Cell **6**, 613-628

Ang LH, Chattopadhyay S, Wei N, Oyyama T, Okada K, Batschauer A, Deng XW (1998). Molecular interaction between COP1 and HY5 defines a regulatory switch for light control of *Arabidopsis* development. Mol Cell **1**, 213-222

Aspinall GO, Kessler G (1957). The Structure of Callose from the Grape Vine, Chem. Ind., London, p.1296

Bauer D, Viczián A, Kircher S, Nobis T, Nitschke R, Kunkel T, Panigrahi KC, Adám E, Fejes E, Schäfer E, Nagy F (2004). Constitutive photomorphogenesis 1 and multiple photoreceptors control degradation of phytochrome interacting factor 3, a transcription factor required for light signaling in *Arabidopsis*. Plant Cell **16**, 1433-1445

Bell CJ, Ecker JR (1994). Assignment of 30 microsatellite loci to the linkage map of *Arabidopsis*. **19**, 137-144

Benvenuto G, Foormiggini F, Laflamme P, Malakhov M, Bowler C (2002) The photomorphogenesis regulator DET1 binds the amino-terminal tail of histone H2B in a nucleosome context. Curr Biol **12**, 1529-1534

Bevan M, **Bancroft I**, **Bent E**, **Love K**, **Goodman H**, **Dean C**, **Bergkamp R**, **Cerdan PD, Chory J** (2003). Regulation of flowering time by light quality. Nature **423**, 881–885

Bevan M, Bancroft I, Chalwatzis N (1998). Analysis of 1.9Mb of contiguous sequence from chromosome 4 of *Arabidopsis thaliana*. Nature **391**, 485-488

Blencowe BJ (2000) Exonic splicing enhancers: mechanism of action, diversity and role in human genetic diseases. Trends Biochem Sci **25**, 106-110

Broothaerts W, Mitchell HJ, Weir B, Kaines S, Smith LM, Yang W, Mayer JE, Roa-Rodrigues C, Jefferson RA (2005). Gene transfer to plants by diverse species of bacteria. Nature **433**, 629-633.

Brown BA, **Cloix C**, **Jiang GH**, **Kaiserli E**, **Herzyk P**, **Kliebenstein DJ**, **Jenkins GI** (2005). A UV-B-specific signaling component orchestrates plant UV protection. Proc Natl Acad Sci USA **102**, 18225-18230

Cabib E, Roh DH, Schmidt M, Crotti LB, Varma A (2001). The yeast cell wall and septum as paradigms of cell growth and morphogenesis. J Biol Chem **276,** 19679–19682

Cai L, Taylor JF, Wing RA, Gallagher DS, Woo SS, Davis SK (1995). Construction and characterization of a bovine bacterial artificial chromosome library. Genomics **29**, 413-425

Cargill M, Altshuler D, Ireland J, Sklar P, Ardlie K, Patil N, Shaw N, Lane CR, Lim EP, Kalyanaraman N, Nemesh J, Ziaugra L, Friedland L, Rolfe A, Warrington J, Lipshutz R, Daley GQ, Lander ES (1999). Characterization of single-nucleotide polymorphisms in coding regions of human genes. Nat Genet **22**, 231-238

Casal JJ, Davis SJ, Kirchenbauer D, Viczian A, Yanovsky MJ (2002). The serine-rich N-terminal domain of oat phytochrome A helps regulate light responses and subnuclear localization of the photoreceptor. Plant Physiol **129**, 1127–1137

Cerdan PD, Chory J (2003). Regulation of flowering time by light quality. Nature **423**, 881-885

Chory J, Peto C, Feinbaum R, Pratt L, Ausubel F (1989). *Arabidopsis thaliana* mutant that develops as a light-grown plant in the absence of light. Cell **58**, 991-999

Chory J (1992). A genetic model for light-regulated seedling development in *Arabidopsis*. Development **115,** 337-354

Clough SJ, Bent AF (1998). Floral dip: a simplified method for *Agrobacterium*-mediated transformation of *Arabidopsis thaliana*. Plant J **16**, 735-743

Cluis CP, Mouchel CF, Hardtke CS (2004). The *Arabidopsis* transcription factor HY5 integrates light and hormone signaling pathways. Plant J **38**, 332–347

Colon-Carmona A, Chen DL, Yeh KC, Abel S (2000). Aux/IAA proteins are phosphorylated by phytochrome *in vitro*. Plant Physiol **124**, 1728–1738

Corbesier L, Vincent C, Jang S, Fornara F, Fan Q, Searle I, Giakountis A, Farrona S, Gissot L, Turnbull C, Coupland G (2007). FT protein movement contributes to long-distance signaling in floral induction of *Arabidopsis*. Science **316**, 1030-1033.

Cui XJ, Shin HS, Song C, Laosinchai W, Amano Y, Brown RM (2001). A putative plant homolog of the yeast β-1,3-glucan synthase subunit FKS1 from cotton (*Gossypium hirsutum* L.) fibers. Planta **213,** 223–230

Currier HB, Webster DH (1964). Callose formation and subsequent disappearance: Studies in ultrasound stimulation. Plant Physiol **39**, 843-847

Deng XW, Matsui M, Wei N, Wagner D, Chu AM, Feldmann KA, Quail PH (1992). COP1, an *Arabidopsis* regulatory gene, encodes a protein with both a zinc-binding motif and a G beta homologous domain. Cell **71**, 791-801

Deng XW, Caspar T, Quail PH (1991). Cop1: a regulatory locus involved in light-controlled development and gene expression in *Arabidopsis*. Genes Dev **5**, 1172-1182

Dijkgraaf GJ, Abe M, Ohya Y, Bussey H (2002). Mutations in Fks1p affect the cell wall content of β-1,3- and β-1,6-glucan in *Saccharomyces cerevisiae*. Yeast **19,** 671–690

Doblin MS, De Melis L, Newbigin E, Bacic A, Read SM (2001). Pollen tubes of *Nicotiana alata* express two genes from different β-glucan synthase families. Plant Physiol **125,** 2040–2052

Dong X, Hong Z, Sivaramakrishnan M, Mahfouz M, Verma DP (2005). Callose synthase (CalS5) is required for exine formation during microgametogenesis and for pollen viability in *Arabidopsis*. Plant J **42**, 315–328

Douglas CM, Foor F, Marrinan JA, Morin N, Nielsen JB, Dahl AM, Mazur P, Baginsky W, Li W, el-Sherbeini M (1994). The *Saccharomyces cerevisiae Fks1* (*Etg1*) gene encodes an integral membrane protein which is a subunit of (1→3)-β-D-glucan synthase. Proc. Natl. Acad. Sci. USA **91,** 12907–12911

Endo M, Mochizuki N, Suzuki T, Nagatani A (2007). CRYPTOCHROME2 in vascular bundles regulates flowering in *Arabodopsis*. Plant Cell **19**, 84-93

Endo M, Nakamura S, Araki T, Mochizuki N, Nagatani A (2005). Phytochrome B in the mesophyll delays flowering by suppressing *FLOWERING LOCUS T* expression in *Arabidopsis* vascular bundles. Plant Cell **17**, 1941–1952

Enns LC, Kanaoka MM, Torii KU, Comai L, Okada K, Cleland RE (2005). Two callose synthases, GSL1 and GSL5, play an essential and redundant role in plant and pollen development and in fertility. Plant Mol Biol **58**, 333-349

Fankhauser C, Yeh KC, Lagarias JC, Zhang H, Elich TD, Chory J (1999). PKS1, a substrate phosphorylated by phytochrome that modulates light signaling in *Arabidopsis*. Science **284**, 1539–1541

Furuya M (1993). Phytochromes; their molecular species, gene family and functions. Annu. Rev. Plant Physiol. Plant Mol Biol **44**, 617-645

Furuya M, Song PS (1994). Assembly and properties of holophytochrome. In Photomorphogenesis in Plants, R.E. Kendrick and G.H.M. Kronenberg, eds, (Dordrecht, Netherlands:Kluwer Academic Publishers), pp. 105-140

Garner WW, Allard HA (1920). Effect of the relative length of day and night and other factors of the environment on growth and reproduction in plants. J. Agric. Res. **18**, 553-606.

Goosey L, Palecanda L, Sharrock RA (1997). Differential patterns of expression of the *Arabidopsis PHYB*, *PHYD*, and *PHYE* phytochrome genes. Plant Physiol **115**, 959–969

Goldberg, R., Beals, T.P. and Sanders, P.M. (1993). Anther development: basic principles and practical applications. Plant Cell **5**, 1217–1229

Guo H, Yang H, Mockler TC, Lin C (1998). Regulation of flowering time by *Arabidopsis* photoreceptors. Science **27**, 1360–1363

Gyula P, Schafer E, Nagy F (2003). Light perception and signaling in higher plants. Curr. Opin. Plant Biol **6**, 446-452

Hajdukiewicz P, Svab Z, Maliga P (1994). The small, versatile pPZP family of Agrobacterium binary vectors for plant transformation. Plant Mol Biol **25**, 989-994

Hardtke CS, Deng XW (2000). The cell biology of the COP/DET/FUS proteins. Regulating proteolysis in photomorphogenesis and beyond? Plant Physiol. **124**, 1548-57.

Hardtke CS, Okamoto H, Stoop-Myer C, Deng XW (2002). Biochemical evidence for ubiquitin ligase activity of the *Arabidopsis* COP1 interacting protein 8 (CIP8). Plant J **30**, 385-394

Heim MA, Jakoby M, Werber M, Martin C, Weisshaar B, Bailey PC (2003). The basic helix-loop-helix transcription factor family in plants: a genome-wide study of protein structure and functional diversity. Mol Biol Evol **20**, 735–747

Heslop-Harrison J, Heslop-Harrison Y (1970). Evaluation of pollen viability by enzymatically induced fluorescence: intracellular hydrolysis of fluorescein diacetate. Stain Tech **45**, 115–120

Holliday KJ, Salter MG, Thingnaes E, Whitelam GC (2003). Phytochrome control of flowering is temperature sensitive and correlates with expression of the floral integrator FT. Plant J **33**, 875-885

Holm M, Deng XW (1999). Structural organization and interactions of COP1, a light-regulated developmental switch. Plant Mol Biol **41**, 151–158

Holm M, Ma LG, Qu LJ, Deng XW (2002). Two interacting bZIP proteins are direct targets of COP1-mediated control of light-dependent gene expression in *Arabidopsis.* Genes Dev **16**, 1247–1259

Hong ZL, Delauney AJ, Verma DPS (2001a). A cell plate–specific callose synthase and its interaction with phragmoplastin. Plant Cell **13,** 755–768

Hong ZL, Zhang ZM, Olson JM, Verma DPS (2001b). A novel UDP-glucose transferase is part of the callose synthase complex and interacts with phragmoplastin at the forming cell plate. Plant Cell **13**, 769-779

Huq E, Quail PH (2002). PIF4, a phytochrome-interacting bHLH factor, functions as a negative regulator of phytochrome B signaling in *Arabidopsis*. EMBO J **21**, 2441–2450

Izhar S, Frankel R (1971). Mechanism of male sterility in *Petunia*: the relationship between pH, callase activity in the anthers, and the breakdown of the microsporogenesis. Theor. Appl. Genet **41**, 104–108

Jacobs AK, Lipka V, Burton RA, Panstruga R, Strizhov N, Schulze-Lefert P, Fincher GB (2003). An *Arabidopsis* callose synthase, GSL5, is required for wound and papillary callose formation. Plant Cell **15**, 2503-2513

Jander G, Norris SR, Rounsley SD, Bush DF, Levin IM, Last RL (2002). *Arabidopsis* map-based cloning in the post-genomic era. Plant Physiol **129,** 440–450

Jang IC, Yang JY, Seo HS, Chua NH (2005). HFR1 is targeted by COP1 E3 ligase for post-translational proteolysis during phytochrome A signaling. Genes Dev **19**, 593–602

Kardailsky I, Shukla VK, Ahn JH, Dagenais N, Christensen SK, Nguyen JT, Chory J, Harrison MJ, Weigel D (1999). Activation tagging of the floral inducer *FT*. Science **286**, 1962–1965

Kauss H, Smallwood M, Knox JP, Bowles DJ (1996). Membranes, Callose synthesis, Specialized Functions in Plants, BIOS Scientific Publishers, Oxford, pp. 77–92

Kendrick RE, Kronenberg GHM (1994). Photomorphogenesis in Plants. Dordrecht, Neth. Kluwer.

Kim J, Yi H, Choi G, Shin B, Song, PS (2003). Functional characterization of phytochrome interacting factor 3 in phytochrome-mediated light signal transduction. Plant Cell **15**, 2399–2407

Knott JE (1934). Effect of localized photoperiod on spinach. Proc Soc Hort Sci **31**, 152–154

Kobayashi Y, Kaya H, Goto K, Iwabuchi M, Araki T (1999). A pair of related genes with antagonistic roles in mediating flowering signals. Science **286**, 1960–1962

Koncz C, De Greve H, Andre D, Deboeck F, Van Montagu M, Schell J (1983). The opine synthase genes carried by Ti plasmids contain all signals necessary for expression in plants. EMBO J **3**, 1029-1037

Konieczny A, Ausubel FM (1993). A procedure for mapping *Arabidopsis* mutations using co-dominant ecotype-specific PCR-based markers. Plant J **4**, 403-410

Koornneef M, Rolff E, Spruit CJP (1980). Genetic control of light-inhibited hypocotyl elongation in *Arabidopsis thaliana.* Z. Pflanzenphysiol **100**, 147-160

Krall L, Reed JW (2000). The histidine kinase-related domain participates in phytochrome B function but is dispensible. Proc Natl Acad. Sci USA **97**, 8169-8174

Lariguet P, Boccalandro HE, Alonso JM, Ecker JR, Chory J (2003). A growth regulatory loop that provides homeostasis to phytochromeA signaling. Plant Cell **15**, 2966–2978

Lukowits W, Gillmor CS, Scheible WR (2000). Positional cloning in *Arabidopsis*. Why it feels good to have a genome initiative working for you. Plant Physiol **123**, 795-805

Ma H (2005). Molecular genetic analyses of microsporogenesis and microgametogenesis in flowering plants. Annu Rev Plant Biol **56**, 393–434

Mathur J, Koncz C (1997). Method for preparation of epidermal imprints using agarose. Biotechniques **22**, 280-282

Martinez-Garcia JF, Huq E, Quail PH (2000). Direct targeting of light signals to a promoter element-bound transcription factor. Science **288**, 859–863

Matsui M, Stoop CD, von Arnim AG, Wei N, Deng XW (1995). *Arabidopsis* COP1 protein specifically interacts *in vitro* with a cytoskeleton-associated protein, CIP1. Proc Natl Acad Sci USA **92**, 4239–4243

Matsushits T, Mochizuki N, Nagatani A (2003). Dimers of N-terminal domain of phytochrome B are functional in the nucleus. Nature **424**, 571-574

McCormick S (1993). Male gametophyte development. Plant Cell **5**, 1265–1275

Mockler T, Yang H, Yu X, Parikh D, Cheng YC, Dolan S, Lin C (2003). Regulation of photoperiodic flowering by *Arabidopsis* photoreceptors. Proc Natl Acad Sci USA **100**, 2140–2145

Montgomery BL, Lagarias JC (2002). Phytochrome ancestry: sensors of bilins and light. Trends Plant Sci **7**, 357-366

Nagy F, Schafer E (2002). Phytochromes control phtomorphogenesis by differentially regulated, interacting signaling pathways in higher plants. Annu. Rev. Plant Mol Biol **53**, 329-355

Nishikawa S, Zinkl GM, Swanson RJ, Maruyama D, Preuss D (2005). Callose (beta-1,3 glucan) is essential for *Arabidopsis* pollen wall patterning, but not tube growth. BMC Plant Biol.**5**, 22-30

Nishimura MT, Stein M, Hou BH, Vogel JP, Edwards H, Somerville SC (2003). Loss of a callose synthase results in salicylic acid-dependent disease resistance. Science **301**, 969–972

Nystrom-Lahti M, Holmberg M, Fidalgo P, Salovaara R, de la Chapelle A, Jiricny J, Peltomaki P (1999). Missense and nonsense mutation in codon 659 of MLH1 cause aberrant splicing of messenger RNA in HNPCC kindreds. Genes Chr Cancer **26**, 372-375

Østergaard L, Petersen M, Mattsson O, Mundy J (2002). An *Arabidopsis* callose synthase. Plant Mol Biol **49,** 559–566

Osterlund MT, Ang LH, Deng XW (1999). The role of COP1 in repression of *Arabidopsis* photomorphogenic development. Trends Cell Biol **9**, 113–118

Osterlund MT, Deng XW (1998). Multiple photoreceptors mediate the light-induced reduction of GUS-COP1 from *Arabidopsis* hypocotyl nuclei. Plant J **16,** 201–208

Osterlund MT, Hardtke CS, Wei N, Deng XW (2000). Targeted destabilization of HY5 during light-regulated development of *Arabidopsis*. Nature **405**, 462–466

Oyama T, Shimura Y, Okada K (1997). The *Arabidopsis HY5* gene encodes a bZIP protein that regulates stimulus-induced development of root and hypocotyls. Genes Dev **11**, 2983–2994

Pepper AE, Chory J (1997). Extragenic suppressors of the *Arabidopsis det1* mutant identify elements of flowering-time and light-response regulatory pathways. Genetics **145**, 1125-1137

Pepper AE, Delaney T, Washburn T, Poole D, Chory J (1994). DET1, a negative regulator of light-mediated development and gene expression in *Arabidopsis*, encodes a novel nuclear-localized protein. Cell **78**, 109-116

Pepper AE, Seong-Kim M, Hebst SM, Ivey KN, Kwak SJ, Broyles DE (2001). *shl*, a new set of *Arabidopsis* mutants with exaggerated developmental responses to available red, far-red, and blue light. Plant Physiol **127**, 295-304

Pertea M, Mount SM, Salzberg SL (2007). A computational survey of candidate exonic splicing enhancer motifs in the model plant *Arabidopsis thaliana*. BMC Bioinformatics **8**, 159-167

Quail PH (2002). Phytochrom photosensory signaling network. Nat. Rev. Mol. Cell Biol **3**, 85-93

Quail PH (1997). An emerging molecular map of the phytochromes. Plant Cell Environ **20**, 657-666

Quail PH, Boylan MT, Parks BM, Short TW, Xu Y, Wagner D (1995). Phytochromes: photosensory perception and signal transduction. Science **268**, 675-680

Regan SM, Moffatt BA (1990). Cytochemical analysis of pollen development in wild-type *Arabidopsis* and a male-sterile mutant. Plant Cell **2**, 877-889

Saijo Y, Sullivan JA, Wang H, Yang J, Shen Y, Rubio V, Ma L, Hoecker U, Deng XW (2003). The COP1-SPA1 interaction defines a critical step in phytochrome A-mediated regulation of HY5 activity. Genes Dev **17**, 2642–2647

Salter MG, Franklin KA, Whitelam GC (2003). Gating of the rapid shade-avoidance response by the circadian clock in plants. Nature **426**, 680–683

Samuels AL, Giddings TH, Staehelin LA (1995). Cytokinesis in tobacco BY-2 and root tip cells: a new model of cell plate formation in higher plants. J Cell Biol **130**, 1345-1357

Sato S, Kotani H, Nakamura Y, Kaneko T, Asamizu E, Fukami M, Miyajima N, Tabata S (1997). Structural analysis of *Arabidopsis thaliana* chromosome 5. I. Sequence features of the 1.6 Mb regions covered by twenty physically assigned P1 clones. DNA Res **4**, 215-230

Scheres B, Wolkenfelt H, Willemsen V, Terlouw M, Lawson E, Dean C, Weisbeek P (1994). Embryonic origin of the *Arabidopsis* primary root and root meristem initials. Development **120,** 2475-2487

Schroeder DF, Gahrtz M, Maxwell BB, Cook RK, Kan JM, Alonso JM, Ecker JR Chory J (2002). De-etiolated 1 and damaged DNA binding protein 1 interact to regulate *Arabidopsis* photomorphogenesis. Curr Biol **12,** 1462–1472

Schwechheimer C, Deng XW (2000). The COP/DET/FUS proteins: regulators of eukaryotic growth and development. Semin Cell Dev Biol **11,** 495–503

Searle, I, Coupland G (2004). Induction of flowering by seasonal changes in photoperiod. EMBO J **23**, 1217-1222

Seo HS, Yang JY, Ishikawa M, Bolle C, Ballesteros ML, Chua NH (2003). LAF1 ubiquitination by COP1 controls photomorphogenesis and is stimulated by SPA1. Nature **423**, 995–999

Sharrock RA, Clark T (2002). Patterns of expression and normalized levels of the five *Arabidopsis* phytochromes. Plant Physiol **130**, 442-456

Simpson GG, Dean C (2002). *Arabidopsis*, the Rosetta stone of flowering time? Science **296**, 285–289

Sivaguru M, Fujiwara T, Samaj J, Baluska F, Yang Z, Osawa H, Maeda T, Mori T, Volkmann D, Matsumoto H (2000). Aluminum-induced 1-->3-beta-D-glucan inhibits cell-to-cell trafficking of molecules through plasmodesmata. A new mechanism of aluminum toxicity in plants. Plant Physiol **124**, 991-1006

Somers DE, Quail PH (1995). Temporal and spatial expression patterns of PHYA and PHYB genes in *Arabidopsis*. Plant J **7**, 413–427

Steiglitz H (1977). Role of *β*-1,3-glucanase in postmeiotic microspore release. Dev Biol **57**, 87–97

Stieglitz H, Stern H (1973). Regulation of β-1,3-glucanase activity in developing anthers of *Lilium*. Dev Biol **34**, 169–173

Stone BA, Clarke AE (1992). Chemistry and Biology of (1→3)-β-D-Glucans. La Trobe University Press, Victoria, Australia

Takada S, Goto K (2003). TERMINAL FLOWER2, an *Arabidopsis* homolog of HETEROCHROMATIN PROTEIN1, counteracts the activation of *FLOWERING LOCUS T* by CONSTANS in the vascular tissues of leaves to regulate flowering time. Plant Cell **15**, 2856–2865

The *Arabidopsis* Genome Initiative (2000) Analysis of the genome sequence of the flowering plant *Arabidopsis thaliana.* Nature **408**, 796-815

Toledo-Ortiz G, Huq E, Quail PH (2003). The *Arabidopsis* basic/helix-loop-helix transcription factor family. Plant Cell **15**, 1749–1770

Torii KU, Stoop-Myer CD, Okamoto H, Coleman JE, Matsui M, Deng XW (1999). The RING finger motif of photomorphogenic repressor COP1 specifically interacts with the RING-H2 motif of novel *Arabidopsis* protein. J Biol Chem **274**, 27674–27681

Toth R, Kevei E, Hall A, Millar AJ, Nagy F, Kozma-Bognar L (2001). Circadian clock-regulated expression of phytochrome and cryptochrome genes in *Arabidopsis*. Plant Physiol **127**, 1607–1616

Ulm R, Baumann A, Oravecz A, Máté Z, Ádám É, Oakeley EJ, Schäfer E, Nagy F (2004). Genome-wide analysis of gene expression reveals function of the bZIP transcription factor HY5 in the UV-B response of *Arabidopsis.* Proc Natl Acad Sci USA **101**, 1397–1402

Valverde F, Mouradov A, Soppe W, Ravenscroft D, Samach A, Coupland G (2004). Photoreceptor regulation of CONSTANS protein in photoperiodic flowering. Science **303**, 1003–1006

Verma DPS (2001). Cytokinesis and building of the cell plate in plants. Annu Rev Plant Physiol Plant Mol Biol **52,** 751-784

Verma DPS, Hong Z (2001). Plant callose synthase complexes. Plant Mol Biol **47**, 693-701

Von Arnim AG, Deng XW (1994). Light inactivation of *Arabidopsis* photomorphogenic repressor COP1 involves a cell-specific regulation of its nucleocytoplasmic partitioning. Cell **79,** 1035–1045

Wang H, Ma LG, Li JM, Zhao HY, Deng XW (2001). Direct interaction of *Arabidopsis* cryptochromes with COP1 in light control development. Science **294,** 154–158

Warmke HE Overman MA (1972) Cytoplasmic male sterility in sorghum. 1. Callose behavior in fertile and sterile anthers. J Hered **63**, 103–108

Wei N, Deng XW (1996). The role of the COP/DET/FUS genes in light control of *Arabidopsis* seedling development. Plant Physiol **112**, 871–878

Wei N, Kwok SF, von Arnim AG, Lee A, McNellis TW, Piekos B, Deng XW (1994). *Arabidopsis COP8*, *COP10*, and *COP11* genes are involved in repression of photomorphogenic development in darkness. Plant Cell **6**, 629-643

Worrall D, Hird DL, Hodge T, Paul W, Draper J (1992). Premature dissolution of the micosporocyte callose wall causes male sterility in transgenic tobacco. Plant Cell **4**, 759-771

Yamamoto YY, Deng X, Matui M (2001). Cip4, a new COP1 target, is a nucleus-localized positive regulator of *Arabidopsis* photomorphogenesis. Plant Cell **13**, 399-411

Yamamoto YY, Matsui M, Ang LH, Deng WD (1998). Role of a COP1 interactive protein in mediating light-regulated gene expression in *Arabidopsis*. Plant Cell **10**, 1083-1094

Yang HQ, Tang RH, Cashmore AR (2001). The signaling mechanism of *Arabidopsis* CRY1 involves direct interaction with COP1. Plant Cell **13**, 2573–2587

Yang J, Lin R, Sullivan J, Hoecker U, Liu B, Xu L, Deng XW, Wang H (2005). Light regulates COP1-mediated degradation of HFR1, a transcription factor essential for light signaling in *Arabidopsis*. Plant Cell **17,** 804–821

Yanisch-Perron C, Vieira J, Messing J (1985). Improved M13 phage cloning vectors and host strains: nucleotide sequences of the M13mp18 and pUC19 vectors. Gene **33**, 103-109

Yeh KC, Lagarias JC (1998). Eukaryotic phytochromes: light-regulated serine/threonine protein kinases with histidine kinase ancestry. Proc Natl Acad Sci USA **95**, 13976-13981

VITA

Name: Bo Hyun Byun

Address: 1094 Wellington Street, Apt # 1002

Halifax, NS B3H 2Z9

CANADA

Email Address: bbyun@bio.tamu.edu

Education: B.S., Genetic Engineering, University of Suwon, 1996

M.S., Seoul National University, 1998

Ph.D. Texas A&M University, 2008